BÉZIER METHOD FOR IMAGE PROCESSING

by

MOHD FIKRI BIN BAHARUDDIN

FINAL PROJECT REPORT

Submitted to the Electrical & Electronics Engineering Programme
in Partial Fulfillment of the Requirements
for the Degree
Bachelor of Engineering (Hons)
(Electrical & Electronics Engineering)

Universiti Teknologi PETRONAS
Bandar Seri Iskandar
31750 Tronoh
Perak Darul Ridzuan

CERTIFICATION OF APPROVAL

BÉZIER METHOD FOR IMAGE PROCESSING

by

MOHD FIKRI BIN BAHARUDDIN

A project dissertation submitted to the
Electrical & Electronics Engineering Programme
Universiti Teknologi PETRONAS
in partial fulfilment of the requirement for the
Bachelor of Engineering (Hons)
(Electrical & Electronics Engineering)

Approved:

MR. SAMSUL ARIFFIN BIN ABDUL KARIM
Project Supervisor

UNIVERSITI TEKNOLOGI PETRONAS
TRONOH, PERAK

December 2010

CERTIFICATION OF ORIGINALITY

This is to certify that I am responsible for the work submitted in this project, that the original work is my own except as specified in the references and acknowledgements, and that the original work contained herein have not been undertaken or done by unspecified sources or persons.

____

Mohd Fikri Bin Baharuddin

ABSTRACT

This project concerns about Bézier method in Computer Aided Geometric Design (CAGD) involving Bézier Curve and Bézier Surface which widely related to the other theorem and method. The aim of this project is to introduce the basic of Bézier method and then generate the Bézier curves, Bézier surfaces, theory and properties and develop Bézier method in image processing application specifically image compression by using MATLAB. The Bézier method was widely applied in many areas especially in Computer Aided Geometric Design (CAGD) but there is only several application in the image processing. This project will focus on Bézier Curve, Bézier Surface, Bernstein Polynomial, de Casteljau Algorithm, Interpolation, Approximation, Quadtree and Parametric Line Fitting, Image Rescaling and Image Compression application. The proof and examples of some theory and properties as well as the application will be shown by using MATLAB and also by using the calculation and analysis. For the main focus of this project which is image compression by RGB Quadtree Decomposition and Parametric Line Fitting method, the analysis have been made for four different images which are Peppers.tiff, Baboon.tiff, Airplane.tiff and Lena.png. From the analysis which being shown in the form of table and graph, the RGB channel threshold effect on the resulted output images being observed.

ACKNOWLEDGMENT

First and foremost, praise to Allah the Almighty, who has helped and gave me courage and strength in completing Final Year Project (FYP). Without His permission, this FYP will not be a success. I would like to take this opportunity to express my deepest gratitude to all parties involved in conducting this project ranging from UTP lecturers, friend and my family who have been supportive in helping me doing the project.

I am profoundly grateful to my supervisor, Mr. Samsul Ariffin Bin Abdul Karim who has guided and given me opportunity to handle the project. Last but not least, many thanks to others whose name was not mentioned in this page but has in one way or another contributed to the accomplishment of this project.

TABLE OF CONTENTS

LIST OF FIGURES

LIST OF TABLES

LIST OF ABBREVIATIONS

WxH	Width x Height
MB	Megabyte
KB	Kilobyte
MSE	Mean Squared Error
RMSE	Root Mean Squared Error
PSNR	Peak Signal Noise Ratio
CR	Compression Ratio
R	Red
G	Green
B	Blue

CHAPTER 1
INTRODUCTION

1.1 Background of Study

Originally, Bézier curves were independently developed in 1959 by Paul de Casteljau and by Pierre Bézier about 1962. The underlying mathematical theory is based on the concept of Bernstein polynomial [1]. The Bernstein polynomial is important and dominant in Bézier spline models for curve and surface design and drawing [2]. de Casteljau directly exploited this relationship, but it was not before 1970 that R. Forrest discovered the connection between Bézier's work and Bernstein polynomials.

Bézier and de Casteljau developed their theories as part of CAD systems that were built up at two French car companies, Renault and Citroën. The Renault system UNISURF was soon described in several publications, this is the reason that the underlying theory now bears Bézier's name [1]. In the late sixties, the Bézier surface description was introduced and has remained one of the most popular schemes. When the Bézier's work on UNISURF first published, the remarkable spline era in computer science started.

The same situation was repeated with the discovery of Ingrid Daubechi's wavelets. Different wavelet splines are now well known and extensively found in the literature. As splines are rich in properties, they provide advantages in many important areas. Bézier and wavelet splines, can, therefore, be regarded as two landmarks in spline theory with wide application in image processing and machine vision [2]. Presently, Bézier curves and surfaces are extensively utilized in many fields like industrial and computer-aided design, vector-based drawing, font design and 3D-modelling.

Two of the most important mathematical representations of curves and surfaces in computer graphics and computer-aided design are the Bézier and B-spline forms. Bézier curves are polynomial curves which have a particular mathematical representation. Their popularity is due to the fact that they posses a number of mathematical properties which enable their manipulation and analysis, and yet no mathematical knowledge is required in order to use the curves [3].

1.2 Problem Statement

The Bézier method was widely applied in many areas especially in Computer Aided Geometric Design (CAGD). The Bézier curves and surfaces were famously used in design problem and play an important role in the construction of quite different products such as car bodies, ship hulls, propeller blades, shoe, and bottles and even in the description of geological, physical and medical phenomena. In image processing, the most famous and familiar techniques being used was wavelet [1]. In order to varies the techniques in image processing and perhaps can improve the available techniques, the author will try to implement the Bézier method for image processing specifically image compression.

1.3 Objectives

The objectives of this project are:

i. To understand the theoretical point of view for Bézier curves and surfaces
ii. To generate the Bézier curves and surfaces using MATLAB software
iii. To implement the Bézier method for image processing specifically image compression and simulating the theory and properties
iv. To apply the Bézier method with another suitable method for image compression

1.4 Scope of Study

This project is aim to implement the Bézier method for image processing using MATLAB. It will cover the theory and properties of Bernstein polynomial, de Casteljau Algorithm, spline, Bézier curves, Bézier surfaces, image processing application such as affine transformations, image rescaling, image reconstruction and image compression. The author will try to implement Bézier method for image processing including cubic interpolation, least square fitting and bilinear interpolation. The author will also apply the method with quadtree decomposition for image compression.

CHAPTER 2
LITERATURE REVIEW

2.1 Bézier Curve

In the mathematical field of numerical analysis, a Bézier curves is a parametric curve important in computer graphics and related fields. Generalizations of Bézier curves to higher dimensions are called Bézier surfaces. ‘Paths” as they are commonly referred to an image manipulation programs are combinations of linked Bézier curves. Bézier curves are also used in animation as a tool to control motion [4]. By simply changing the control points, the Bézier curve will change. The examples are attached in appendices (refer Appendix A).

2.1.1 Linear Bézier Curves

A linear Bézier curve is a line segment joining two control points $\mathbf{b}_0(p_0, q_0)$ and $\mathbf{b}_1(p_1, q_1)$, parameterized by

$$\big(x(t), y(t)\big) = (1-t)(p_0, q_0) + t(p_1, q_{1)}, \quad for\ t \in [0,1] \tag{2.1}$$

so that $x(t) = (1-t)p_0 + tp_1$, and $y(t) = (1-t)q_0 + tq_1$. Letting $\mathbf{B}(t) = (x(t), y(t))$, the curve can be written in the vector form

$$\mathbf{B}(t) = (1-t)\mathbf{b}_0 + t\mathbf{b}_1 \tag{2.2}$$

The curve is defined on the interval [0, 1], so the starting point of the curve is $\mathbf{B}(0) = \mathbf{b}_0$ and the finishing point is $\mathbf{B}(1) = \mathbf{b}_1$, that is, the Bézier curve interpolates the first and last control points [3].

2.1.2 Quadratic Bézier Curves

Suppose three control points $\mathbf{b}_0(p_0, q_0)$, $\mathbf{b}_1(p_1, q_1)$ and $\mathbf{b}_2(p_2, q_2)$ are specified. Then the quadratic Bézier curve is defined to be

$$\mathbf{B}(t) = (1-t)^2(p_0, q_0) + 2(1-t)t(p_1, q_1) + t^2(p_2, q_2) \quad \text{for } t \in [0,1] \quad (2.3)$$

The starting points of the curve is $\mathbf{B}(0) = \mathbf{b}_0$ and the finishing point is $\mathbf{B}(1) = \mathbf{b}_2$. The curve can be expressed in the parametric for $(x(t), y(t))$ where

$$x(t) = (1-t)^2 p_0 + 2(1-t)tp_1 + t^2 p_2, \quad (2.4)$$

$$y(t) = (1-t)^2 q_0 + 2(1-t)tq_1 + t^2 q_2, \quad (2.5)$$

The triangle $\mathbf{b}_0\mathbf{b}_1\mathbf{b}_2$ obtained by joining the control points with line segments, in their prescribed order, is called the control polygon [3].

2.1.3 Cubic Bézier Curves

Suppose four control points $\mathbf{b}_0$, $\mathbf{b}_1$, $\mathbf{b}_2$, and $\mathbf{b}_3$ are specified, then the cubic Bézier curve is defined to be

$$\mathbf{B}(t) = (1-t)^3\mathbf{b}_0 + 3(1-t)^2t\mathbf{b}_1 + 3(1-t)t^2\mathbf{b}_2 + t^3\mathbf{b}_3, \quad t \in [0,1] \quad (2.6)$$

As in the quadratic case, the polygon obtained by joining the control points in the specified order is called the control polygon.

Cubic Bézier curves provide a greater range of shapes than quadratic Bézier curves, since they can exhibit loops, sharp corners and inflections [3].

2.1.4 Deriving the Curve

The first step to understand Bézier curve is knows how the curves are geometrically formed. The construction of a Bézier curve begins with picking three or more points, called control points. For example, we use four control points, P_0, P_1, P_2, and P_3 (refer Figure 1) to create Cubic Bézier curve [5].

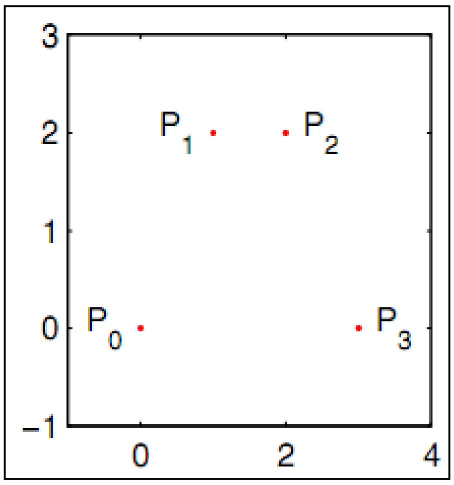

Figure 1: Four Control Points

The next step is to find the points on the line segments P_0P_1, P_1P_2, and P_2P_3. This is best done when thinking about the points as vectors. The first point is P_{1a} and it lies t% of the way from point P_0 to P_1 (refer Figure 2).

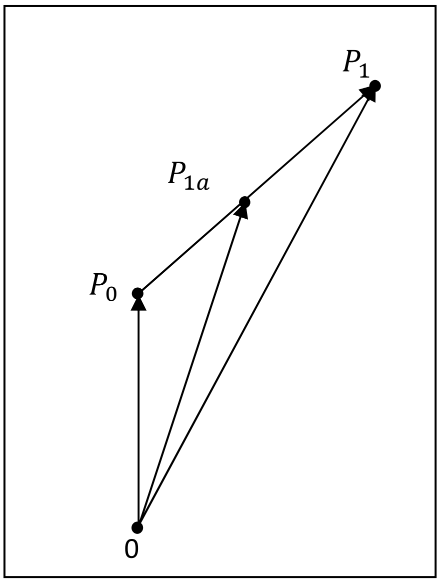

Figure 2: Formation of Individual Points

This point is derived by:

$$\begin{aligned} P_{1a} &= P_0 + t(P_1 - P_0) \\ &= P_0 + tP_1 - tP_0 \\ &= (1-t)P_0 + tP_1 \end{aligned} \tag{2.7}$$

Repeating the process five more times as below;

$$\begin{aligned} P_{1a}(t) &= (1-t)P_0 + tP_1 \\ P_{2a}(t) &= (1-t)P_1 + tP_2 \\ P_{3a}(t) &= (1-t)P_2 + tP_3 \\ P_{1b}(t) &= (1-t)P_{1a}(t) + tP_{2a}(t) \\ P_{2b}(t) &= (1-t)P_{2a}(t) + tP_{3a}(t) \end{aligned} \tag{2.8}$$

we get the other points that form Figure 3.

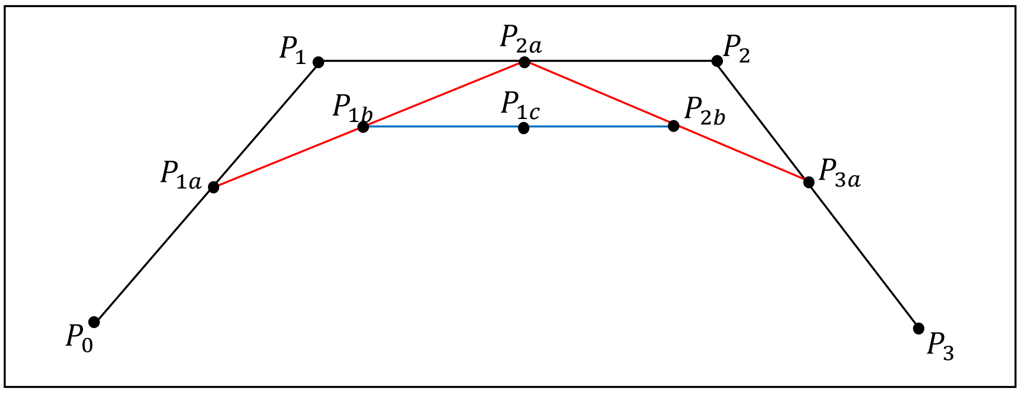

Figure 3: Formation of the First Points P_{1c} on the Curve

Only P_{1c} is on the actual curve. To find other points on the curve we repeat the process with a different t value, ranging from 0 to 1.

$$P_{1c}(t) = (1-t)P_{1b}(t) + tP_{2b}(t) \tag{2.9}$$

Using equation (2.9) we can form a specific polynomial called the Bernstein Polynomial (refer equation (2.11)) with the variable t. The Bernstein Polynomial can be derived by setting $P(t) = P_{1c}(t)$.

$$\begin{aligned} P(t) = P_{1c}(t) &= (1-t)P_{1b}(t) + tP_{2b}(t) \\ &= (1-t)[(1-t)P_{1a}(t) + tP_{2a}(t)] + t[(1-t)P_{2a}(t) + tP_{3a}(t)] \\ &= (1-t)\Big[(1-t)\big[(1-t)P_0 + tP_1 + t\big((1-t)P_1 + tP_2\big)\big]\Big] \\ &\quad +t\Big[(1-t)\big[(1-t)P_1 + tP_2 + t\big((1-t)P_2 + tP_3\big)\big]\Big] \\ &= (1-t)[(1-t)^2P_0 + t(1-t)P_1 + t(1-t)P_1 + t^2P_2] \\ &\quad +t[(1-t)^2P_1 + t(1-t)P_2 + t(1-t)P_2 + t^2P_3 \\ &= (1-t)^3P_0 + t(1-t)^2P_1 + t(1-t)^2P_1 + t^2(1-t)P_2 \end{aligned} \tag{2.10}$$

$$P(t) = (1-t)^3P_0 + 3t(1-t)^2P_1 + 3t^2(1-t)P_2 + t^3P_3 \tag{2.11}$$

Because now we have a polynomial that can give us the points on the curve we could consider ourselves lucky; however, since there are points P_0, P_1, P_2, P_3 in the polynomial the desired curve is a little hard to generate. To find other points on the curve without having to recalculate P_{1c} every time we put the Bernstein Polynomial in matrix form. This is done by looking at the polynomial as a linear combination of the four control points and their coefficients. We can then break the coefficient vector into a vector times a matrix.

$$P(t) = [(1-t)^3 \quad 3t(1-t)^2 \quad 3t^2(1-t) \quad t^3] \begin{bmatrix} P_0 \\ P_1 \\ P^2 \\ P^3 \end{bmatrix} \tag{2.12}$$

To break the coefficients into a vector and a matrix, the coefficients have to be expanded.

$$P(t) = [1 - 3t + 3t^2 \quad 3t - 6t^2 + 3t^3 \quad 3t^2 - 3t^3 \quad t^3] \begin{bmatrix} P_0 \\ P_1 \\ P^2 \\ P^3 \end{bmatrix} \tag{2.13}$$

Now the vector can be expanded to include a matrix which will isolate the t values and allow us to quickly calculate multiple points on our Bézier curve.

$$P(t) = \begin{bmatrix} 1 & t & t^2 & t^3 \end{bmatrix} \begin{bmatrix} 1 & 0 & 0 & 0 \\ -3 & 3 & 0 & 0 \\ 3 & -6 & 3 & 0 \\ -1 & 3 & -3 & 1 \end{bmatrix} \begin{bmatrix} P_0 \\ P_1 \\ P_2 \\ P_3 \end{bmatrix} \qquad (2.14)$$

With the matrix representation of the Bernstein Polynomial, multiple values of t can be quickly entered and calculated using a computer to generate points on the Bézier curve.

2.1.5 Subdivisions and Generating New Control Points

Sometimes it is useful to adjust part of a curve and not the whole thing. The easiest way to do this is to subdivide the curve into parts and find new control points for each of the subdivisions. To do this, take the matrix form of the Bernstein Polynomial equation (2.14), then decide which part of the curve needs to be changed. For this example, the curve will be divided into two equal parts. In order to do this, the Bernstein Polynomial needs to be reparameterized, which is easily done by adjusting t [5].

$$P(t) = R\left(\frac{t}{2}\right) + R\left(\frac{1}{2} + \frac{t}{2}\right) \qquad (2.15)$$

Taking the first part of the reparameterization of $P(t)$, $R(\frac{t}{2})$, which is the first half of $P(t)$, and writing in matrix form, the control points of the matrix can be determined. Reparameterizing $P(t)$ we get the matrix equation:

$$\begin{bmatrix} 1 & t/2 & (\frac{t}{2})^2 & (\frac{t}{2})^3 \end{bmatrix} \begin{bmatrix} 1 & 0 & 0 & 0 \\ -3 & 3 & 0 & 0 \\ 3 & -6 & 3 & 0 \\ -1 & 3 & -3 & 1 \end{bmatrix} \begin{bmatrix} P_0 \\ P_1 \\ P_2 \\ P_3 \end{bmatrix}$$

Next we expand the vector T_t into a vector matrix form labeling the matrix $N_{(\frac{1}{2t})}$.

We get:

$$\begin{bmatrix}1 & t/2 & (\frac{t}{2})^2 & (\frac{t}{2})^3\end{bmatrix} = [1 \quad t \quad t^2 \quad t^3] \begin{bmatrix}1 & 0 & 0 & 0\\ 0 & 1/2 & 0 & 0\\ 0 & 0 & 1/4 & 0\\ 0 & 0 & 0 & 1/8\end{bmatrix}$$

Putting this new matrix into our equation $P(t)$ we get $R(t)$ which is exactly half of $P(t)$ but this does not find the new control points. To find these points we have to multiply the P_p vector of the points by a relationship of N. In other words we need to put the matrix equation into a form resembling $R(t) = T_t * M * N_{(0,1,2)} * P_p$. We know $R(t) = T_t * N_{(\frac{t}{2})} * M * P_p$, which leaves us with the matrix equation $N_{(\frac{t}{2})} * M = M * N_{(0,1/2)}$.

$$\begin{bmatrix}1 & 0 & 0 & 0\\ 0 & 1/2 & 0 & 0\\ 0 & 0 & 1/4 & 0\\ 0 & 0 & 0 & 1/8\end{bmatrix}\begin{bmatrix}1 & 0 & 0 & 0\\ -3 & 3 & 0 & 0\\ 3 & -6 & 3 & 0\\ -1 & 3 & -3 & 1\end{bmatrix} = \begin{bmatrix}1 & 0 & 0 & 0\\ -3 & 3 & 0 & 0\\ 3 & -6 & 3 & 0\\ -1 & 3 & -3 & 1\end{bmatrix}\begin{bmatrix}? & ? & ? & ?\\ ? & ? & ? & ?\\ ? & ? & ? & ?\\ ? & ? & ? & ?\end{bmatrix}$$

Multiplying both sides by M^{-1}, we get our $N_{(0,1/2)}$.

$$\begin{bmatrix}1 & 0 & 0 & 0\\ 1 & 1/3 & 0 & 0\\ 1 & 2/3 & 1/3 & 0\\ 1 & 1 & 1 & 1\end{bmatrix}\begin{bmatrix}1 & 0 & 0 & 0\\ 0 & 1/2 & 0 & 0\\ 0 & 0 & 1/4 & 0\\ 0 & 0 & 0 & 1/8\end{bmatrix}\begin{bmatrix}1 & 0 & 0 & 0\\ -3 & 3 & 0 & 0\\ 3 & -6 & 3 & 0\\ -1 & 3 & -3 & 1\end{bmatrix} = \begin{bmatrix}? & ? & ? & ?\\ ? & ? & ? & ?\\ ? & ? & ? & ?\\ ? & ? & ? & ?\end{bmatrix}$$

Now we have calculated the matrix $N_{(0,1/2)}$.

$$N_{(0,1/2)} = \begin{bmatrix}1 & 0 & 0 & 0\\ 1/2 & 1/2 & 0 & 0\\ 1/4 & 1/2 & 1/4 & 0\\ 1/8 & 3/8 & 3/8 & 1/8\end{bmatrix} \tag{2.16}$$

Using the $N_{(0,1/2)}$ we found we can now multiply our control points vector P_p on the left by $N_{(0,1/2)}$ to generate our new points for $R(t)$. This same process can be done for $R(\frac{1}{2}+\frac{t}{2})$ to generate the $N_{(0,1/2)}$ matrix which can be used to find the new control points for the other half of the curve $P(t)$.

$$N_{\left(0,\frac{1}{2}\right)}\begin{bmatrix}P_0\\P_1\\P_2\\P_3\end{bmatrix}=\begin{bmatrix}P_0'\\P_1'\\P_2'\\P_3'\end{bmatrix} \tag{2.17}$$

$$\begin{bmatrix}P_0'\\P_1'\\P_2'\\P_3'\end{bmatrix}=\begin{bmatrix}P_0\\1/2P_1\ +1/2P_0\\1/4P_2\ +1/2P_1+1/4P_0\\1/8P_3\ +3/8P_2+3/8P_1+1/8P_0\end{bmatrix} \tag{2.18}$$

Calculating $N_{(\frac{1}{2}+1/2t)}$, similarly to what we did for $N_{(t/2)}$

$$N_{(\frac{1}{2}+t/2)}=\begin{bmatrix}1&1/2&1/4&1/8\\0&1/2&1/2&3/8\\0&0&1/4&3/8\\0&0&0&1/8\end{bmatrix} \tag{2.19}$$

$$N_{(\frac{1}{2},1)}=\begin{bmatrix}1/8&3/8&3/8&1/8\\0&1/4&1/2&1/4\\0&0&1/2&1/2\\0&0&0&1\end{bmatrix} \tag{2.20}$$

$N_{(\frac{1}{2}+t/2)}$ is similar to $N_{(\frac{1}{2},1)}$ as $N_{(t/2)}$ is similar to $N_{(0,1/2)}$. Once we have one we can easily find the other using the matrix M. This works for any subdivision of the original matrix and allows us to find the new control points for the subdivision. Once the subdivisions are found we can move two of the control points, P_1' or P_2', to change just part of the curve. This tool is highly practical in drafting and allows for more complex changes.

2.1.6 *Properties of Bézier Curves* [3]

- ***Endpoint Interpolation Property***: $\mathbf{B}(0) = \mathbf{b}_0$ and $\mathbf{B}(1) = \mathbf{b}_n$

- ***Endpoint Tangent Property***:

$$\mathbf{B}'(0) = n(\mathbf{b}_1 - \mathbf{b}_0) \quad \text{and} \quad \mathbf{B}'(1) = n(\mathbf{b}_n - \mathbf{b}_{n-1})$$

- ***Convex Hull Property (CHP)***: For all $t \in [0,1]$, $\mathbf{B}(t) \in \mathrm{CH}\{\mathbf{b}_0, \ldots.., \mathbf{b}_n\}$ Thus every point of a Bézier curve lies inside the convex hull of its defining control points. The convex hull of the control points is often referred to as the convex hull of the Bézier curve.

- ***Invariance under Affine Transformations***: Let $\mathbf{T}$ be an (affine) transformation (for example rotation, reflection, translation or scaling). Then

$$\mathbf{T}\left(\sum_{i=0}^{n} \mathbf{b}_i \, B_{i,n}(t)\right) = \sum_{i=0}^{n} \mathbf{T}\,(\mathbf{b}_i) B_{i,n}(t) \qquad (2.21)$$

- ***Variation Diminishing Property (VDP)***: For a planar Bézier curve $\mathbf{B}(t)$, the VDP states that the number of intersections of a given line with $\mathbf{B}(t)$ is less than or equal to the number of intersections of that line with the control polygon.

2.2 Bézier Surface

A species of mathematical spline used in computer graphics, computer-aided design and finite element modeling. Bézier surface is defined by a set of control points. Similar to interpolation in many respects, a key difference is that the surface does not, in general, pass through the central control points; rather, it is "stretched" toward them as though each were an attractive force. They are visually intuitive, and for many applications [6].

A Bézier surface of order (n, m) is defined by a set of $(n+1)(m+1)$ control points $\mathbf{k}_{i,j}$. It maps the unit square into a smooth continuous surface embedded within a space of the same dimensionality as $\{\mathbf{k}_{i,j}\}$. For example, if **k** are all points in a four-dimensional space, then the surface will be within a four-dimensional space [5]. A two-dimensional Bézier surface can be defined as a parametric surface where the position of a point **p** as a function of the parametric coordinates u, v is given by:

$$\mathbf{p}(u, v) = \sum_{i=0}^{n} \sum_{j=0}^{m} B_i^n(u) B_j^m(v) \mathbf{k}_{i,j} \tag{2.22}$$

evaluated over the unit square where

$$B_i^n(u) = \binom{n}{i} u^i (1-u)^{n-i} \tag{2.23}$$

is a Bernstein polynomial and $\binom{n}{i} = \frac{n!}{i!(n-i)!}$ is the binomial coefficient.

2.2.1 Bilinear Bézier Surfaces

The simple method to define bilinear Bézier surface is (linear curve)(linear curve). So we can define bilinear Bézier surface by

$$\begin{aligned} S(u,v) = {} & (1-u)(1-v)\mathbf{b}_0\mathbf{b}_0 + (1-u)v\mathbf{b}_1\mathbf{b}_0 + (1-v)u\mathbf{b}_0\mathbf{b}_1 \\ & +uv\mathbf{b}_1\mathbf{b}_1 \end{aligned} \tag{2.24}$$

2.2.2 Biquadratic Bézier Surfaces

The simple method to define biquadratic Bézier surface is (quadratic curve)(quadratic curve). So we can define biquadratic Bézier surface by

$$\begin{aligned} S(u,v) = {} & (1-u)^2(1-v)^2\mathbf{b}_0\mathbf{b}_0 + (1-u)^2 2(1-v)v\mathbf{b}_0\mathbf{b}_1 \\ & +(1-u)^2v^2\mathbf{b}_0\mathbf{b}_2 + 2(1-u)u(1-v)^2\mathbf{b}_1\mathbf{b}_0 \\ & +2(1-u)u2(1-v)v\mathbf{b}_1\mathbf{b}_1 + 2(1-u)uv^2\mathbf{b}_1\mathbf{b}_2 \\ & +u^2(1-v)^2\mathbf{b}_2\mathbf{b}_0 + u^2 2(1-v)v\mathbf{b}_2\mathbf{b}_1 + u^2v^2\mathbf{b}_2\mathbf{b}_2 \end{aligned} \tag{2.25}$$

2.2.3 Bicubic Bézier Surfaces

The simple method to define bicubic Bézier surface is (cubic curve)(cubic curve). So we can define bicubic Bézier surface by

$$\begin{aligned} S(u,v) = {} & \mathbf{b}_0\mathbf{b}_0(1-u)^3(1-v)^3 + 3\mathbf{b}_0\mathbf{b}_1u(1-u)^2(1-v)^3 \\ & +3\mathbf{b}_0\mathbf{b}_2u^2(1-u)(1-v)^3 + \mathbf{b}_0\mathbf{b}_3u^3(1-v)^3 \\ & +3\mathbf{b}_1\mathbf{b}_0(1-u)^3v(1-v)^2 + 9\mathbf{b}_1\mathbf{b}_1u(1-u)^2v(1-v)^2 \\ & +9\mathbf{b}_1\mathbf{b}_2u^2(1-u)v(1-v)^2 + 3\mathbf{b}_1\mathbf{b}_3u^3v(1-v)^2 \\ & +3\mathbf{b}_2\mathbf{b}_0(1-u)^3v^2(1-v) + 9\mathbf{b}_2\mathbf{b}_1u(1-u)^2v^2(1-v) \\ & +9\mathbf{b}_2\mathbf{b}_2u^2(1-u)v^2(1-v) + 3\mathbf{b}_2\mathbf{b}_3u^3v^2(1-v) \\ & +\mathbf{b}_3\mathbf{b}_0(1-u)^3v^3 + 3\mathbf{b}_3\mathbf{b}_1u(1-u)^2v^3 + 3\mathbf{b}_3\mathbf{b}_2u^2(1-u)v^3 \\ & +\mathbf{b}_3\mathbf{b}_3u^3v^3 \end{aligned} \tag{2.26}$$

2.2.4 *Properties of Bézier Surfaces* [7]

- ***Endpoint interpolation***: Analogous to the curve case, the patch passes through the four corner control points, that is

$$\mathbf{x}(0,0) = \mathbf{b}_{0,0} \quad \mathbf{x}(1,0) = \mathbf{b}_{m,0}$$
$$\mathbf{x}(0,1) = \mathbf{b}_{0,n} \quad \mathbf{x}(1,1) = \mathbf{b}_{m,n}$$

- ***Symmetry***: We could re-index the control net so that any of the corners corresponds to $\mathbf{b}_{0,0}$ and evaluation would result in a patch with the same shape as the original one.

- ***Affine invariance***: Apply an affine map to the control net, and then evaluate the patch. This surface will be identical to the surface created by applying the same affine map to the original patch.

- ***Convex hull property***: For $(u, v) \in [0,1] \times [0,1]$, the patch $\mathbf{x}(u, v)$ is in the convex hull of the control net.

- ***Bilinear precision***: A degree $m \times n$ patch with boundary control points which are evenly spaced on lines connecting the corner control points, and the interior control points are evenly-spaced on lines connecting boundary control points on adjacent edges. This patch is identical to the bilinear interpolant to the four corner control points.

- ***Tensor product***: Bézier patches are in the class of tensor product surfaces. This property allows Bézier patches to be dealt with in terms of isoparametric curves, which in turn simplifies evaluation and other operations.

2.3 Bernstein Polynomial

In the mathematical field of numerical analysis, a Bernstein polynomial is a polynomial in the Bernstein form that is linear combination of Bernstein basis polynomials. A numerically stable way to evaluate polynomials in Bernstein form is de Casteljau's algorithm. With the advent of computer graphics, Bernstein polynomials restricted to the interval $x \in [0, 1]$, became important in the form of Bézier curves [8].

The $n + 1$ Bernstein basis polynomials of degree n are defined as

$$B_{i,n}(t) = \binom{n}{i} t^i (1-t)^{n-i}, \quad i = 0, \ldots., n \tag{2.27}$$

A linear combination of Bernstein basis polynomials is called a Bernstein polynomial

$$B(t) = \sum_{i=0}^{n} b_i B_{i,n}(t) \tag{2.28}$$

2.3.1 Properties of Bernstein Polynomials [3]

- ***Partition of Unity***: The Bernstein polynomials of degree *n* sum to one

$$\sum_{i=0}^{n} B_{i,n}(t) = 1, \;\; t \in [0,1) \tag{2.29}$$

- ***Positivity***: The Bernstein polynomials are non-negative on the interval [0, 1]

$$B_{i,n}(t) \geq 0, \;\; t \in [0,1] \tag{2.30}$$

- ***Symmetry***:

$$B_{n-i,n}(t) = B_{i,n}(1-t), \quad \text{for} \quad i = 0, \dots, n \tag{2.31}$$

  So, the graph of $B_{n-i,n}(t)$ is a reflection of the graph of $B_{i,n}(1-t)$.

- ***Recursion***: The Bernstein polynomials of degree n can be expressed in terms of the polynomials of degree $n-1$

$$B_{i,n}(t) = (1-t)B_{i,n-1}(t) + tB_{i-1,n-1}(t), \quad \text{for } i = 0, \dots, n \tag{2.32}$$

  where $B_{-1,n-1}(t) = 0$ and $B_{n,n-1}(t) = 0$

The partition of unity and positivity properties gives rise to two important properties of Bézier curves namely invariance under transformations and the convex hull property. As a consequence of the symmetry property, a symmetrical control polygon gives rise to a symmetrical curve. The recursion property gives rise to the de Casteljau algorithm.

2.4 de Casteljau Algorithm

In the mathematical subfield of numerical analysis, de Casteljau algorithm is a recursive method to evaluate polynomials in Bernstein form or Bézier curves. This algorithm can also be used to split a single Bézier curve into two Bézier curves at an arbitrary parameter value. Although the algorithm is slower when compared with the direct approach it is numerically stable [9].

The de Casteljau algorithm provides a method for evaluating the point on a Bézier curve corresponding to the parameter value $t \in [0,1]$. For the case of a cubic Bézier curve with control points $\mathbf{b}_0$, $\mathbf{b}_1$, $\mathbf{b}_2$, and $\mathbf{b}_3$, and for a specified parameter value $t \in [0,1]$, the de Casteljau algorithm is expressed by the recursive formula

$$\begin{cases} \mathbf{b}_i^0 = \mathbf{b}_i \\ \mathbf{b}_i^j = (1-t)\mathbf{b}_i^{j-1} + t\mathbf{b}_{i+1}^{j-1}, \end{cases} \tag{2.33}$$

for $j = 1, 2, 3$ and $i = 0, \dots, 3 - j$. The formula generates a triangular set of values as below for which $\mathbf{b}_0^3 = \mathbf{B}(t)$ for the specified value of t [3].

$$\begin{array}{llll} \mathbf{b}_0^0 & \mathbf{b}_1^0 & \mathbf{b}_2^0 & \mathbf{b}_3^0 \\ \mathbf{b}_0^1 & \mathbf{b}_1^1 & \mathbf{b}_2^1 & \\ \mathbf{b}_0^2 & \mathbf{b}_1^2 & & \\ \mathbf{b}_0^3 & & & \end{array}$$

2.5 Spline

In mathematics, a spline is a special function defined piecewise by polynomials. In the computer science subfields of computer-aided design and computer graphics, the term ‘spline’ more frequently refers to a piecewise polynomial (parametric) curve. Splines are popular curves in these subfields because of the simplicity of their construction, their ease and accuracy of evaluation, and their capacity to approximate complex shapes through curve fitting and interactive curve design [10].

2.6 Bernstein – Bézier – Spline

In fact, Bernstein polynomial can be thought of as the gateway to splines, namely the Bézier spline. Bézier polynomial can be made to act in either as a spline or non-spline. When it acts as a spline, it does piecewise approximation of a data set with some smoothness conditions satisfying at the break points, but when it acts as a non-spline to approximate, it does not take into consideration the smoothness conditions to satisfy at the break points. Bézier curves is influenced by Bernstein polynomial. As Bézier curves and surfaces are driven by Bernstein basis, they can also be thought of, respectively, the Bernstein polynomial pieces of curves and surfaces.

The basic philosophy behind the Bernstein polynomial approximation is that this polynomial is very convenient to free-form drawing. In fact, some of the properties of this Bernstein polynomial are so attractive that no sooner than the technique was published by Bézier, it became widely popular in many industries. In order to design the body of an automobile, Bézier developed a spline model that became the first widely accepted spline model in computer graphics and computer-aided design, due to its flexibility and ease over the then-used drawing and design techniques. This model, therefore, helps to design and draw smooth curves and surfaces of different shapes and sizes, corresponding to different arbitrary objects, based on a set of control points.

Bézier spline model, can also be used to approximate data points originated from different functions. Notice that Bézier spline-based drawing technique starts from the zeroth order Bernstein approximation (which is exactly the line drawing between control points) of the data points and goes to some higher order (quadratic or cubic) approximation, until it mimics the shape of the object. The Bézier splines are effective, efficient, and easy to implement, and have a strong and elegent mathematical background as well. In computer graphics, their significant role is well documented. Unfortunately it is not the case in image processing and machine vision [2].

2.7 Image Processing

Image processing is any form of signal processing for which the input is an image or frames of video, the output of image processing can be either an image or a set of characteristics or parameters related to the image. Most image-processing techniques involve treating the image as a two-dimensional signal and applying standard signal-processing techniques to it. The typical operations involved in image processing were denoising, compressing, reduction, rotation, and color corrections [11].

2.8 Image Compression

Image compression is minimizing the size in bytes of a graphics file without degrading the quality of the image to an unacceptable level. The reduction in file size allows more images to be stored in a given amount of disk or memory space. It also reduces the time required for images to be sent over the internet or downloaded from web pages.

There are several different ways in which image files can be compressed. For internet use, the two most common compressed graphic image formats are the JPEG format and the GIF format. The JPEG method is more often used for photographs, while the GIF method is commonly used for line art and other images in which geometric shapes are relatively simple.

Other techniques for image compression include the use of fractal and wavelets. These methods have not gained widespread acceptance for use on the internet as of this writing. However, both methods offer promise because they offer higher compressions ratio than the JPEG or GIF methods for some types of images. Another new method that may in time replace the GIF format is the PNG format.

A text file or program can be compressed without the introduction of errors, but only up to a certain extent. This is called lossless compression. Beyond this point, errors are introduced. In text and program files, it is crucial that compression be lossless because a single error can seriously damage the meaning of a text file, or cause a program not to run. In image compression, a small loss in quality is usually not noticeable. There is no ‘critical point’ up to which compression works perfectly, but beyond which it becomes impossible. When there is some tolerance for loss, the compression factor can be greater than it can where there is no loss tolerance. For this reason, graphic images can be compressed more than text files or programs [12].

2.9 Cubic Interpolation

Suppose we are given four points p_0, p_1, p_2, p_3 and we wish to pass a curve through them, just like the situation shown in Figure 4. There, the points are 2D, but they might as well be 3D. This is called interpolation [7].

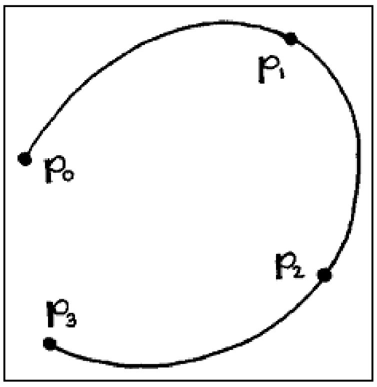

Figure 4: Cubic Bézier Curve Through Four Given Points

Every point on a Bézier curve has a parameter value; in order to solve our problem, we have to assign a parameter value t_i to every p_i. A natural choice is to associate each p_i with a parameter value $t_i = \frac{i}{3}$. Now, our interpolation problem becomes:

Given four point / parameter pairs (p_i, t_i), find a cubic Bézier curve $x(t)$ such that:

$$x(t_i) = p_i; \quad i = 0,1,2,3. \tag{2.34}$$

This simply states that we want the Bézier curve to pass through the data points at the right parameter values. The desired Bézier curve will be of the form

$$x(t) = B_0^3(t)b_o + B_1^3(t)b_1 + B_2^3(t)b_2 + B_3^3(t)b_3 \tag{2.35}$$

Writing out all interpolation conditions (2.34) yields

$$\begin{aligned}
p_0 &= B_0^3(t_0)b_o + B_1^3(t_0)b_1 + B_2^3(t_0)b_2 + B_3^3(t_0)b_3 \\
p_1 &= B_0^3(t_1)b_o + B_1^3(t_1)b_1 + B_2^3(t_1)b_2 + B_3^3(t_1)b_3 \\
p_2 &= B_0^3(t_2)b_o + B_1^3(t_2)b_1 + B_2^3(t_2)b_2 + B_3^3(t_2)b_3 \\
p_3 &= B_0^3(t_3)b_o + B_1^3(t_3)b_1 + B_2^3(t_3)b_2 + B_3^3(t_3)b_3
\end{aligned}$$

These are four equations in the four unknowns $b_0, \dots, b_3$. In order to find a solution, it helps to write them in matrix form:

$$\begin{bmatrix} p_0 \\ p_1 \\ p_2 \\ p_3 \end{bmatrix} = \begin{bmatrix} B_0^3(t_0) & B_1^3(t_0) & B_2^3(t_0) & B_3^3(t_0) \\ B_0^3(t_1) & B_1^3(t_1) & B_2^3(t_1) & B_3^3(t_1) \\ B_0^3(t_2) & B_1^3(t_2) & B_2^3(t_2) & B_3^3(t_2) \\ B_0^3(t_3) & B_1^3(t_3) & B_2^3(t_3) & B_3^3(t_3) \end{bmatrix} \begin{bmatrix} b_o \\ b_1 \\ b_2 \\ b_3 \end{bmatrix} \tag{2.36}$$

We further abbreviate this as

$$P = MB \tag{2.37}$$

The solution is now simply

$$B = M^{-1}P \tag{2.38}$$

2.10 Image Rescaling Using Bilinear Interpolation

In computer graphics, image scaling is the process of resizing a digital image. Scaling is a non-trivial process that involves a trade-off between efficiency, smoothness and sharpness. As the size of an image is increased, so the pixels which comprise the image become increasingly visible, making the image appears ‘soft’. Conversely, reducing an image will tend to enhance its smoothness and apparent sharpness [13].

In mathematics, bilinear interpolation is an extension of linear interpolation for interpolating function of two variables for example x and y on a regular grid. The key idea is to perform linear interpolation first in one direction, and then again in the other direction. Although each step is linear in the sampled values and in the position, the interpolation as a whole is not linear but rather quadratic in the sample location [14].

When an image needs to be scaled up, each pixel of the original image needs to be moved in a certain direction based on the scale constant. However, when scaling up an image by a non-integral scale factor, there are pixels (holes) that are not assigned appropriate pixel values. In this case, those holes should be assigned appropriate RGB or grayscale values so that the output image does not have non-valued pixels. Based on [15], the examples of image rescaling using bilinear interpolation performed by using MATLAB are attached in the appendices (refer Appendix B).

2.11 Cubic Bézier Curve Least Square Fitting

According to [16], Bézier curve is a parametric curve. A Bézier curve of degree m can be generalized as follows:

$$q(t_i) = \sum_{k=0}^{m} \binom{m}{k} P_k (1-t_i)^{m-k} {t_i}^{k}, \quad 0 \le t_i \le 1, \tag{2.39}$$

where $q(t_i)$ is an interpolated point at parameter value t_i, m is degree of Bézier curve and P_k is k^{th} control point. To generate n points (n is count of interpolating points) between first and last control points inclusive, the parameter t_i is uniformly divided into $n-1$ intervals between 0 and 1 inclusive. Equations of cubic Bézier curves can be derived from Eq. (2.39) as follows:

$$q(t_i) = (1-t_i)^3 P_0 + 3t_i(1-t_i)^2 P_1 + 3{t_i}^2(1-t_i)P_2 + {t_i}^3 P_3 \qquad (2.40)$$

Bézier curve passes through its first and last control points which are P_0 and P_3. The middle control points, P_1 and P_2 determine the shape of curve.

2.11.1 Least Square Bézier fitting

For data to be fit by cubic Bézier, the first and last control points of Bézier curve are first and last point of the input data segment. The input data can be divided into many segments or just one segment by specifying initial set of break point, but the middle control points P_1 and P_2 for cubic Bézier must be determined. We used least square method to find the middle control points. Least square method gives the best value of middle control points that minimize the squared distance between original and fitted data and is well suited for approximating data. If there are n data points and p_i and $q(t_i)$ are values of original and approximated points respectively then we can write the least square equation as follows:

$$S = \sum_{i=1}^{n} [p_i - q(t_i)]^2 \qquad (2.41)$$

Equation above can be written as follows:

$$S = \sum_{i=1}^{n} [p_i - (1-t_i)^3 P_0 + 3t_i(1-t_i)^2 P_1 + 3{t_i}^2(1-t_i)P_2 + {t_i}^3 P_3]^2 \quad (2.42)$$

P_1 and P_2 can be determined by:

$$\frac{\partial S}{\partial P_1} = 0$$
$$\frac{\partial S}{\partial P_2} = 0$$

Solving for P_1 and P_2 gives:

$$P_1 = {(A_2C_1 - A_{12}C_2)}\Big/{(A_1A_2 - A_{12}A_{12})}, \tag{2.43}$$

$$P_2 = {(A_1C_2 - A_{12}C_1)}\Big/{(A_1A_2 - A_{12}A_{12})}, \tag{2.44}$$

where

$$A_1 = 9\sum_{i=1}^{n} {t_i}^2\,(1 - t_i)^4,$$
$$A_2 = 9\sum_{i=1}^{n} {t_i}^4\,(1 - t_i)^2,$$
$$A_{12} = 9\sum_{i=1}^{n} {t_i}^3\,(1 - t_i)^3,$$
$$C_1 = \sum_{i=1}^{n} 3t_i\,(1 - t_i)^2[p_i - (1 - t_i)^3P_0 - {t_i}^3P_3],$$
$$C_2 = \sum_{i=1}^{n} 3{t_i}^2\,(1 - t_i)[p_i - (1 - t_i)^3P_0 - {t_i}^3P_3],$$

After determining the control points, Bézier curves can be fitted to large number of original data points with very few control points using Bézier interpolation.

2.11.2 Fitting strategy

Suppose we have set of points (original data) $O = \{p_1, p_2, \dots, p_n\}$ and we want to approximate it using cubic Bézier. As in input we specify the value of limit of error (maximum allowed square distance between original and fitted data) and provide initial set of breakpoints. At least two breakpoints are required, the first point and the last point of original data. Input data is divided into segments based on initial set of breakpoints. A segment is set of all points between two consecutive breakpoints. We have to fit each segment using cubic Bézier curve. Now the fitting process begins. We generate n points (approximated data) $Q = \{q_1, q_{2,} \dots, q_n\}$ using cubic Bézier interpolation such that cubic Bézier curve passes through breakpoints. Then we measure the error between original and approximated (fitted) data.

When approximated data is not close enough to original data, limit of error bound is violated then an existing segment is split (break) into two segments at a point called new breakpoint. After splitting, number of segments are increased by one (splitted segment is replaced by two new segments). Number of breakpoints are also increased by one (new breakpoint is added in the set of existing breakpoints). The point where the error is maximum between original and approximated data is selected as new breakpoint and this point is added in the set of breakpoints.

After splitting, repeat the same fitting procedure using updated set of segments and breakpoints until error is less than or equal to limit of error. We call this technique as fitting *break and fit* strategy.

2.12 Quadtree and Parametric Line Fitting

Quadtree is a data structure that is widely used for image storage, representation and processing [17, 18]. Quadtree is most often used to partition a 2-D space by recursively subdividing it into four quadrants or blocks until each quadrant contains only pixels of one color or luminance. Recursive subdivision may result a quadrant contains only single pixel. This conventional quadtree decomposition has following drawbacks:

(1) The overhead of representing a single pixel by quadtree is not desirable for image compression. It may take more space to represent a single pixel by quadtree that without using it.

(2) Due to subdividing criteria, even if a single pixel in a quadrant is of different color or luminance then quadtree decomposition would divide that quadrant into four quadrants.

As a consequence of this, there may be three quadrants with same luminance value. In other words, the boundaries between quadrants does not necessary represent quadrant of different luminance. To overcome the first drawback; in our method we imposed a constraint of minimum block size on quadtree decomposition. It means that a quadrant would not be further divided into four quadrants if its size is equal to the predefined minimum block size. The constraint of minimum block size safeguards our method from the overhead of representing very small quadrants (quadrants of size less than 4x4) by a quadtree. The constraint based quadtree decomposition results in two types of quadrants:

(a) Homogeneous quadrants: quadrants that contain only pixels of one color or luminance

(b) Non-homogeneous quadrants: quadrants that contain pixels of more than one color or luminance

We represented only homogeneous quadrants using quadtree. Non-homogeneous quadrants are represented by parametric line [19].

Parametric line is essentially a straight line obtained by linear interpolation between two points (control points). To generate a parametric line that interpolates $k + 1$ points, k line segments are used. Equation of j^{th} segment between points p_j and p_{j+1} can be written as follows:

$$q_j(t) = (1 - t)p_j + tp_{j+1}, \quad t \in [0,1], \quad 1 \le j \le k, \tag{2.45}$$

where $q_j(t)$ is an interpolated point between control points p_j and p_{j+1} at parameter value t. To generate n points between p_j and p_{j+1} inclusive, the parameter t is divided into $n - 1$ intervals between 0 and 1 inclusive such that $q_j(0) = p_j$ and $q_j(1) = p_{j+1}$. In order to represent the non-homogeneous quadrants, we scanned the image data row wise and fitted the parametric line to pixels of non-homogeneous quadrants. Parametric line fitting helps to further reduce the data size in two ways. First, the parametric line fitting helps to represent the pixels of one color/luminance with smaller data set. Second, the parametric line fitting merges the data of a row, belong to more than one non-homogeneous quadrant, as a single data set. This single merged row removes the artificial boundaries between quadrants that have been imposed by quadtree decomposition. It is very likely that at the boundaries of two adjacent non-homogeneous quadrants, pixels have same luminance. By merging quadrants, large number of pixels can be represented by small output data obtained from parametric line fitting. This also solves the second drawback of conventional quadtree representation of image [19].

2.13 Application: A New Method For Video Data Compression By Quadratic Bézier Curve Fitting

The input points are approximated using quadratic Bézier least square fitting. The output data consists of quadratic Bézier control points and difference between original and fitted data. In order to understand how quadratic Bézier curve can be used to fit video data, we need to understand the nature of video data. Digital video data consists of sequence of frames which is images. Each frame consists of rectangular 2-D array of pixels. An important factor in fitting of data via quadratic Bézier curve is finding least number of control points [20].

Fitting process is applied to temporal data of each spatial location (x, y) individually. Let n is the number of frames in a video sequence, let W and H are width and height of a frame respectively. At frame i, where $1 \leq i \leq n$, let p_i as luminance or color value of a spatial location (x, y). We have to approximate the n values of each spatial location by quadratic Bézier curve. As an input to algorithm the user specifies breakpoint interval δ.Luminance or color values of a spatial location after every δ^{th} frames are taken as a breakpoint (control point). The fitting process divides the data into segments based on breakpoints. A segment is a set of all points (luminance or color values) between two adjacent breakpoints. Each segment is fitted (approximated) by a quadratic Bézier curve. The first and the last breakpoints of a segment are taken as end control points, for example P_0 and $P_2$of quadratic Bézier curve, while middle control point, $P_1$is obtained by least square method. Once all the three control points, P_0, P_1 and $P_2$are known, then approximated data of a segment using Bézier curve is obtained using following equation:

$$Q(t_i) = (1 - t_i)^2 P_0 + 2t_i(1 - t_i)P_1 + {t_i}^2 P_2 \tag{2.46}$$

Note that the first and last points of input data and interpolated data are always same, because $Q(t_i = 0) = P_0$ and $Q(t_i = 1) = P_2$. Interpolated points other than first and last points may or may not have the same values as corresponding points of input data. In order to reconstruct the original video data without any loss, first interpolated frames are generated using keyframes of end control points (KFE) and keyframes of middle control points (KFM), then adding the difference between original and quadratic Bézier approximated (interpolated) frames other than keyframes, frame difference (FD) to interpolated frames reproduces the original video frames.

The most important application of the method is data compression. A fundamental approach of prevalent video data compression techniques such as MPEG-1, MPEG-2 and H.263 [21, 22] is to reduce the entropy of data by applying Discrete Cosine Transform. Data with reduced entropy can be encoded with less number of bits. In this method, the overall entropy of KFE, KFM and FD is much less than the entropy of original video data. So, it can be encoded with less number of bits. This less entropy of output data is mainly due to the fact that quadratic Bézier curve approximates the original video data with quite good level of accuracy.

2.14 Application: An Innovative Scheme For Effectual Fingerprint Data Compression Using Bézier Curve Representation

This kind of application utilizes the Bézier curve representations for effective compression of fingerprint image. It is designed in a way to preserve the fine details in the fingerprint image such as ridge endings and bifurcations. It is employed for achieving better compression with some cost to quality. A fingerprint image can have hundreds of ridges each having its own structure. In the proposed scheme, each ridge is visualized as a cubic Bézier curve and it's Bézier control points are determined. The set of four Bézier control points determined, serve as compressed form of an individual ridge. So every fingerprint image with n ridges can be compressed into a file containing 4*n Bézier control points. A desirable property of these curves is that the curve can be translated and rotated by performing these operations on the control points. It is sufficient to store all the four Bézier control points instead of storing the actual Bézier curve (ridge). The original ridge can be reproduced from these stored control points by the properties of Bézier curve. Thus, the proposed scheme for fingerprint compression achieves an effective reduction in the memory space required to store the fingerprint [23].

CHAPTER 3
METHODOLOGY

3.1 Procedure Identification

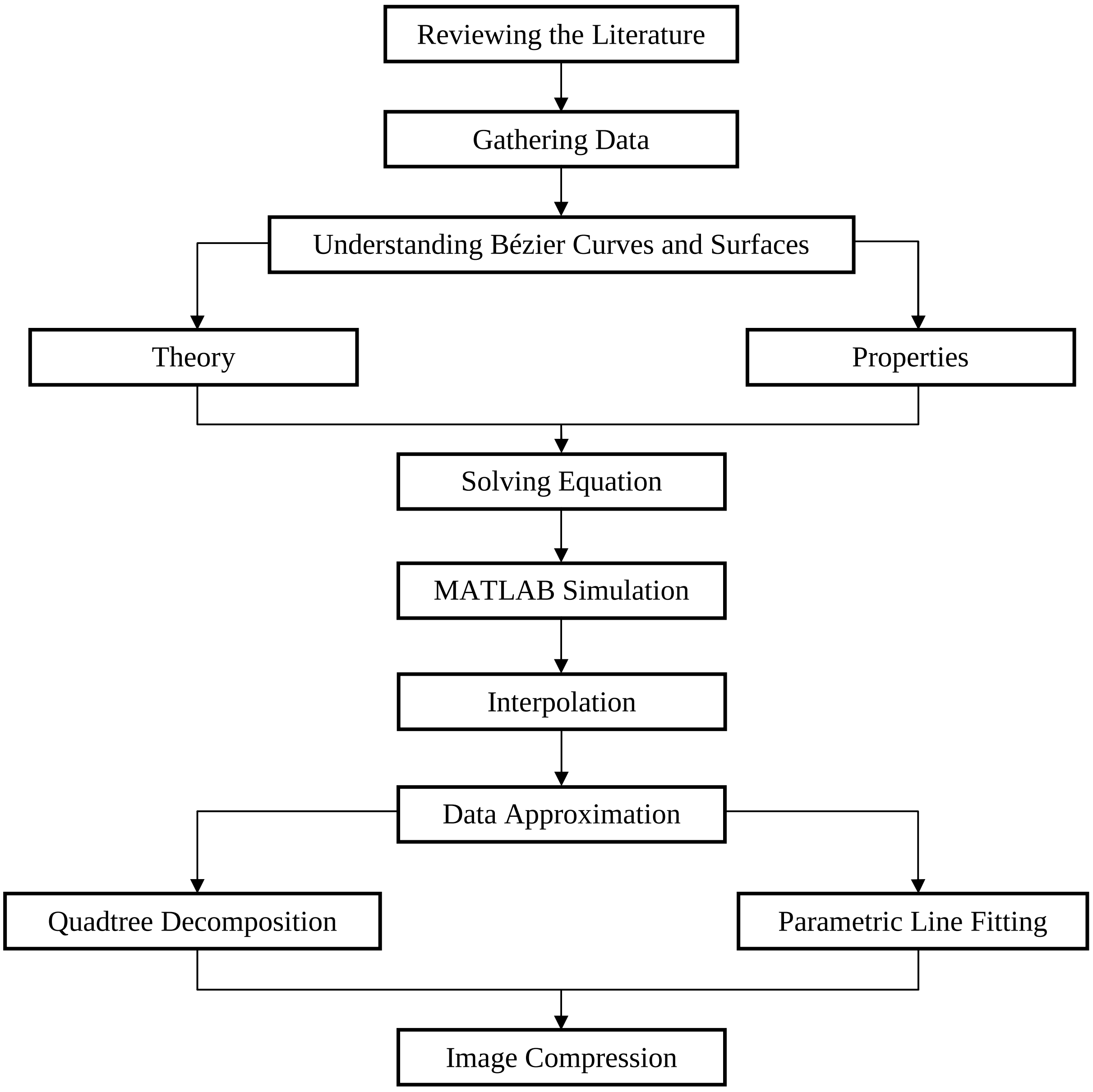

Figure 5: Flowchart of The Project

3.2 Tools used

3.2.1 Software

- MATLAB 7.4.0 (R2007a)
- GPL Ghostscript 8.64
- GSview 4.9

CHAPTER 4
RESULTS AND DISCUSSION

4.1 Linear Bézier Curve

The following figures show the examples of linear Bézier curve. The following figures vary from its control points. The comparison between the equation and the coding are as followed:

$$\text{Equation: } \mathbf{B}(t) = (1-t)\mathbf{b}_0 + t\mathbf{b}_1 \tag{4.1}$$

$$\text{Coding: } px(i) = (1-t)^{*}cx(1) + t^{*}cx(2)$$

So, we can see that the different is $\mathbf{b}_0 = cx(1)$ and $\mathbf{b}_1 = cx(2)$

- ➢ Linear Curve

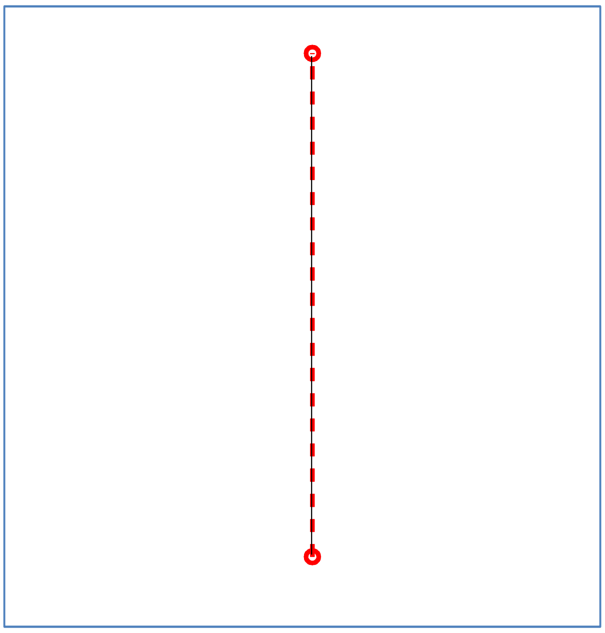

Figure 6: Linear Curve

- Linear Curve

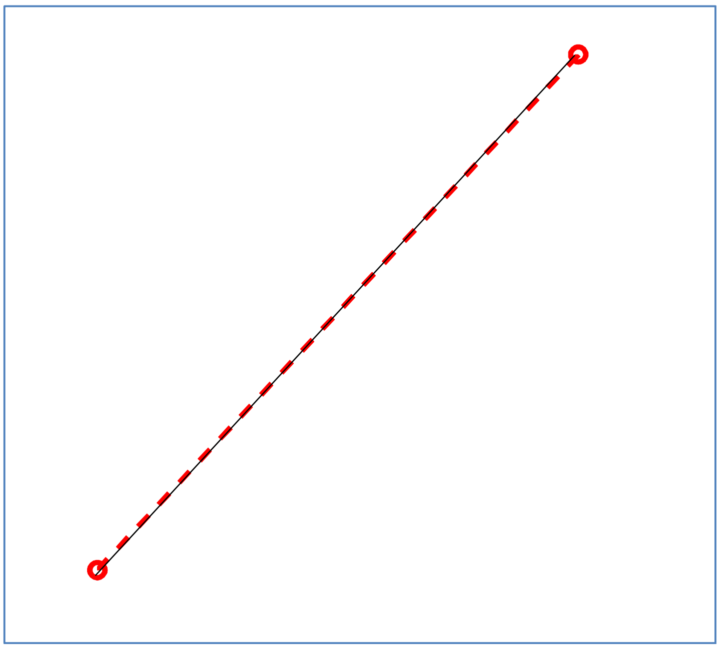

Figure 7: Linear Curve

- Linear Curve

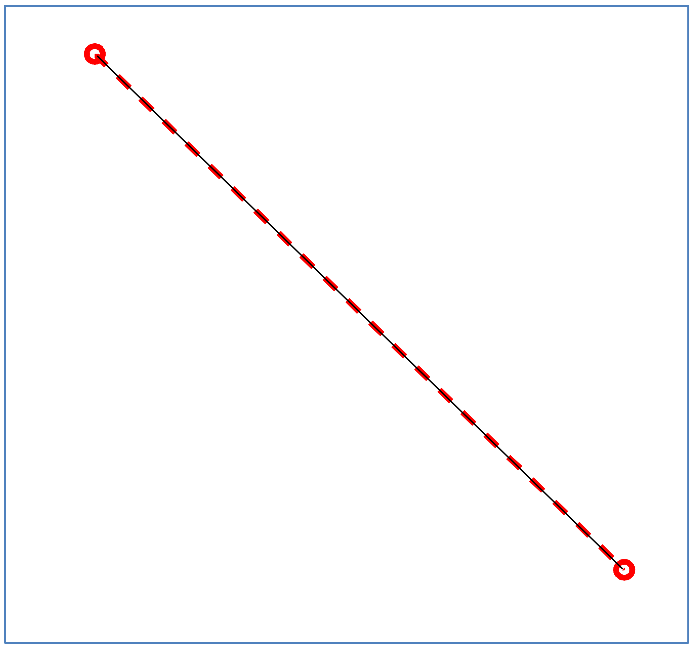

Figure 8: Linear Curve

- Linear Curve

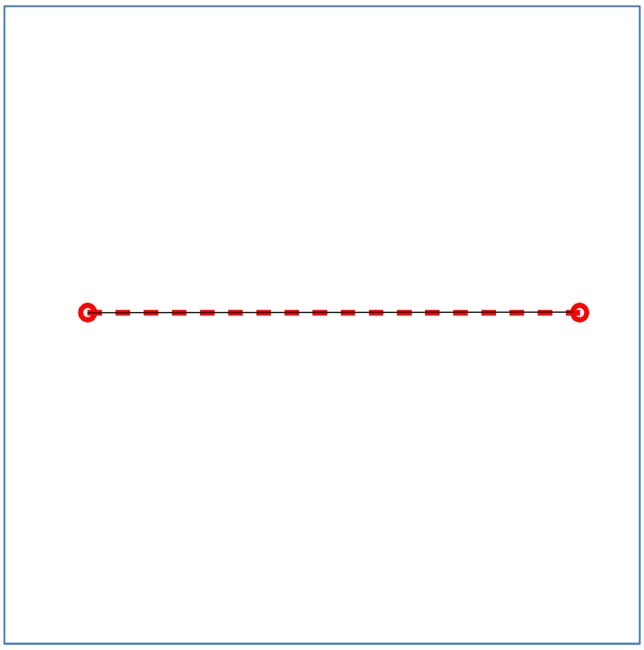

Figure 9: Linear Curve

4.2 Quadratic Bézier Curve

The following figures show the examples of quadratic Bézier curve. The following figures vary from its control points. The comparison between the equation and the coding are as followed:

Equation: $\mathbf{B}(t) = (1-t)^2\mathbf{b}_0 + 2(1-t)t\mathbf{b}_1 + t^2\mathbf{b}_2$ (4.2)

Coding: $px(i)$ =(1-t)^2*cx(1)+2*(1-t)*t*cx(2)+t^2*cx(3)

So, we can see that the different is $\mathbf{b}_0 = cx(1)$, $\mathbf{b}_1 = cx(2)$, and $\mathbf{b}_2 = cx(3)$

- Quadratic Curve

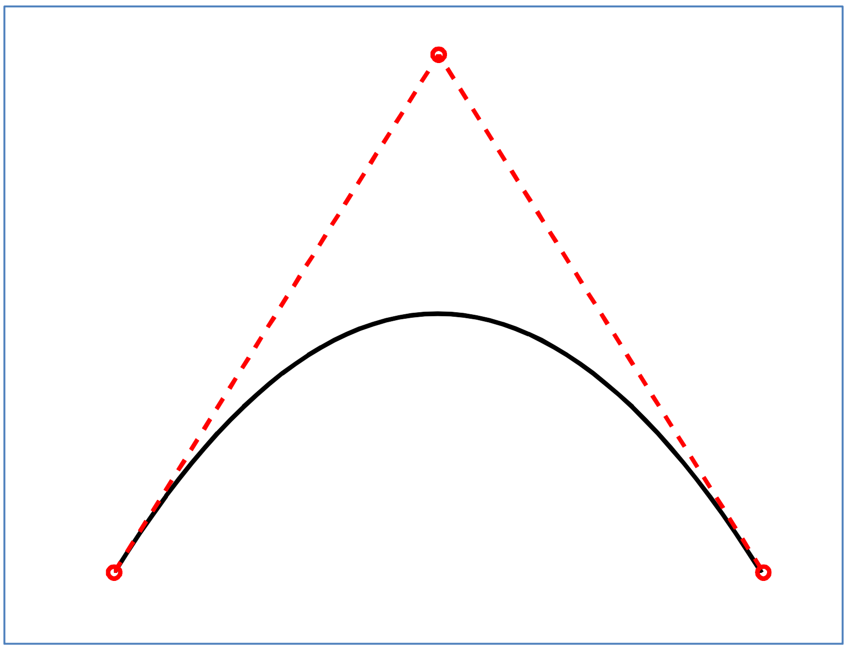
Figure 10: Quadratic Curve

- Quadratic Curve

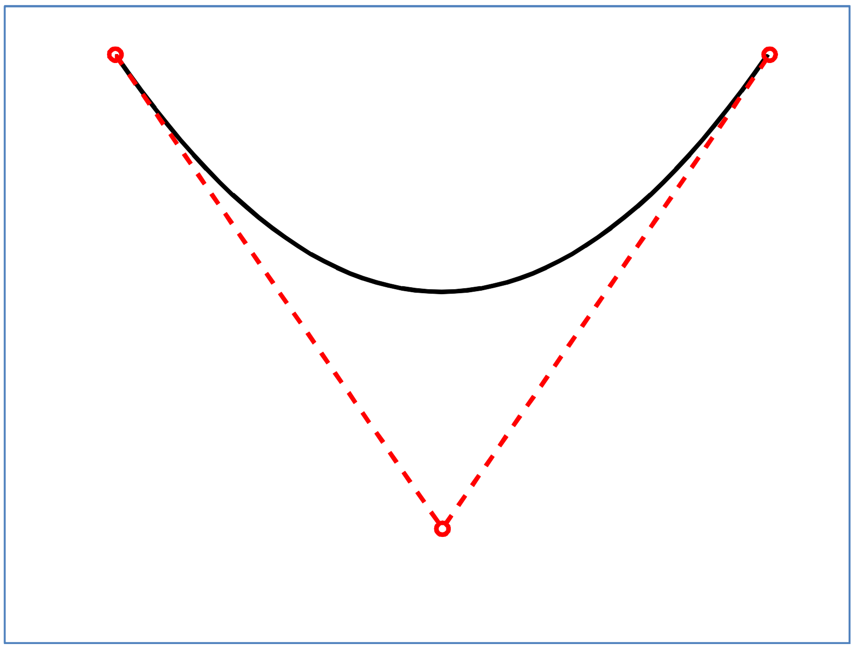
Figure 11: Quadratic Curve

- Quadratic Curve

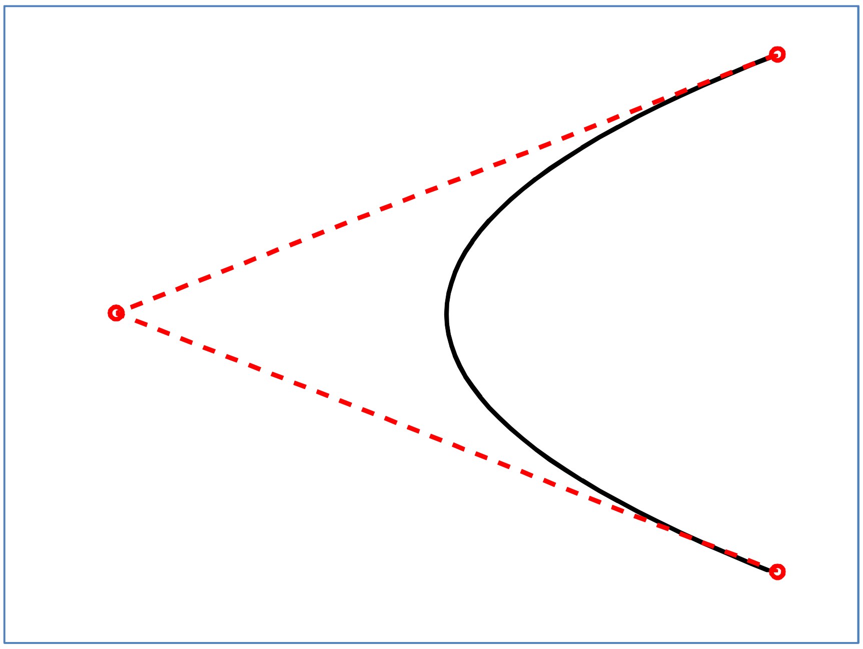
Figure 12: Quadratic Curve

- Quadratic Curve

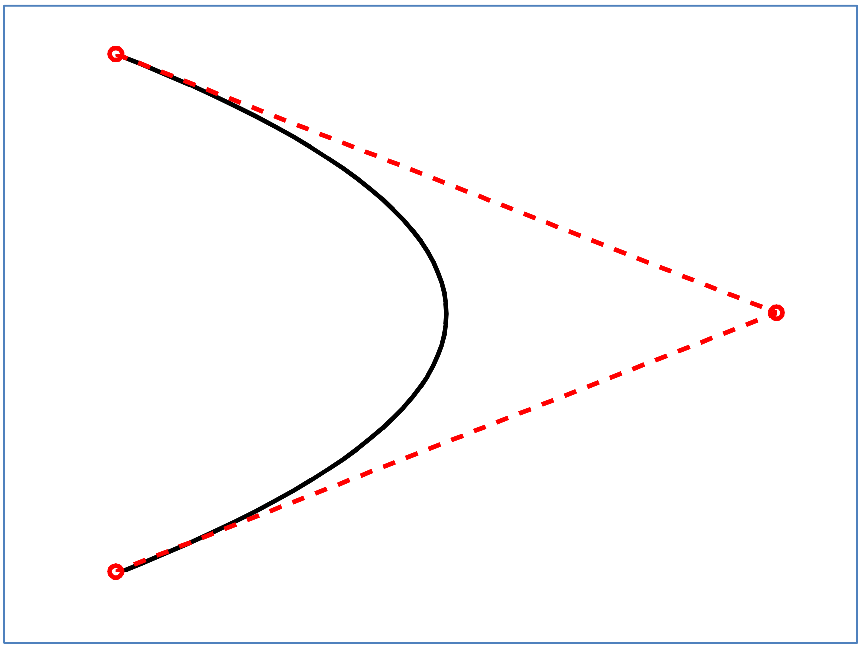
Figure 13: Quadratic Curve

4.3 Cubic Bézier Curve

The following figures show the examples of cubic Bézier curve. The following figures vary from its control points. The comparison between the equation and the coding are as followed:

Equation: $\mathbf{B}(t) = (1-t)^3\mathbf{b}_0 + 3(1-t)^2t\mathbf{b}_1 + 3(1-t)t^2\mathbf{b}_2 + t^3\mathbf{b}_3$ (4.3)

Coding: cx(1)*(1-t)^3+3*cx(2)*t*(1-t)^2+3*cx(3)*(1-t)*t^2+cx(4)*t^3

So, we can see that the different is $\mathbf{b}_0 = cx(1)$, $\mathbf{b}_1 = cx(2)$, $\mathbf{b}_2 = cx(3)$, and $\mathbf{b}_3 = cx(4)$

- Cubic Curve

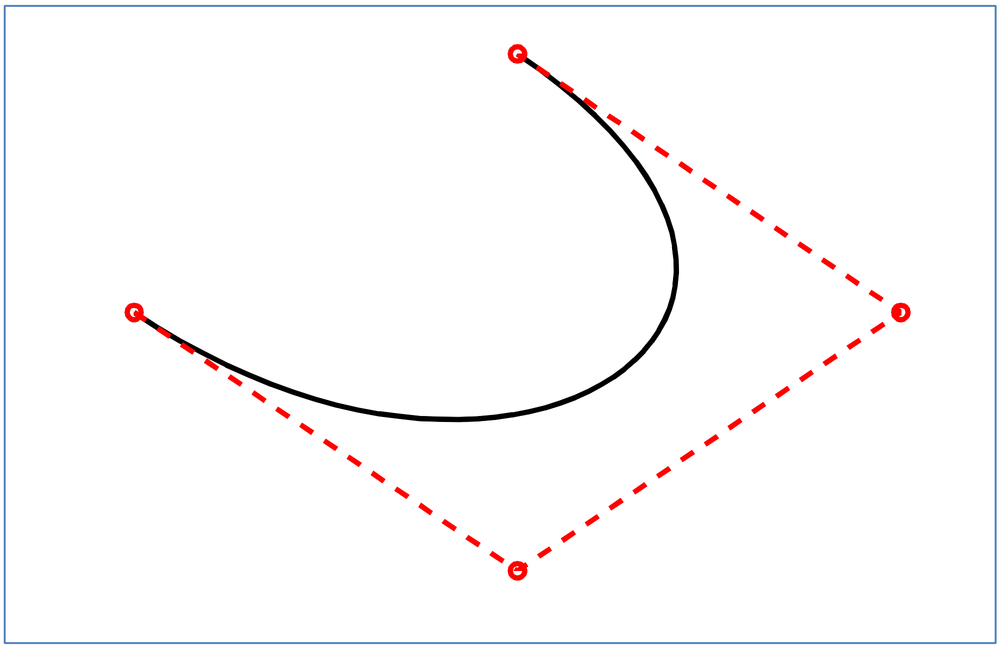

Figure 14: Cubic Curve

- Cubic Curve

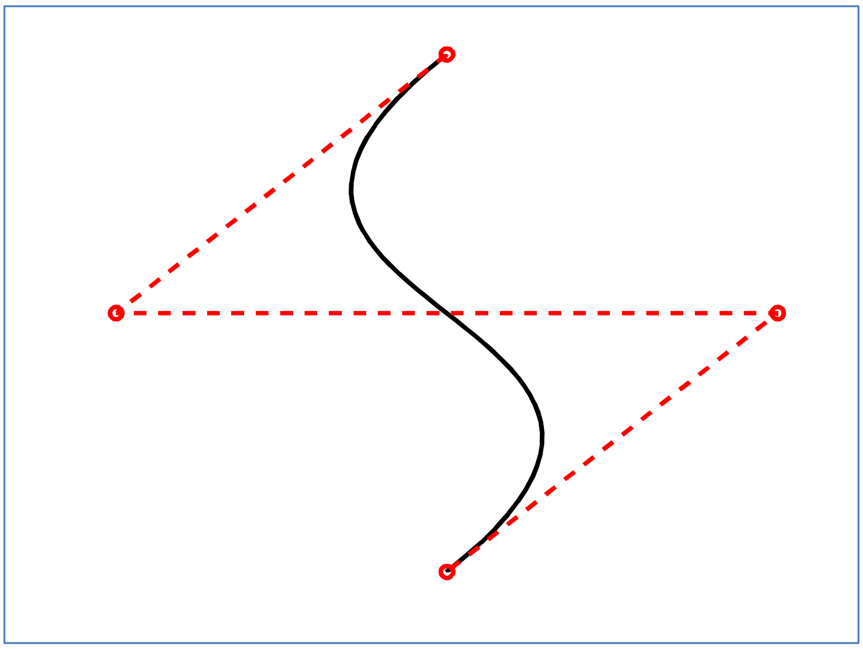

Figure 15: Cubic Curve

- Cubic Curve

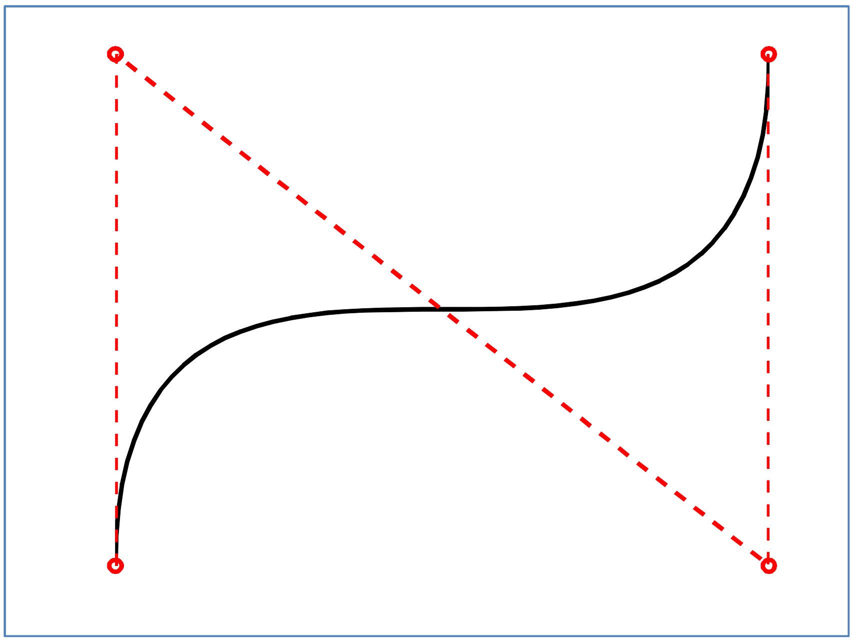

Figure 16: Cubic Curve

- Cubic Curve

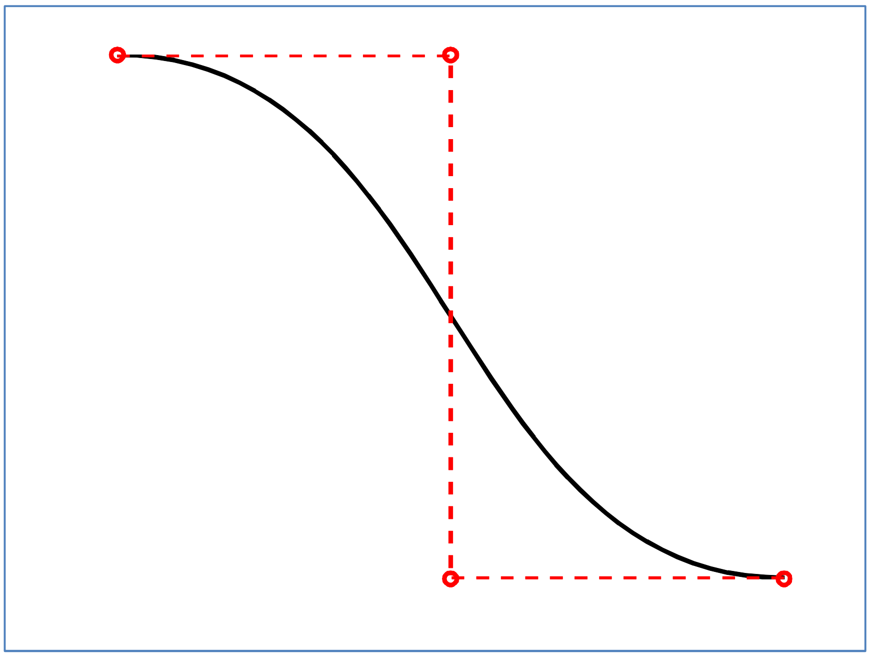

Figure 17: Cubic Curve

4.4 Bilinear Bézier Surface

The following figures show the examples of bilinear Bézier surface. The following figures vary from its control points. The difference between the equation and coding is from its control points representation:

$\mathbf{b}_0\mathbf{b}_0 = cx(1,1)$, $\mathbf{b}_0\mathbf{b}_1 = cx(1,2)$, $\mathbf{b}_1\mathbf{b}_0 = cx(2,1)$, and $\mathbf{b}_1\mathbf{b}_1 = cx(2,2)$

- Bilinear Surface

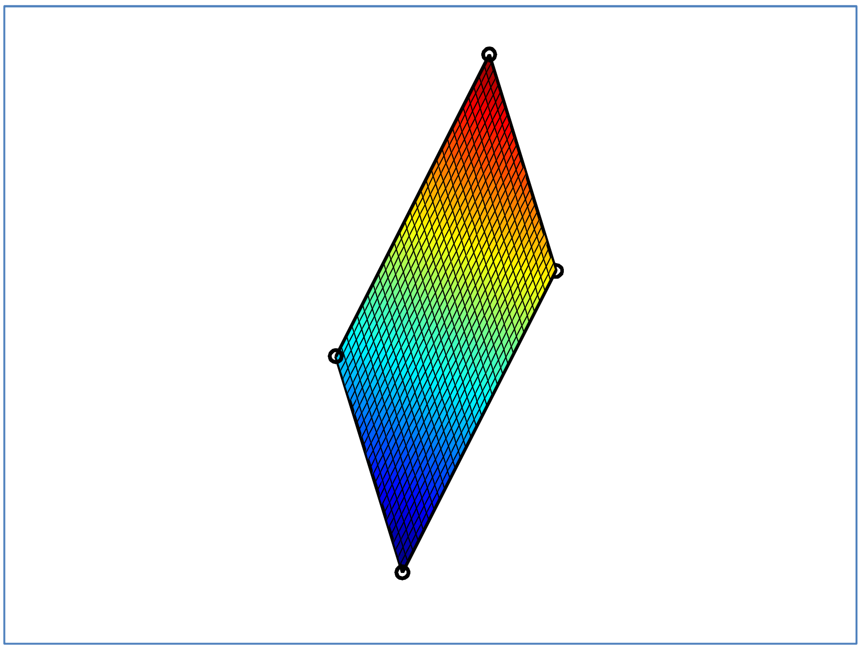

Figure 18: Bilinear Surface

- Bilinear Surface

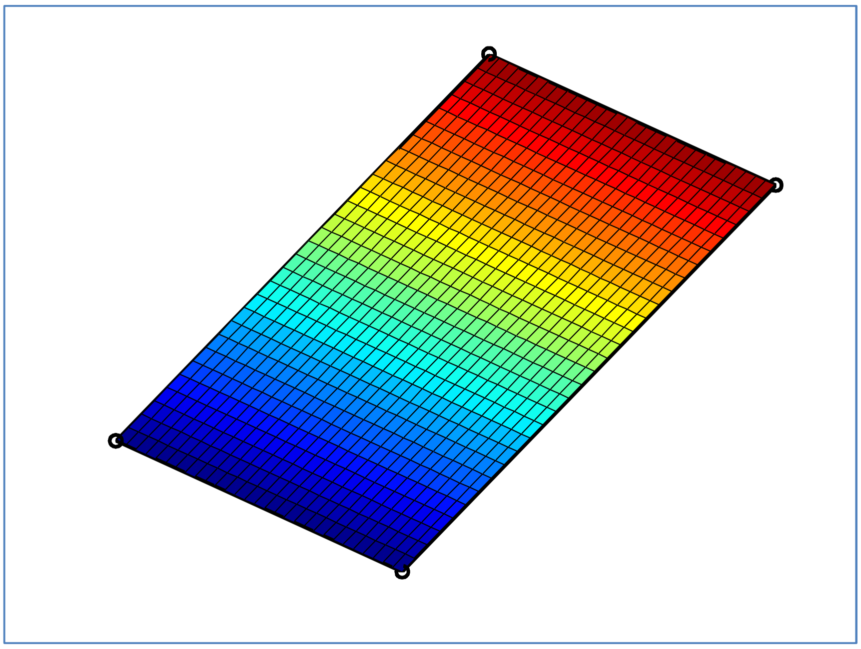

Figure 19: Bilinear Surface

- Bilinear Surface

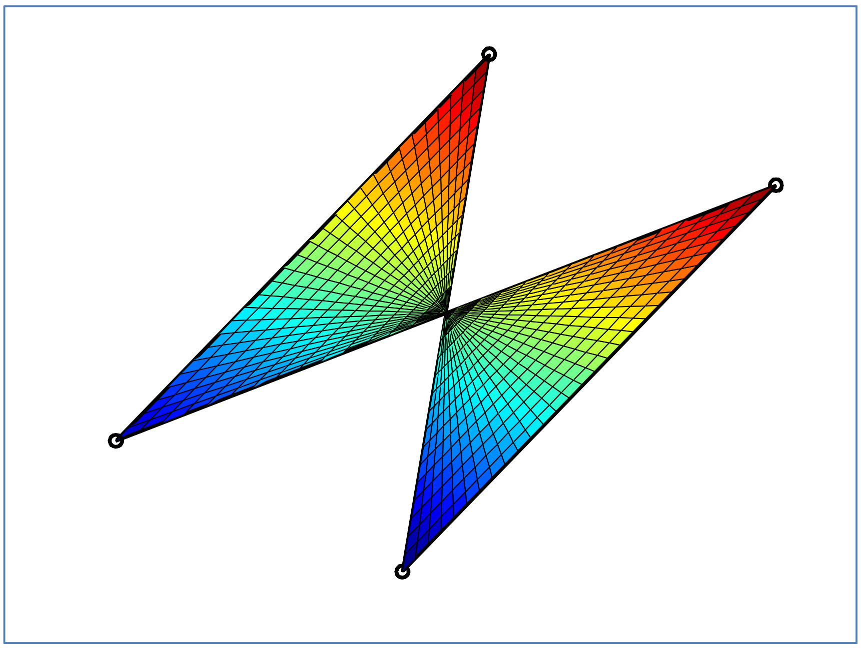

Figure 20: Bilinear Surface

- Bilinear Surface

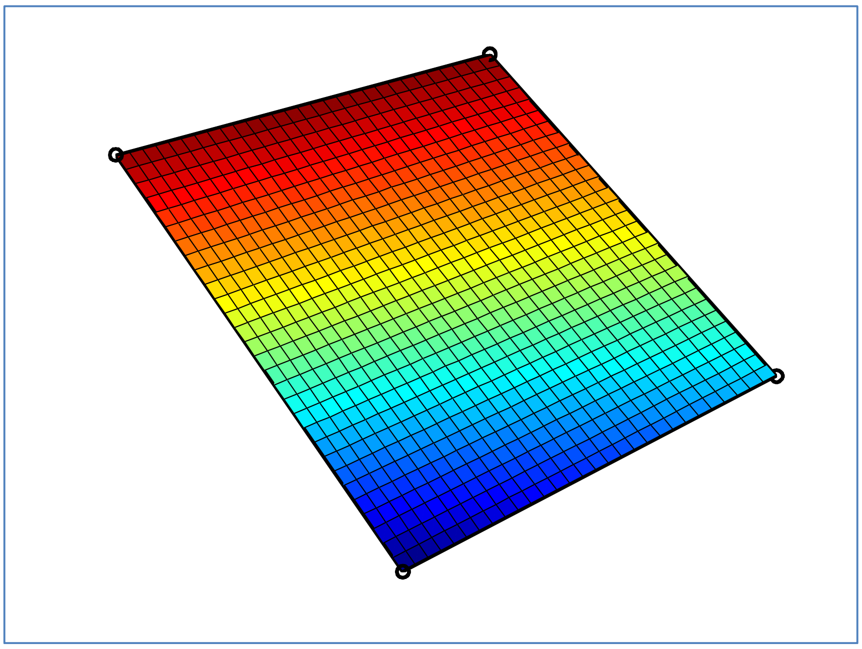

Figure 21: Bilinear Surface

4.5 Biquadrtic Bézier Surface

The following figures show the examples of biquadratic Bézier surface. The following figures vary from its control points. The difference between the equation and coding is from its control points representation:

$\mathbf{b}_0\mathbf{b}_0 = cx(1{,}1)$, $\mathbf{b}_0\mathbf{b}_1 = cx(1{,}2)$, $\mathbf{b}_0\mathbf{b}_2 = cx(1{,}3)$, $\mathbf{b}_1\mathbf{b}_0 = cx(2{,}1)$,
$\mathbf{b}_1\mathbf{b}_1 = cx(2{,}2)$, $\mathbf{b}_1\mathbf{b}_2 = cx(2{,}3)$, $\mathbf{b}_2\mathbf{b}_0 = cx(3{,}1)$, $\mathbf{b}_2\mathbf{b}_1 = cx(3{,}2)$, and
$\mathbf{b}_2\mathbf{b}_2 = cx(3{,}3)$

- Biquadratic Surface

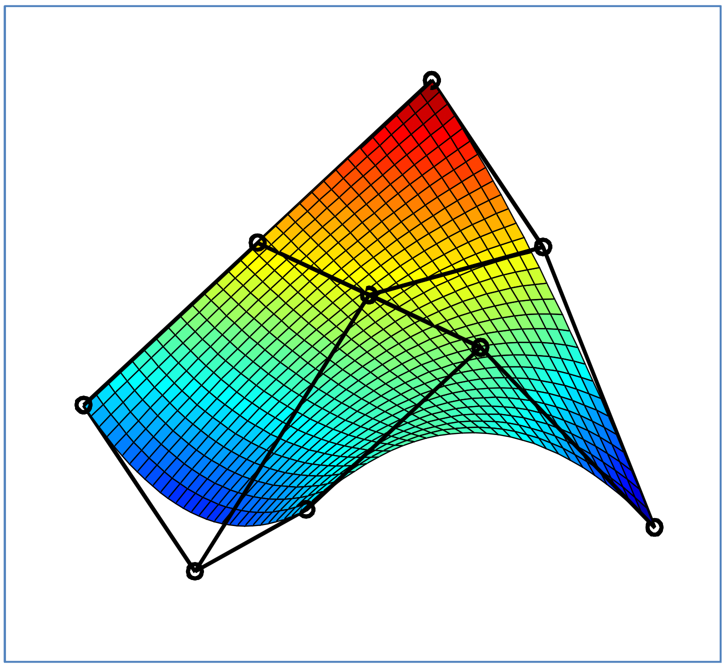

Figure 22: Biquadratic Surface

- Biquadratic Surface

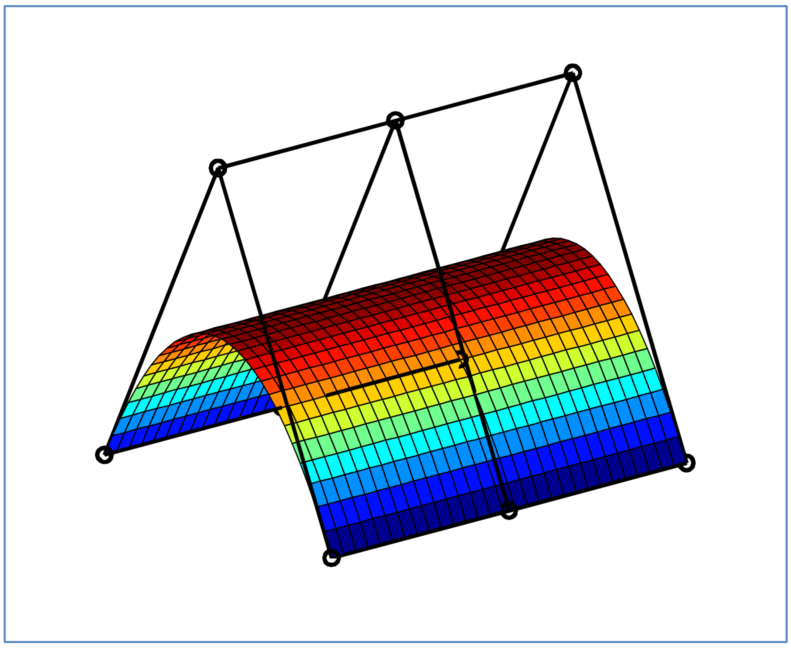

Figure 23: Biquadratic Surface

- Biquadratic Surface

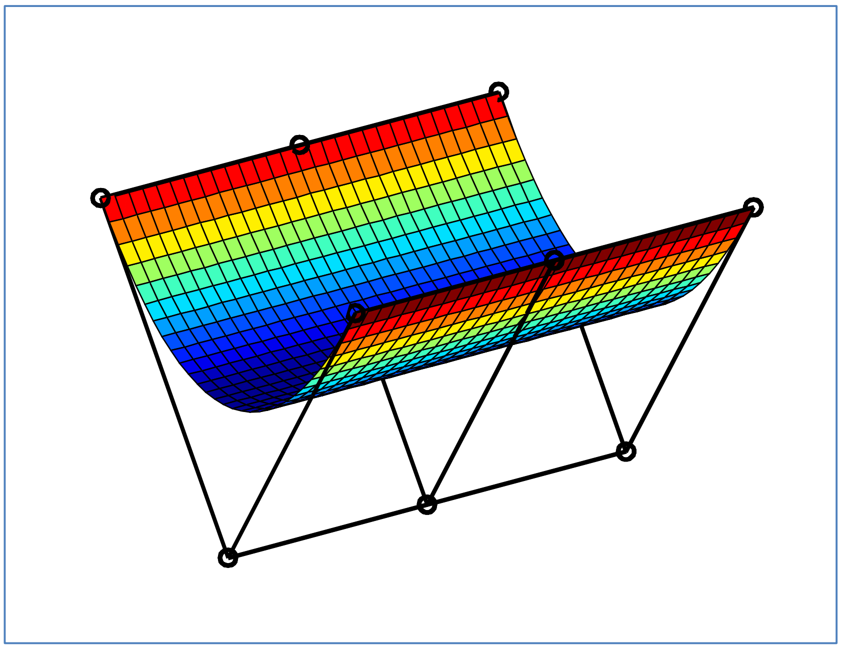

Figure 24: Biquadratic Surface

- Biquadratic Surface

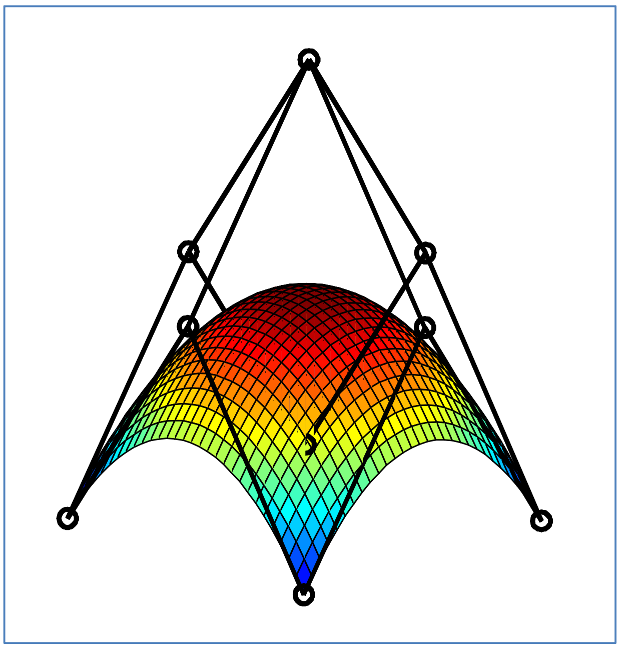

Figure 25: Biquadratic Surface

4.6 Bicubic Bézier Surface

The following figures show the examples of bicubic Bézier surface. The following figures vary from its control points. The difference between the equation and coding is from its control points representation:

$\mathbf{b}_0\mathbf{b}_0 = cx(1,1)$, $\mathbf{b}_0\mathbf{b}_1 = cx(1,2)$, $\mathbf{b}_0\mathbf{b}_2 = cx(1,3)$, $\mathbf{b}_0\mathbf{b}_3 = cx(1,4)$,
$\mathbf{b}_1\mathbf{b}_0 = cx(2,1)$, $\mathbf{b}_1\mathbf{b}_1 = cx(2,2)$, $\mathbf{b}_1\mathbf{b}_2 = cx(2,3)$, $\mathbf{b}_1\mathbf{b}_3 = cx(2,4)$,
$\mathbf{b}_2\mathbf{b}_0 = cx(3,1)$, $\mathbf{b}_2\mathbf{b}_1 = cx(3,2)$, $\mathbf{b}_2\mathbf{b}_2 = cx(3,3)$, $\mathbf{b}_2\mathbf{b}_3 = cx(3,4)$,
$\mathbf{b}_3\mathbf{b}_0 = cx(4,1)$, $\mathbf{b}_3\mathbf{b}_1 = cx(4,2)$, $\mathbf{b}_3\mathbf{b}_2 = cx(4,3)$, and $\mathbf{b}_3\mathbf{b}_3 = cx(4,4)$

➢ Bicubic Surface

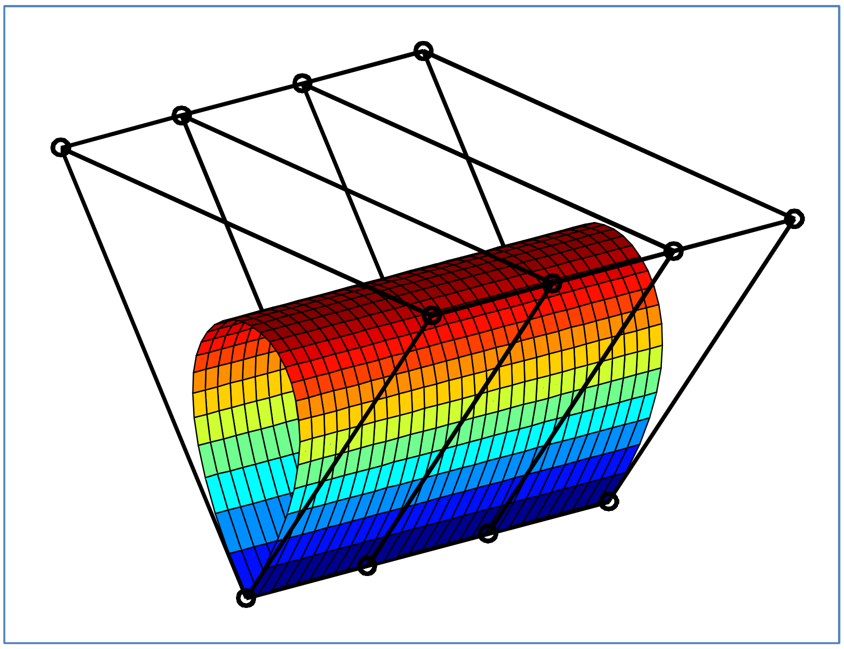
Figure 26: Bicubic Surface

➢ Bicubic Surface

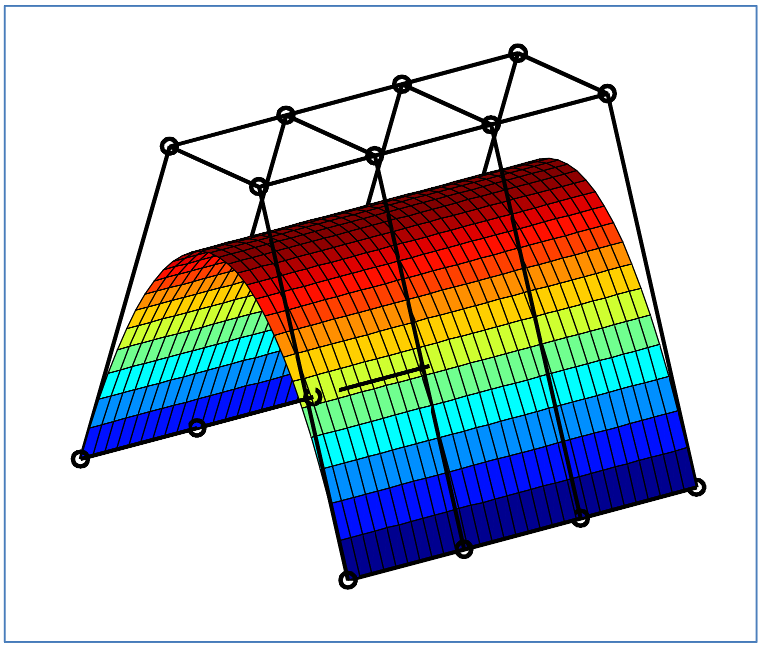
Figure 27: Bicubic Surface

- Bicubic Surface

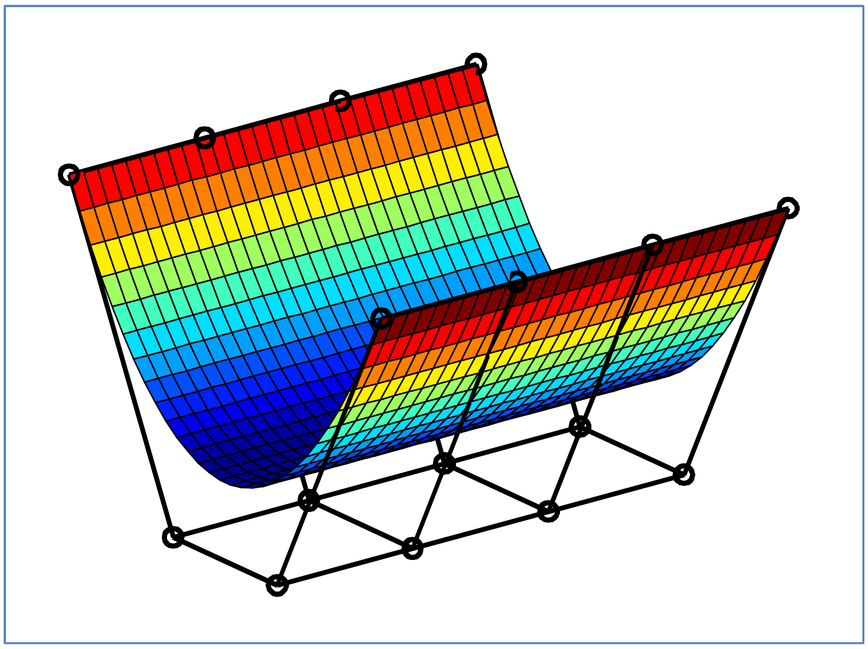

Figure 28: Bicubic Surface

- Bicubic Surface

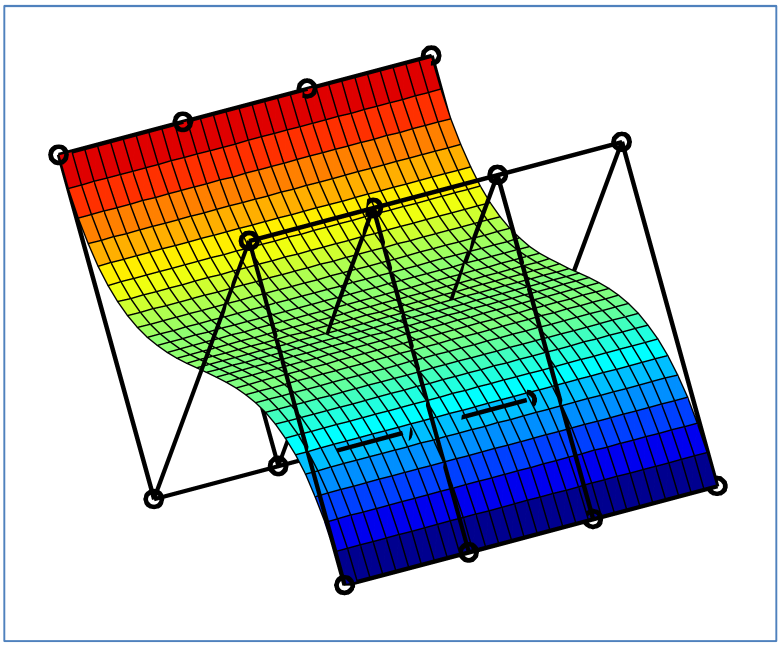

Figure 29: Bicubic Surface

4.7 Bernstein Polynomial of degree 2

This figure displayed the Bernstein Polynomial of degree 2.

- ➢ Degree 2

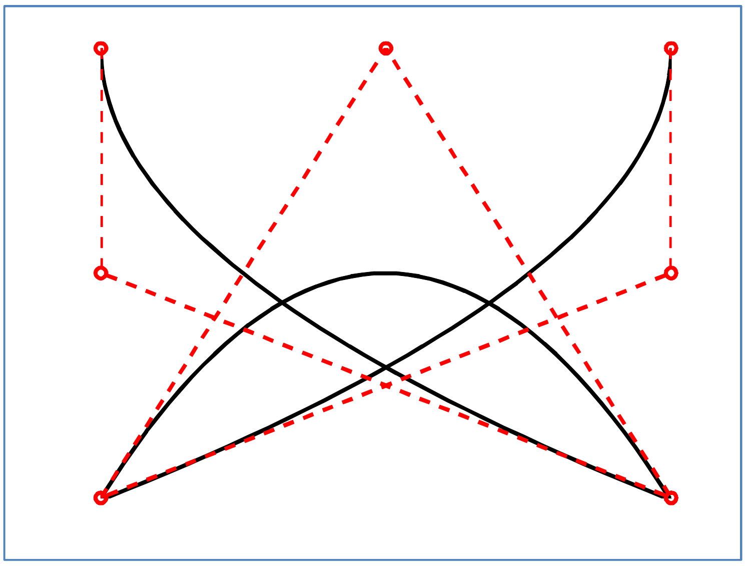

Figure 30: Bernstein Polynomial of Degree 2

4.8 Convex Hull Property (CHP)

- ➢ Convex Hull (The curve lies in the control polygon) [7]

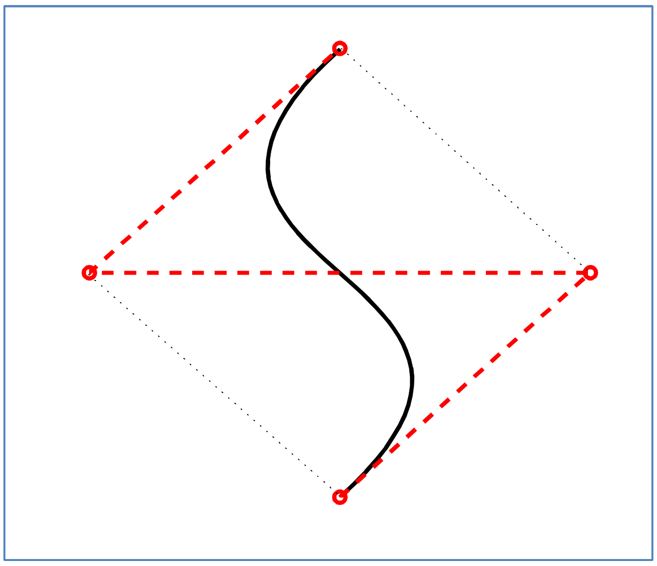

Figure 31: Convex Hull Property

4.9 Rotation of Cubic Bézier Curve

Consider a cubic Bézier curve with vertices $\mathbf{b}_0(1,0)$, $\mathbf{b}_1(2,3)$, $\mathbf{b}_2(5,4)$, and $\mathbf{b}_3(2,1)$. [3]

Apply a rotation through an angle $^{\pi}/_{4}$ about the origin in the anticlockwise direction to the curve.

$$\begin{pmatrix} 1 & 0 & 1 \\ 2 & 3 & 1 \\ 5 & 4 & 1 \\ 2 & 1 & 1 \end{pmatrix} \begin{pmatrix} \cos {}^{\pi}/_{4} & \sin {}^{\pi}/_{4} & 0 \\ -\sin {}^{\pi}/_{4} & \cos {}^{\pi}/_{4} & 0 \\ 0 & 0 & 1 \end{pmatrix} = \begin{pmatrix} 0.707 & 0.707 & 1.0 \\ -0.707 & 3.536 & 1.0 \\ 0.707 & 6.364 & 1.0 \\ 0.707 & 2.121 & 1.0 \end{pmatrix} \qquad (4.4)$$

The control points of the rotated curve are $\mathbf{b}_0(0.707,0.707)$, $\mathbf{b}_1(-0.707,3.536)$, $\mathbf{b}_2(0.707,6.364)$, and $\mathbf{b}_3(0.707,2.121)$. The curve and its rotated image are illustrated in Figure 32.

- Rotation of Cubic Curve

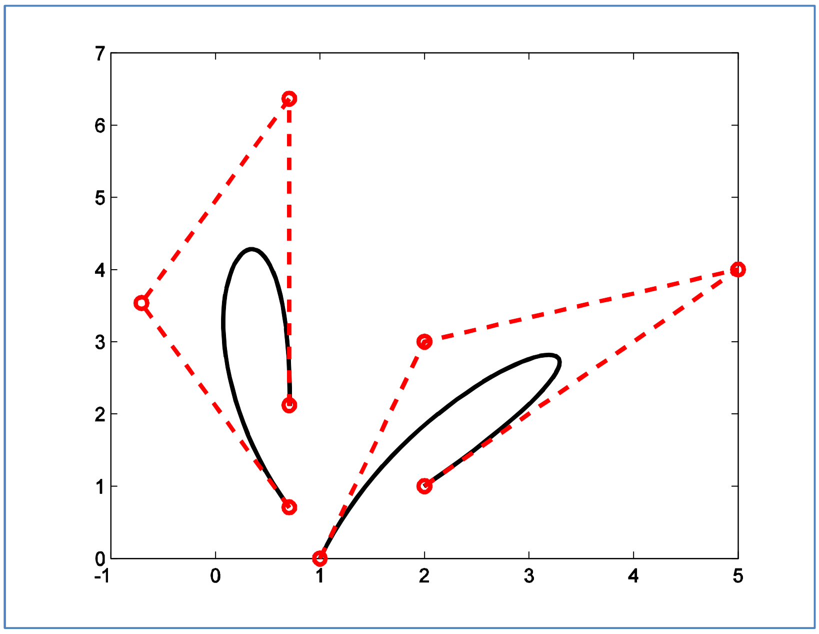

Figure 32: Rotation of Cubic Curve

4.10 Cubic Bézier curve with loop

- Loop (It self-intersects) [7]

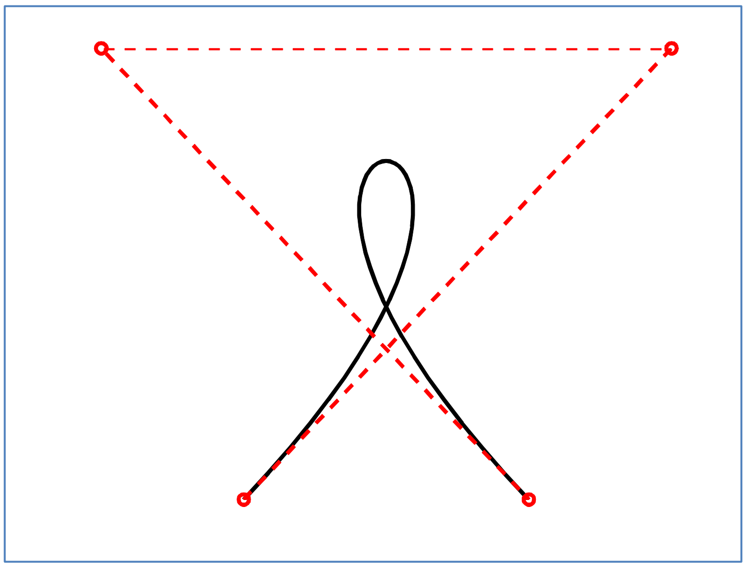

Figure 33: Loop

4.11 Cubic Bézier curve with two inflection points

- Two inflection points [7]

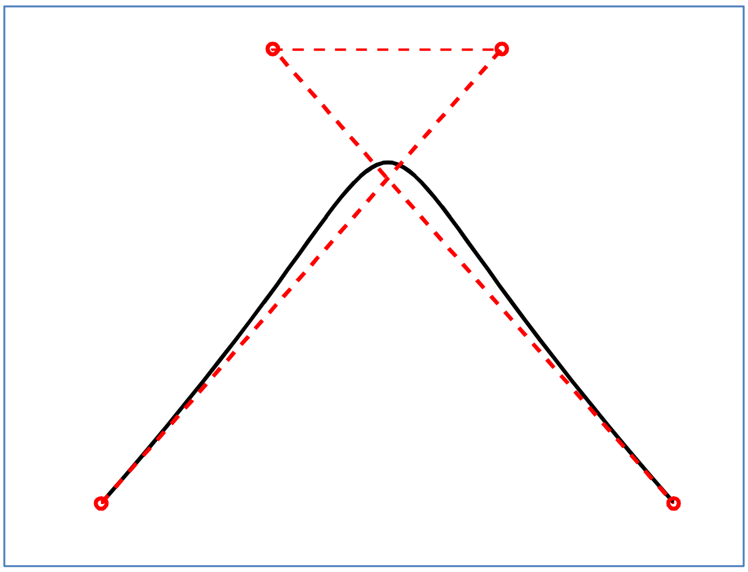

Figure 34: Two Inflection Points

4.12 Cubic Bézier curve with cusp

- Cusp (Points where the first derivative vector vanishes) [7]

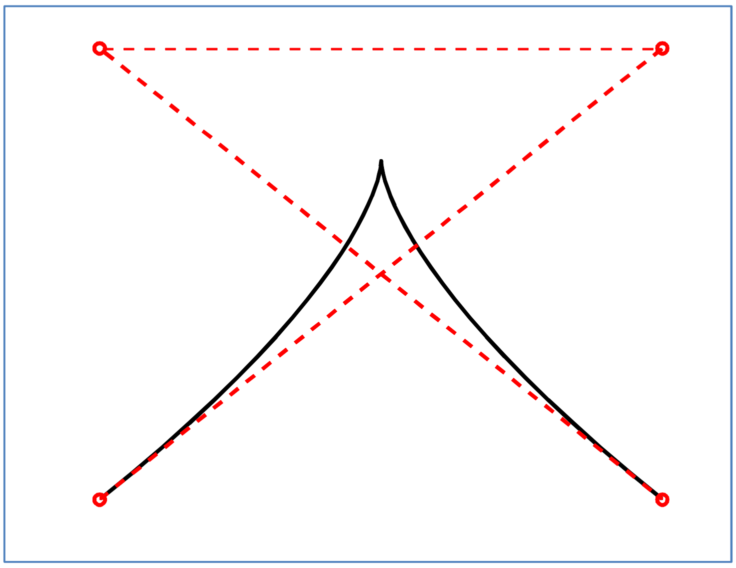

Figure 35: Cusp

4.13 Variation Diminishing Property

- Variation Diminishing Property [7]

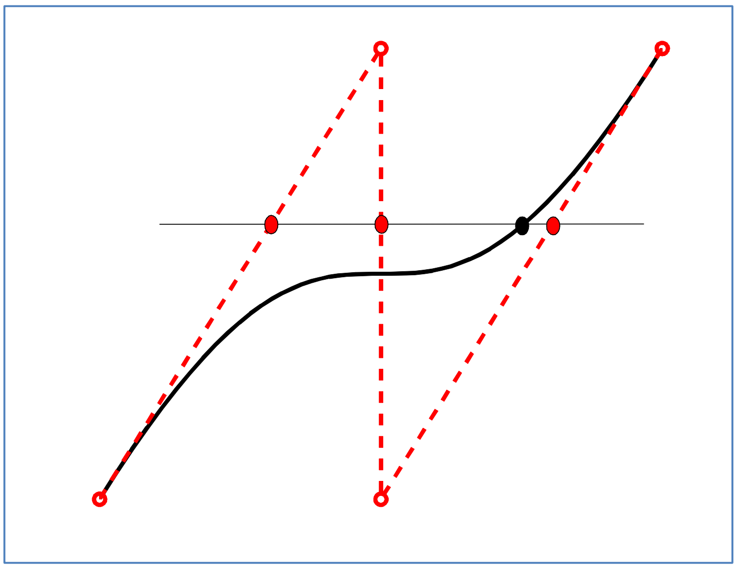

Figure 36: Variation Diminishing Property

4.14 Combination of Bézier Curve

- 8 segments of Cubic Curve

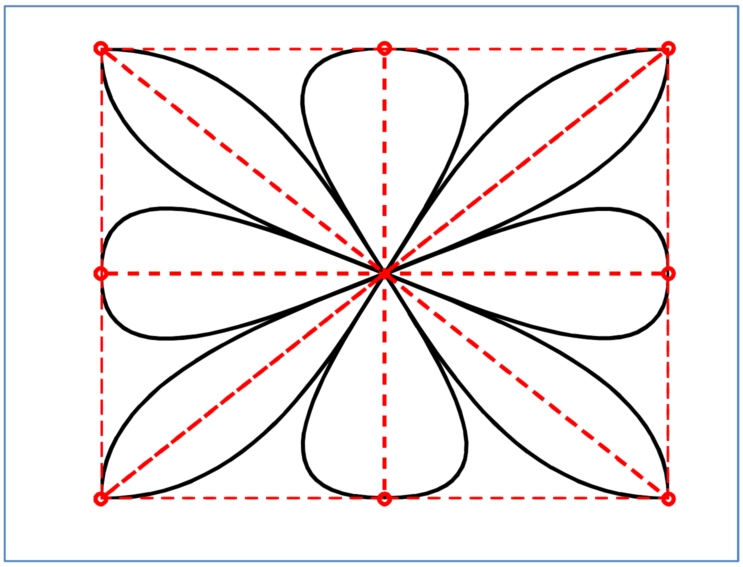

Figure 37: 8 Segments of Cubic Curve

- 2 segments of Cubic Curve

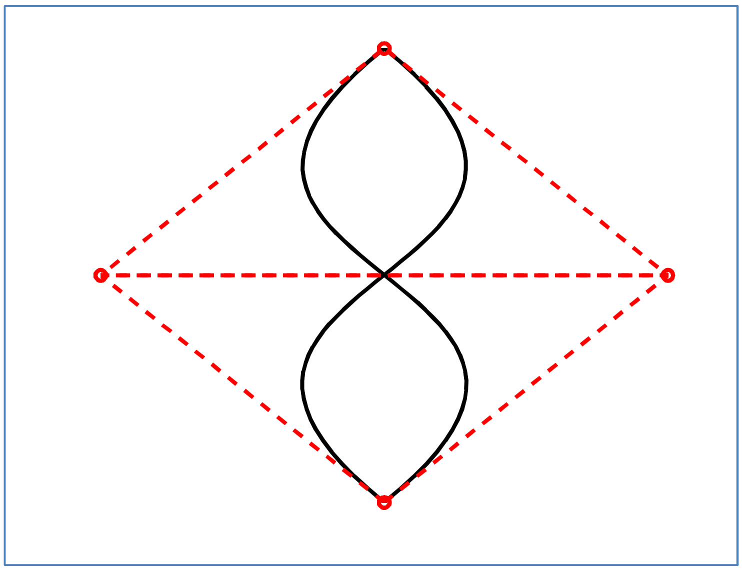

Figure 38: 2 Segments of Cubic Curve

- 4 segments of Quadratic, 2 segments of Linear Curve

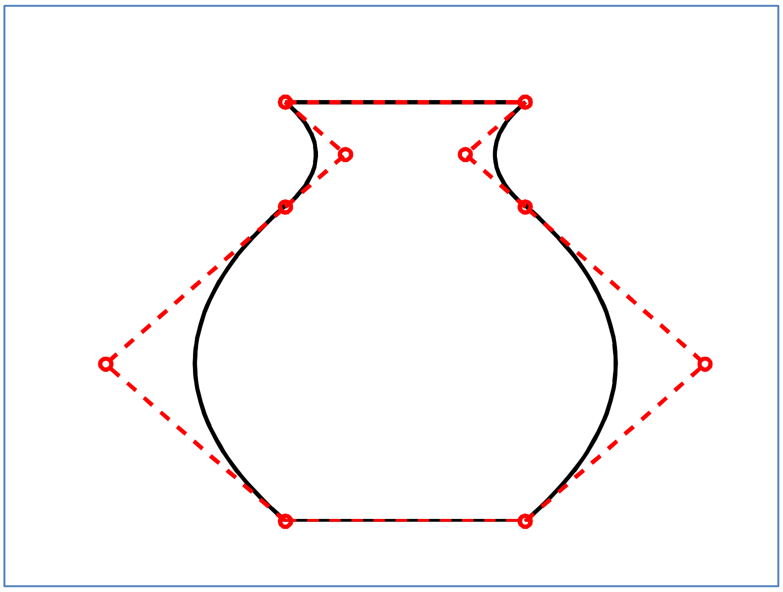

Figure 39: 4 Segments of Quadratic, 2 Segments of Linear Curve

4.15 Combination of Bézier Surface

- 2 segments of Biquadratic Surface

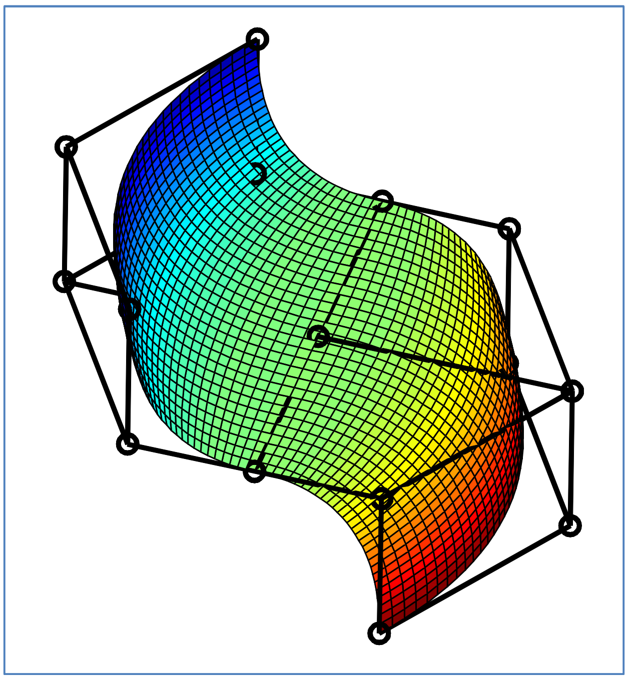

Figure 40: 2 Segments of Biquadratic Surface

4.16 Utah Teapot

The teapot data was created in 1975 by early computer graphics researcher Martin Newell, a member of the pioneering graphic program at the University of Utah. Newell needed a moderately simple mathematical model of a familiar object for his work, and his wife’s teapot (a Melitta) provided a convenient solution. The shape contains a number of elements that make it ideal for the graphics experiments of the time. Its round, contains saddle-points, has a concave element (the hole in the handle), and looks reasonable when displayed without a complex surface texture [24].

Newell made the mathematical data which describes the teapot’s geometry (largely a set of three-dimensional coordinates) publicly available and soon other researches needed something with roughly the same characteristics that Newell had, and using the teapot data meant they didn’t have to laboriously enter geometric data for some other object. The actual teapot is about 30% taller than many of its computer-generated images because the data was originally recorded for the rectangular pixels of early displays [24].

The following figures showed the Utah teapot which being generated by MATLAB. The model is designed by using 32 bicubic Bézier surfaces [25]. Another images for Utah teapot are attached in appendices (refer Appendix C)

- Utah Teapot

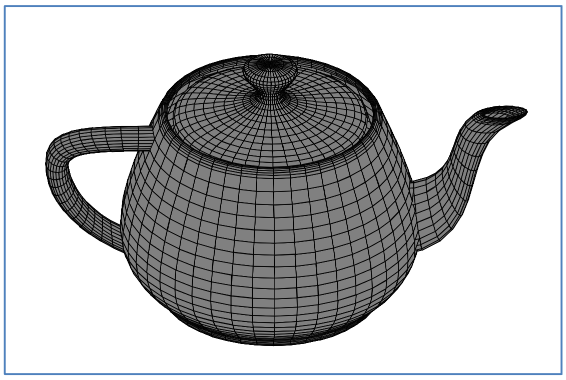
Figure 41: Utah Teapot

4.17 Cubic Interpolation

Let the p_i be given by

$$p_0 = \begin{bmatrix}-1\\0\end{bmatrix}, \quad p_1 = \begin{bmatrix}0\\1\end{bmatrix}, \quad p_2 = \begin{bmatrix}0\\-1\end{bmatrix}, \quad p_3 = \begin{bmatrix}1\\0\end{bmatrix},$$

and set $t_i = \frac{i}{3}$. Then the matrix M for our linear system becomes

$$M = \begin{bmatrix} 1 & 0 & 0 & 0 \\ \frac{8}{27} & \frac{4}{9} & \frac{2}{9} & \frac{1}{27} \\ \frac{1}{27} & \frac{2}{9} & \frac{4}{9} & \frac{8}{27} \\ 0 & 0 & 0 & 1 \end{bmatrix}$$

Now we inverse the matrix M becomes

$$M^{-1} = \begin{bmatrix} 1.0000 & 0 & 0 & 0 \\ -0.8333 & 3.0000 & -1.5000 & 0.3333 \\ 0.3333 & -1.5000 & 3.0000 & -0.8333 \\ 0 & 0 & 0 & 1.0000 \end{bmatrix} \tag{4.5}$$

With the p_i given above, first we solve for x- coordinate

$$B_x = M^{-1}P_x = \begin{bmatrix} -1.0000 \\ 1.1667 \\ -1.1667 \\ 1.0000 \end{bmatrix} \tag{4.6}$$

Then for y- coordinate

$$B_y = M^{-1}P_y = \begin{bmatrix} 0 \\ 4.5 \\ -4.5 \\ 0 \end{bmatrix} \tag{4.7}$$

Thus, the Bézier ponts for interpolating cubic are

$$b_0 = \begin{bmatrix}-1\\0\end{bmatrix}, \qquad b_1 = \begin{bmatrix}1.1667\\4.5\end{bmatrix}, \qquad b_2 = \begin{bmatrix}-1.1667\\-4.5\end{bmatrix}, \qquad b_3 = \begin{bmatrix}1\\0\end{bmatrix},$$

This example is outlined in Figure 42 below:

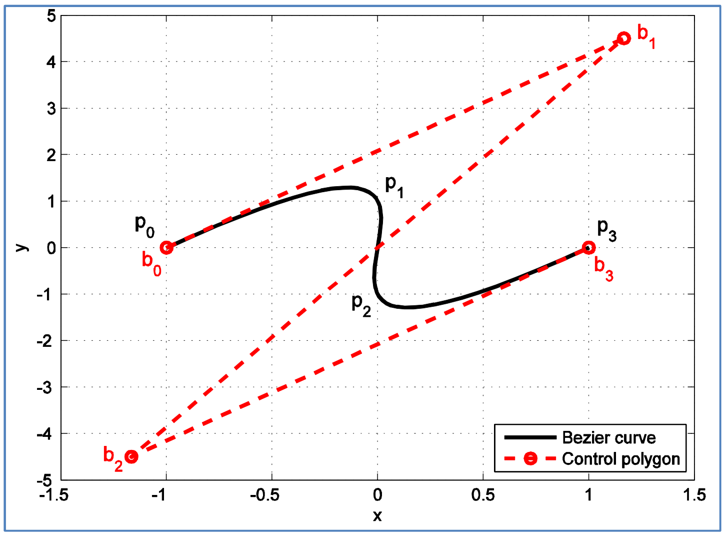

Figure 42: Cubic Bézier Interpolation

4.18 Image Rescaling Using Bilinear Interpolation

- Lake.tif

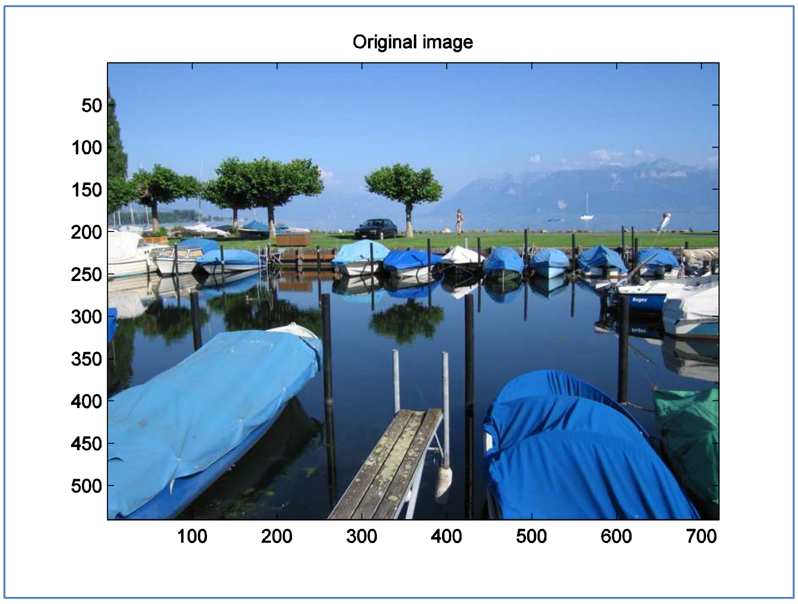

Figure 43: Original Image Lake.tif

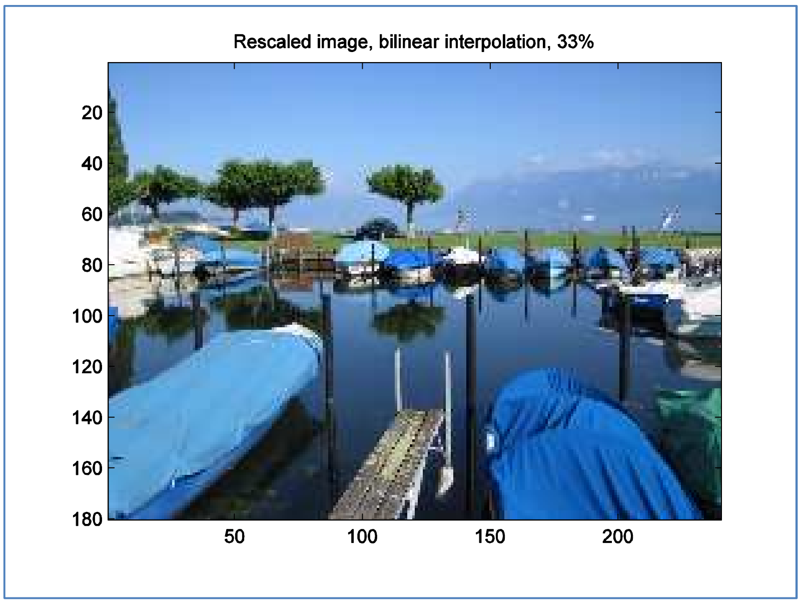

Figure 44: Rescale 33%

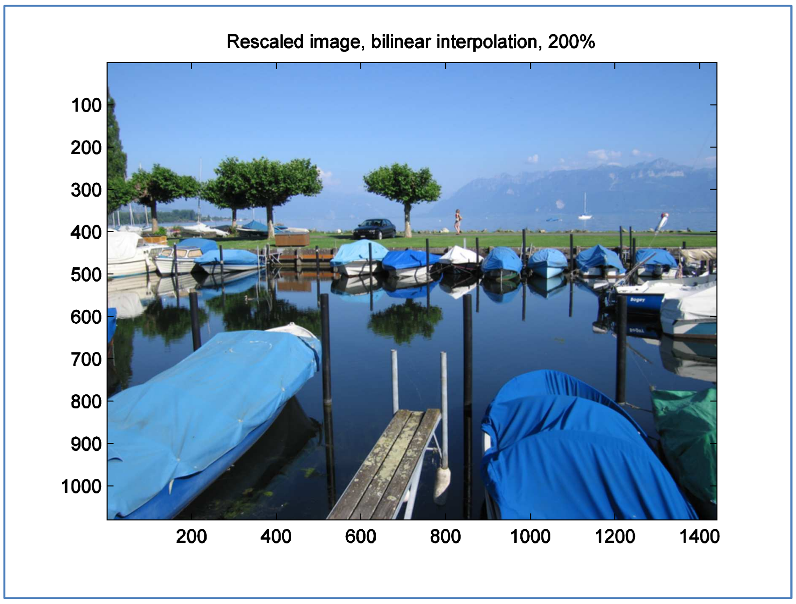

Figure 45: Rescale 200%

➢ Mosque.jpg

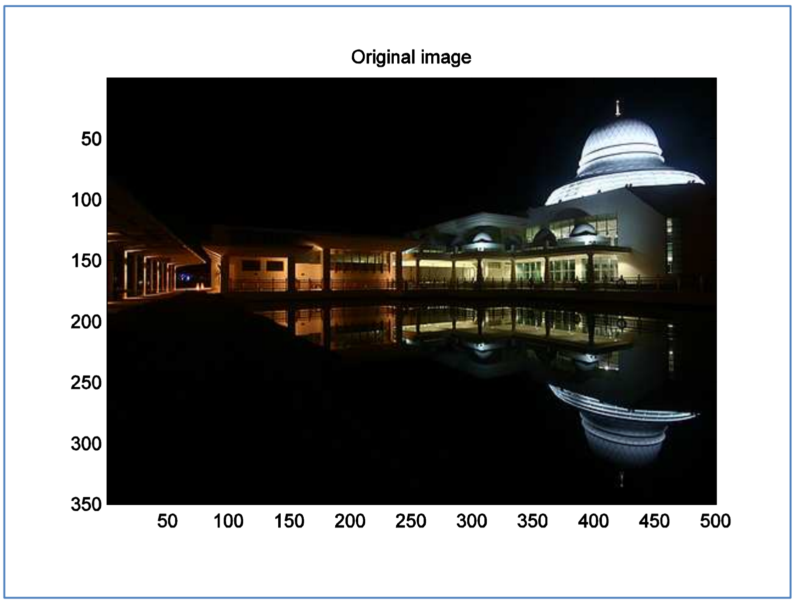

Figure 46: Original Image Mosque.jpg

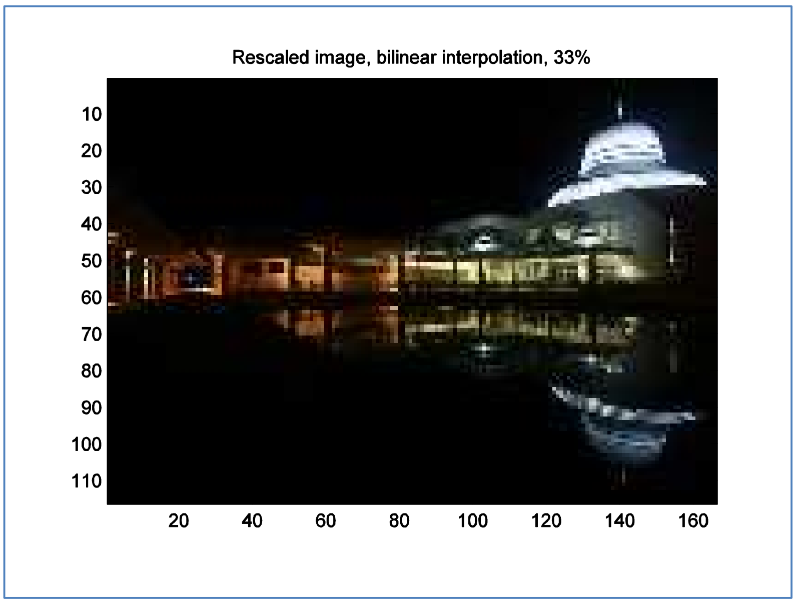

Figure 47: Rescale 33%

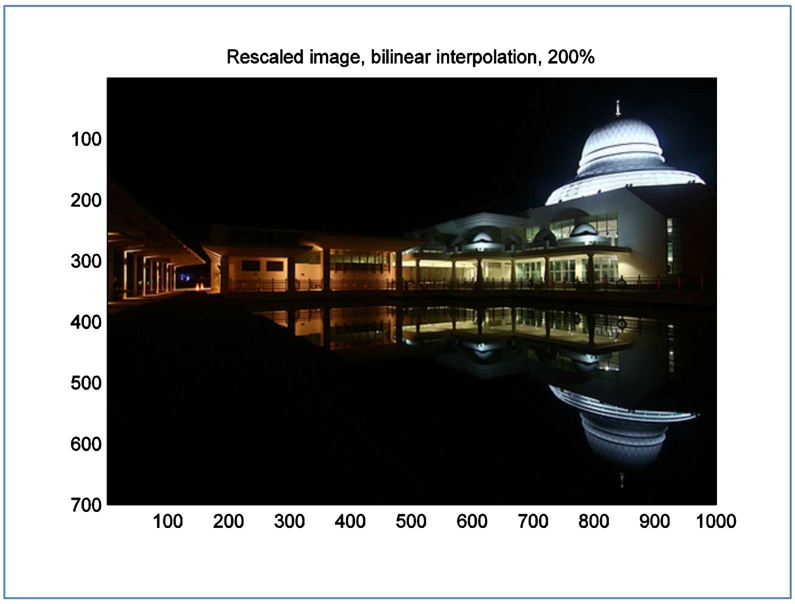

Figure 48: Rescale 200%

The comparison of WxH and file size for each images are showed as follow:

Table 1: Quantitative Analysis for Image Rescaling

Image		Lake.tif	Mosque.jpg
Original Image	WxH	720x540	500x350
	File Size	2.25 MB	1.01 MB
Rescale 33%	WxH	238x178	165x116
	File Size	264 KB	122 KB
Rescale 200%	WxH	140x1080	1000x700
	File Size	8.98 MB	4.04 MB

4.19 Bézier Curve Least Square Fitting

- Circle Approximation [16]

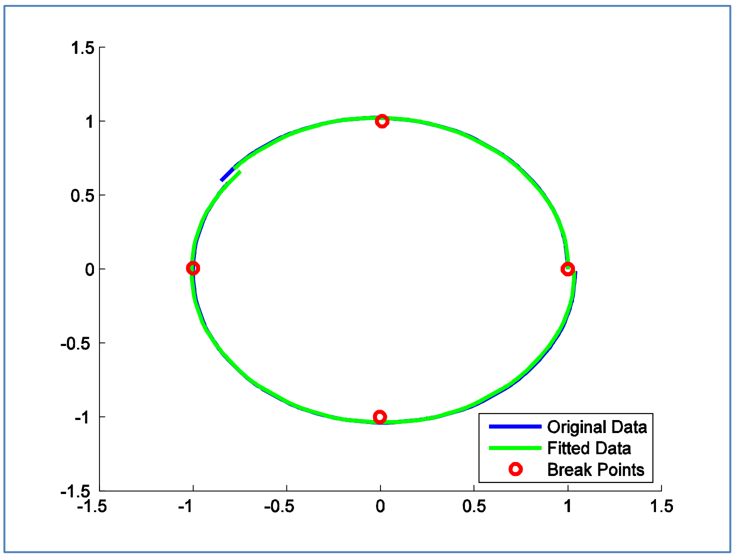

Figure 49: Circle Approximation

- Sine Approximation (sin (x)) [16]

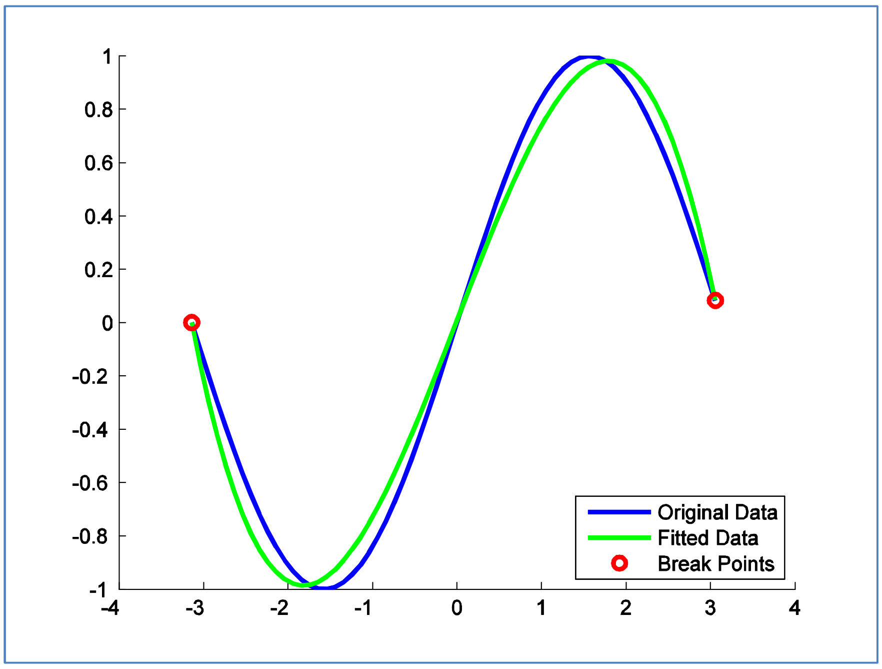

Figure 50: Sine Approximation

➢ Five Text Approximation [16]

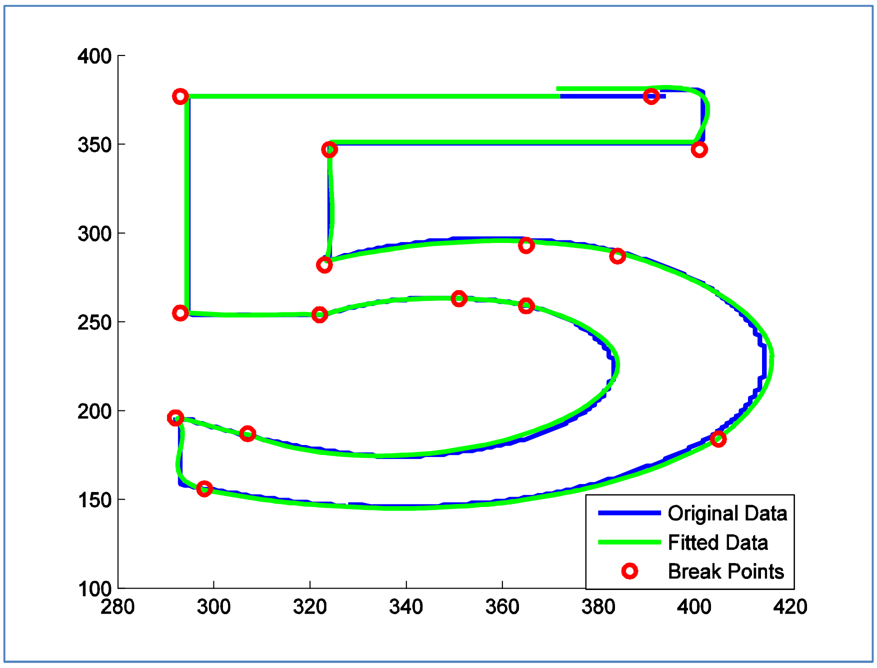

Figure 51: Five Text Approximation

➢ Tangent Approximation (tan (x))

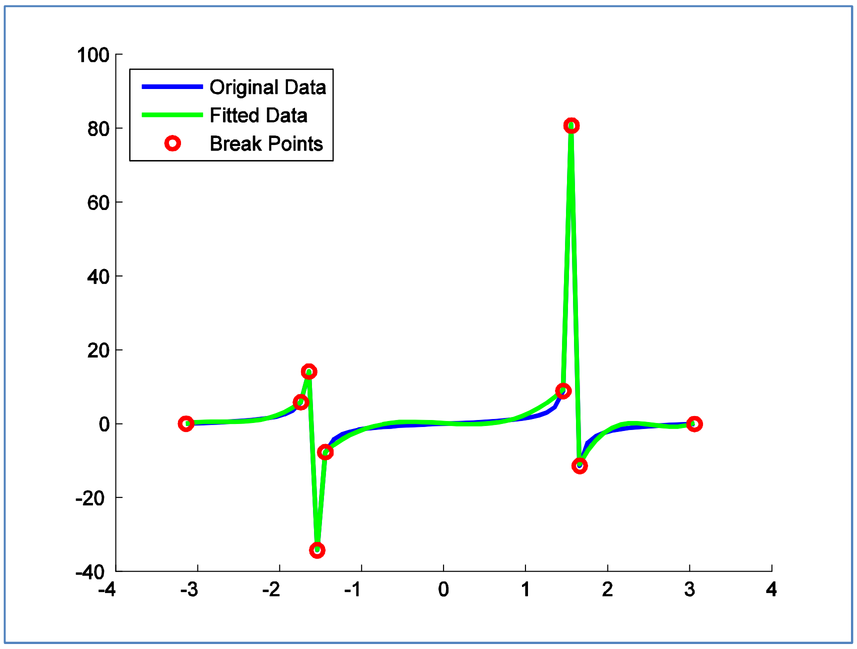

Figure 52: Tangent Approximation

4.20 RGB Quadtree Decomposition and Parametric Line Fitting

4.20.1 Uniform Threshold Variation

- Peppers.tiff

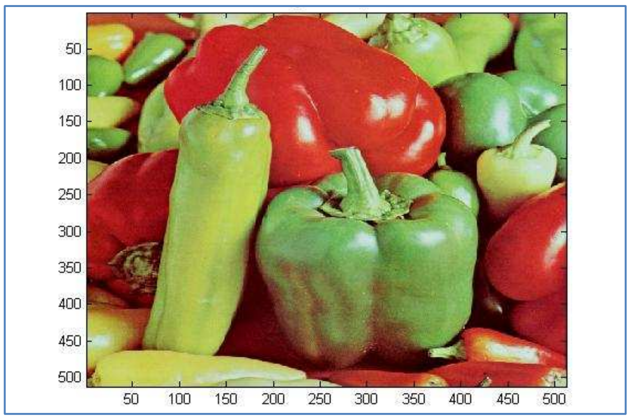

Figure 53: Original Image Peppers.tiff

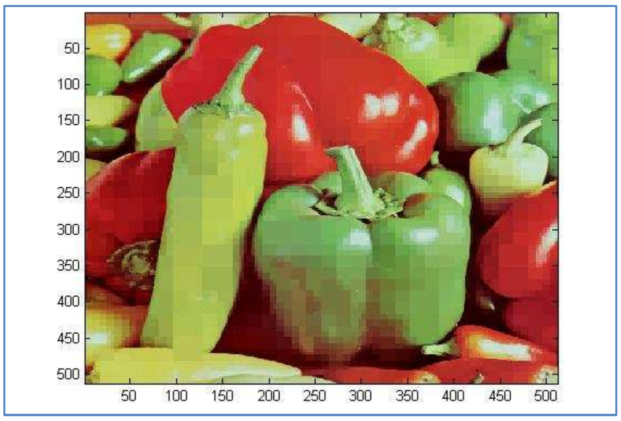

Figure 54: Decoded Image Peppers.tiff Threshold (0.3, 0.3, 0.3)

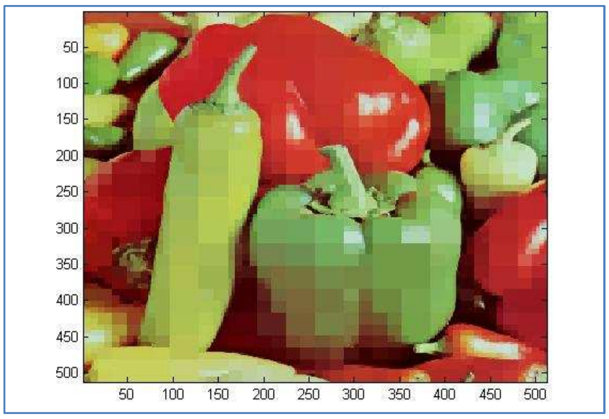

Figure 55: Decoded Image Peppers.tiff Threshold (0.5, 0.5, 0.5)

- Baboon.tiff

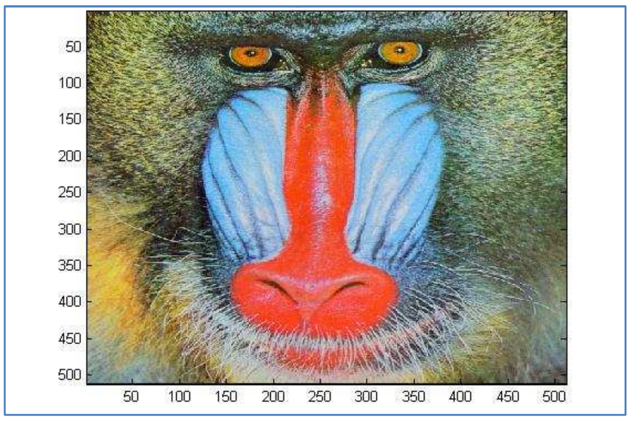

Figure 56: Original Image Baboon.tiff

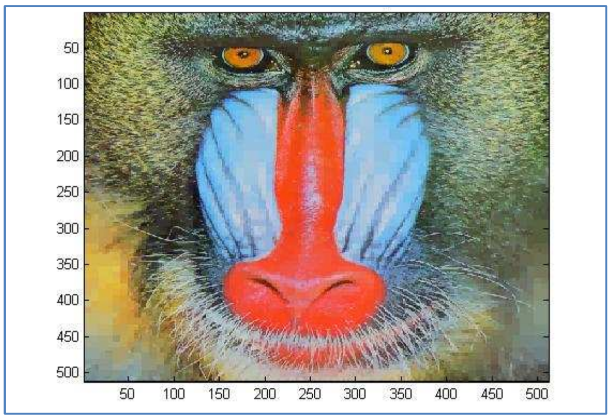

Figure 57: Decoded Image Baboon.tiff Threshold (0.3, 0.3, 0.3)

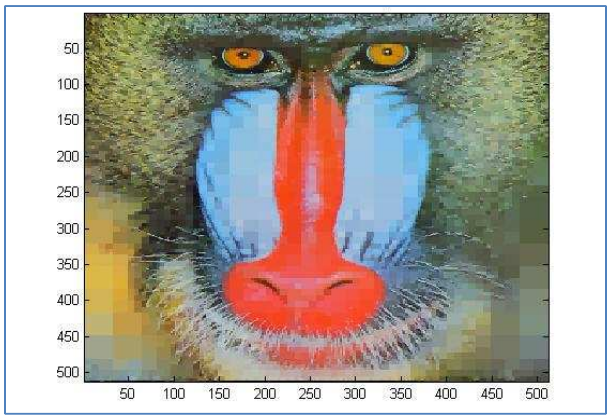

Figure 58: Decoded Image Baboon.tiff Threshold (0.5, 0.5, 0.5)

- Airplane.tiff

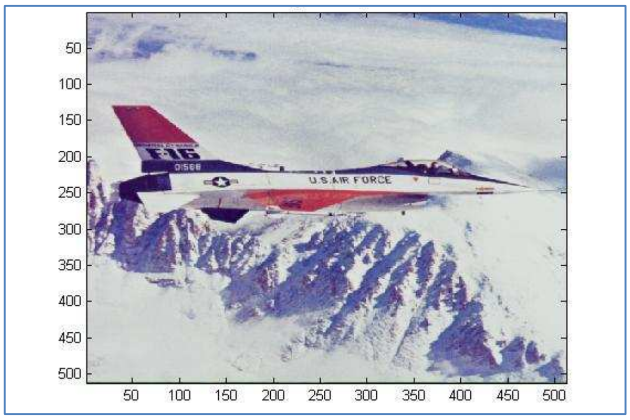

Figure 59: Original Image Airplane.tiff

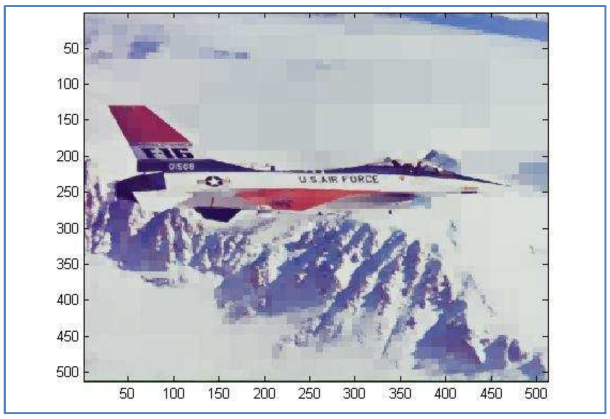

Figure 60: Decoded Image Airplane.tiff Threshold (0.3, 0.3, 0.3)

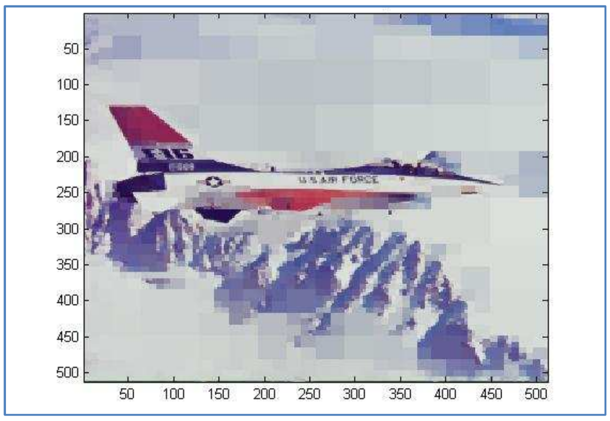

Figure 61: Decoded Image Airplane.tiff Threshold (0.5, 0.5, 0.5)

➢ Lena.png

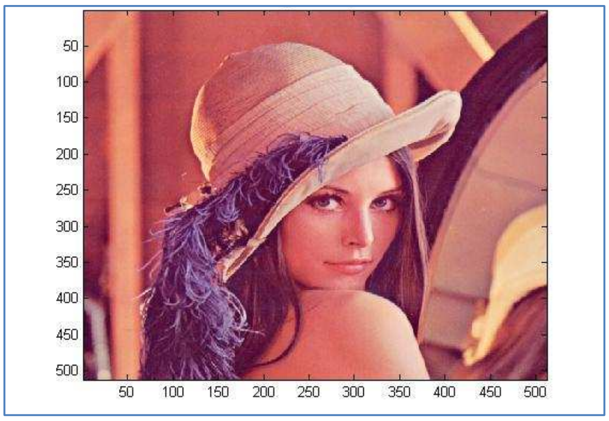

Figure 62: Original Image Lena.png

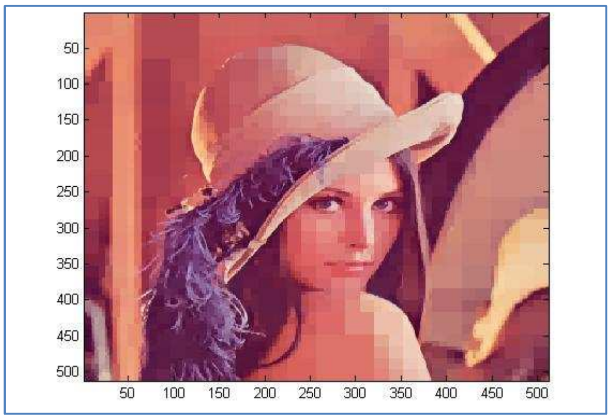

Figure 63: Decoded Image Lena.png Threshold (0.3, 0.3, 0.3)

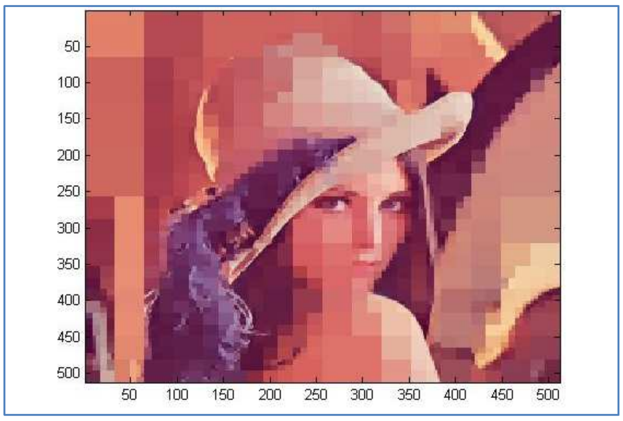

Figure 64: Decoded Image Lena.png Threshold (0.5, 0.5, 0.5)

➢ Threshold (0.3, 0.3, 0.3)

Table 2: Quantitative Analysis for Threshold (0.3, 0.3, 0.3)

Image		Peppers.tiff	Baboon.tiff	Airplane.tiff	Lena.png
MSE	R	56.0000	54.0000	56.0000	63.0000
	G	68.0000	56.0000	63.0000	60.0000
	B	63.0000	57.0000	58.0000	66.0000
RMSE	R	7.4833	7.3485	7.4833	7.9373
	G	8.2462	7.4833	7.9373	7.7460
	B	7.9373	7.5498	7.6158	8.1240
PSNR	R	30.6489	30.8069	30.6489	30.1374
	G	29.8057	30.6489	30.1374	30.3493
	B	30.1374	30.5721	30.4965	29.9354
File Size	Original	35.7 KB	54.7 KB	33.7 KB	34.3 KB
	Decoded	34.0 KB	50.2 KB	30.9 KB	31.7 KB

➢ Threshold (0.5, 0.5, 0.5)

Table 3: Quantitative Analysis for Threshold (0.5, 0.5, 0.5)

Image		Peppers.tiff	Baboon.tiff	Airplane.tiff	Lena.png
MSE	R	107.0000	97.0000	101.0000	102.0000
	G	112.0000	98.0000	108.0000	106.0000
	B	99.0000	103.0000	81.0000	100.0000
RMSE	R	10.3441	9.8489	10.0499	10.0995
	G	10.5830	9.8995	10.3923	10.2956
	B	9.9499	10.1489	9.0000	10.0000
PSNR	R	27.8370	28.2631	28.0876	28.0448
	G	27.6386	28.2185	27.7966	27.8777
	B	28.1745	28.0024	29.0460	28.1308
File Size	Original	35.7 KB	54.7 KB	33.7 KB	41.2 KB
	Decoded	32.8 KB	41.3 KB	28.5 KB	35.9 KB

From the quantitative analysis in two tables above, we can see the comparison of value for MSE, RMSE and PSNR for each RGB channel and also file size for original and decoded of the images. The compression ratio for threshold (0.3, 0.3, 0.3) is 1.43 and for threshold (0.5, 0.5, 0.5) is 2.00 for all images. From the above value, we can observe the best result by looking at lowest MSE and RMSE value and highest PSNR value. The lowest MSE and RMSE and highest PSNR determine the best quality of image compression. From the four tested image, we can see that the best result is Baboon.tiff and if we observe the image itself, we can see the quality is better from others.

4.20.2 Non-uniform Threshold Variation

For the non-uniform threshold variation, there are three patterns of variation being used to examine and analyze the quality of the image. The lists of non-uniform threshold being used are as followed:

Table 4: Non-uniform Threshold Variation

First Pattern	Second Pattern	Third Pattern
0.3, 0.5, 0.7	0.8, 0.3, 0.3	0.8, 0.8, 0.3
0.3, 0.7, 0.5	0.3, 0.8, 0.3	0.3, 0.8, 0.8
0.5, 0.3, 0.7	0.3, 0.3, 0.8	0.8, 0.3, 0.8
0.5, 0.7, 0.3		
0.7, 0.3 0.5		
0.7, 0.5, 0.3		

The images of Peppers.tiff, Baboon.tiff, Airplane.tiff and Lena.png with the non-uniform threshold variation are as followed:

- Peppers.tiff

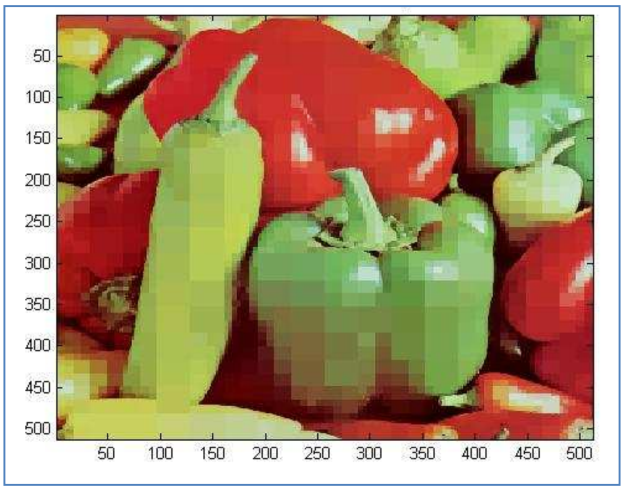

Figure 65: Decoded Image Peppers.tiff Threshold (0.3, 0.5, 0.7)

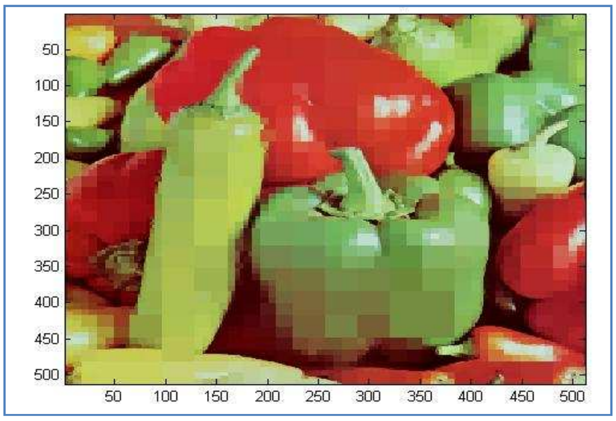

Figure 66: Decoded Image Peppers.tiff Threshold (0.3, 0.7, 0.5)

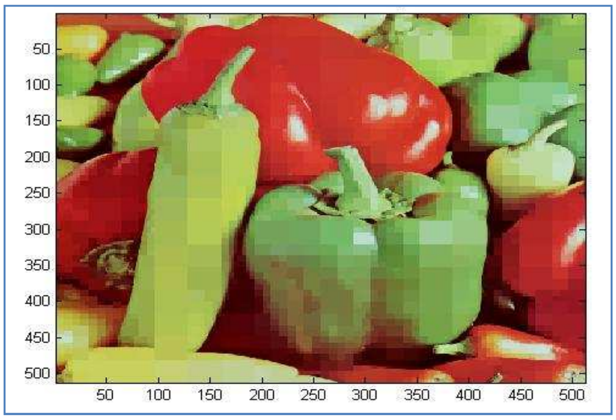

Figure 67: Decoded Image Peppers.tiff Threshold (0.5, 0.3, 0.7)

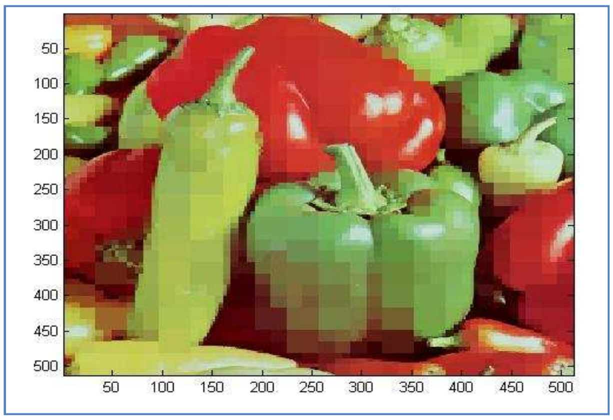

Figure 68: Decoded Image Peppers.tiff Threshold (0.5, 0.7, 0.3)

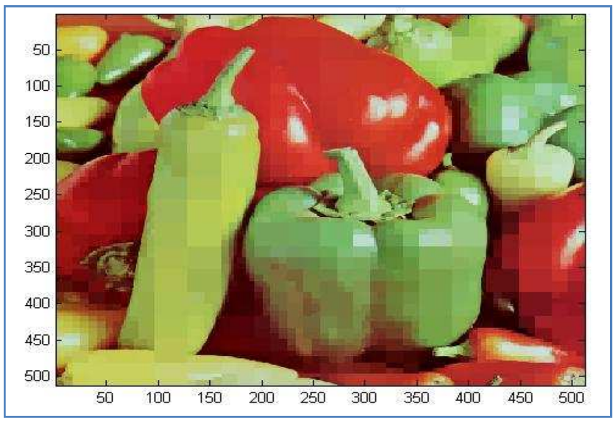

Figure 69: Decoded Image Peppers.tiff Threshold (0.7, 0.3, 0.5)

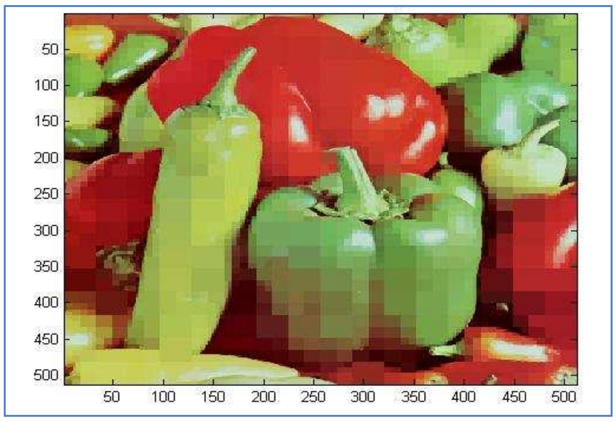

Figure 70: Decoded Image Peppers.tiff Threshold (0.7, 0.5, 0.3)

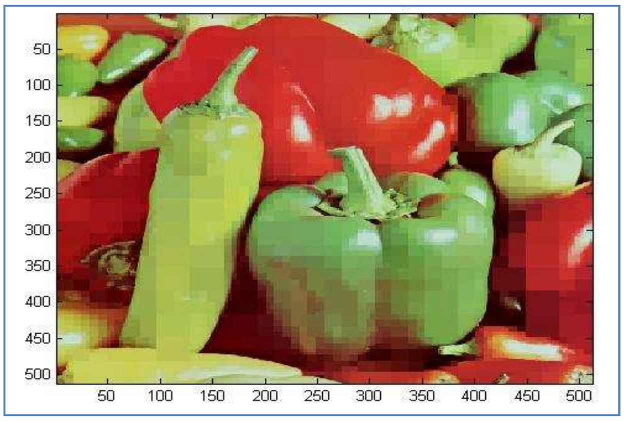

Figure 71: Decoded Image Peppers.tiff Threshold (0.8, 0.3, 0.3)

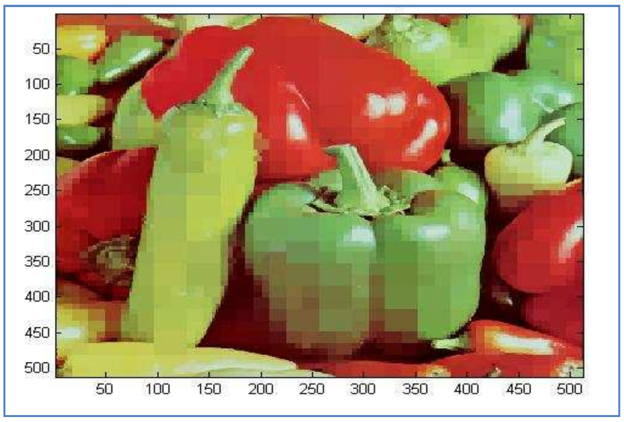

Figure 72: Decoded Image Peppers.tiff Threshold (0.3, 0.8, 0.3)

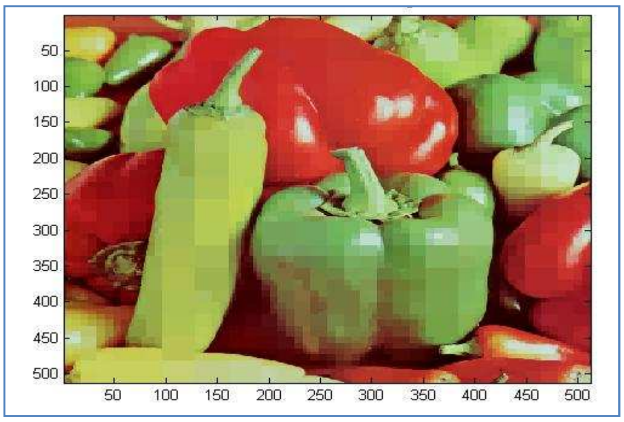

Figure 73: Decoded Image Peppers.tiff Threshold (0.3, 0.3, 0.8)

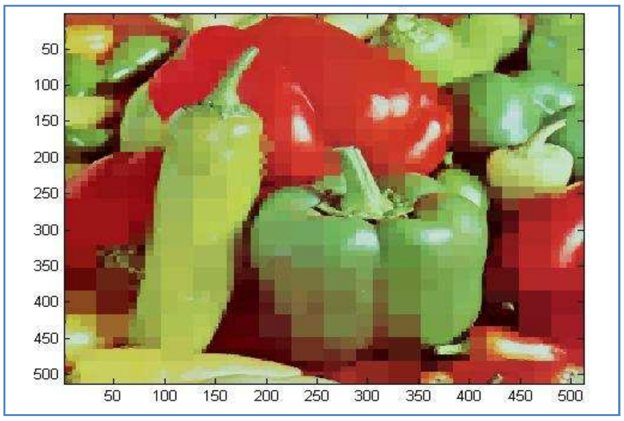

Figure 74: Decoded Image Peppers.tiff Threshold (0.8, 0.8, 0.3)

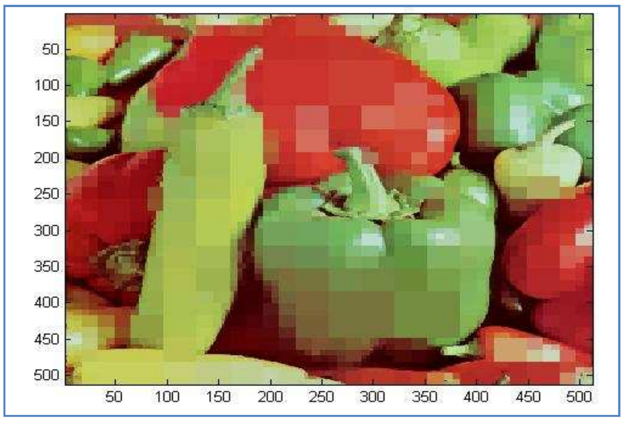

Figure 75: Decoded Image Peppers.tiff Threshold (0.3, 0.8, 0.8)

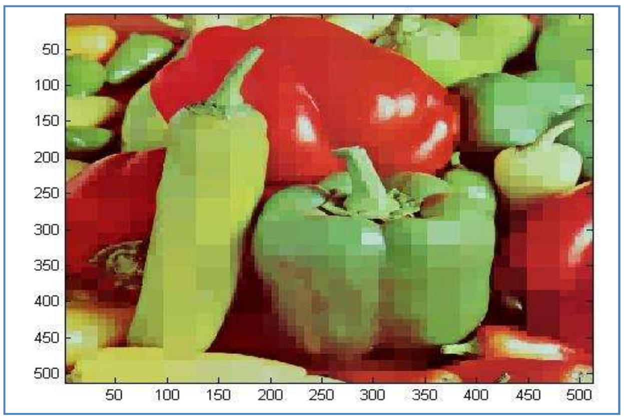

Figure 76: Decoded Image Peppers.tiff Threshold (0.8, 0.3, 0.8)

- Baboon.tiff

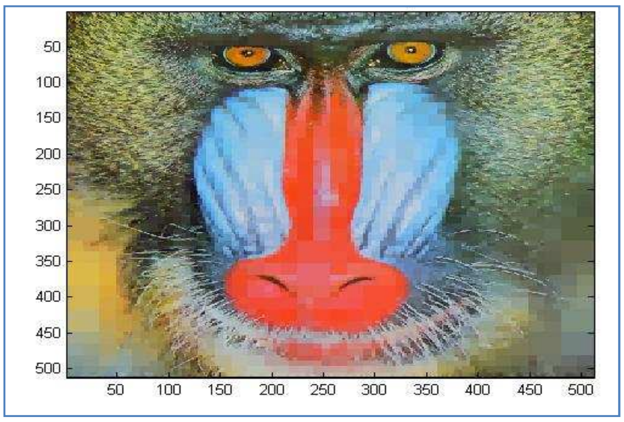

Figure 77: Decoded Image Baboon.tiff Threshold (0.3, 0.5, 0.7)

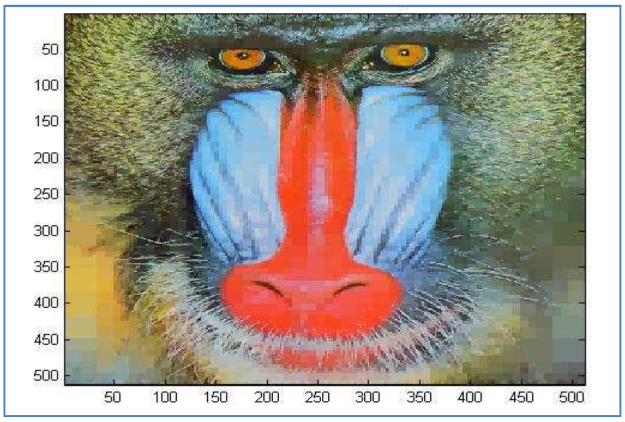

Figure 78: Decoded Image Baboon.tiff Threshold (0.3, 0.7, 0.5)

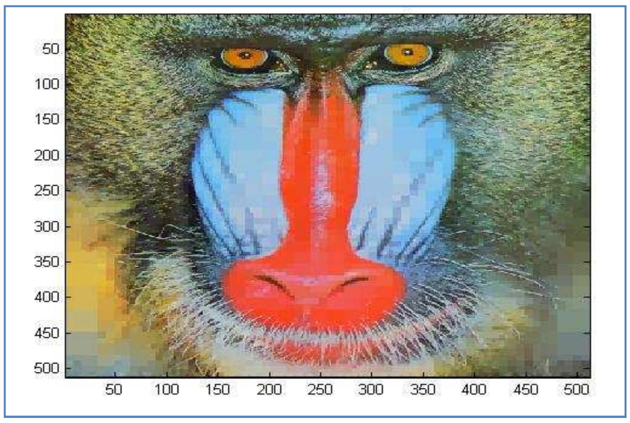

Figure 79: Decoded Image Baboon.tiff Threshold (0.5, 0.3, 0.7)

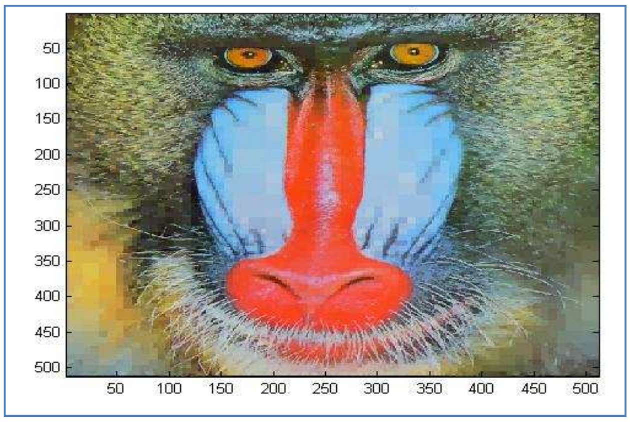

Figure 80: Decoded Image Baboon.tiff Threshold (0.5, 0.7, 0.3)

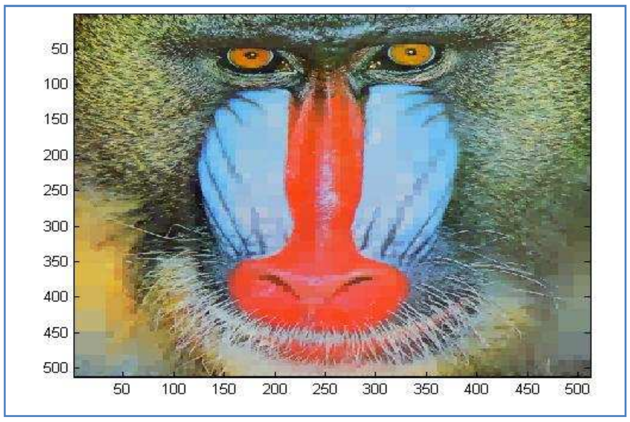

Figure 81: Decoded Image Baboon.tiff Threshold (0.7, 0.3, 0.5)

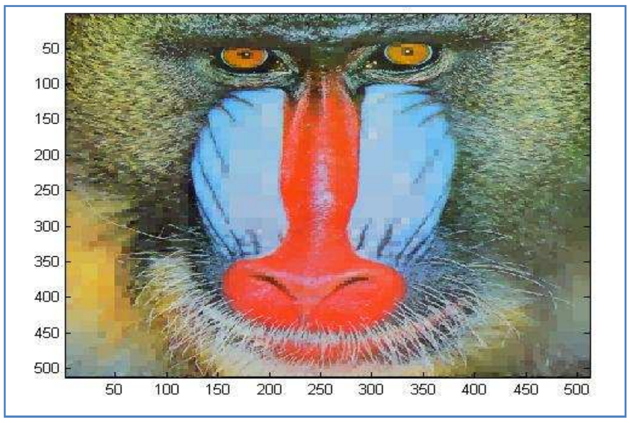

Figure 82: Decoded Image Baboon.tiff Threshold (0.7, 0.5, 0.3)

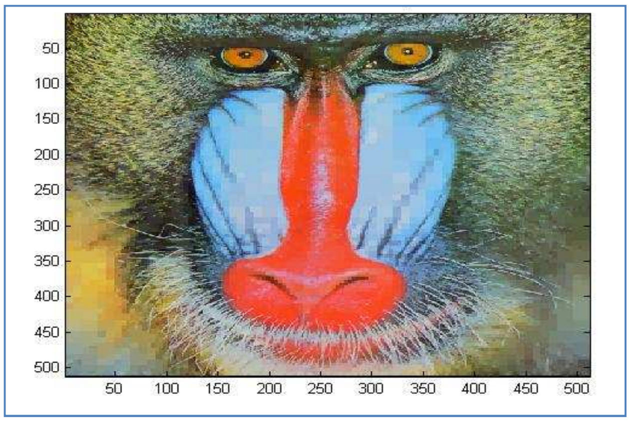

Figure 83: Decoded Image Baboon.tiff Threshold (0.8, 0.3, 0.3)

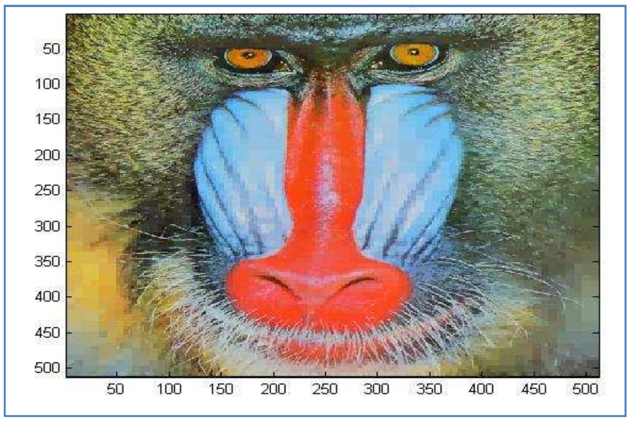

Figure 84: Decoded Image Baboon.tiff Threshold (0.3, 0.8, 0.3)

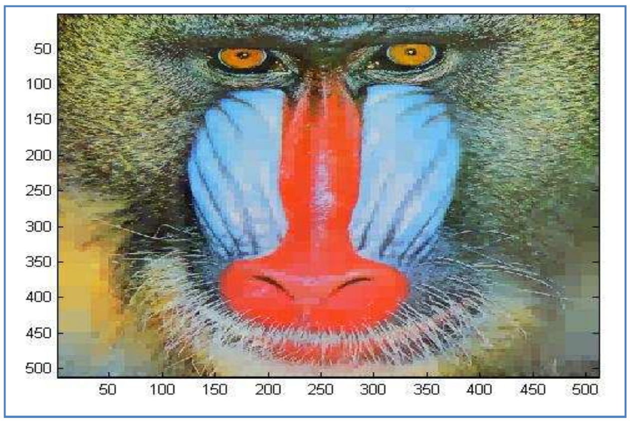

Figure 85: Decoded Image Baboon.tiff Threshold (0.3, 0.3, 0.8)

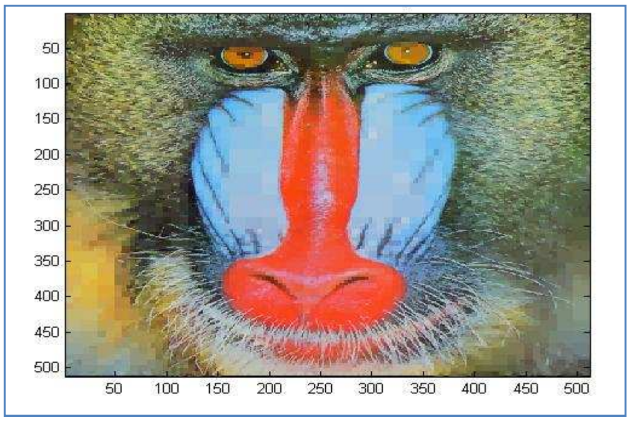

Figure 86: Decoded Image Baboon.tiff Threshold (0.8, 0.8, 0.3)

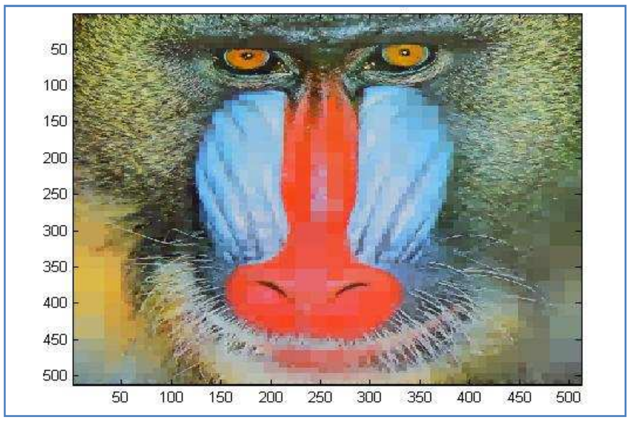

Figure 87: Decoded Image Baboon.tiff Threshold (0.3, 0.8, 0.8)

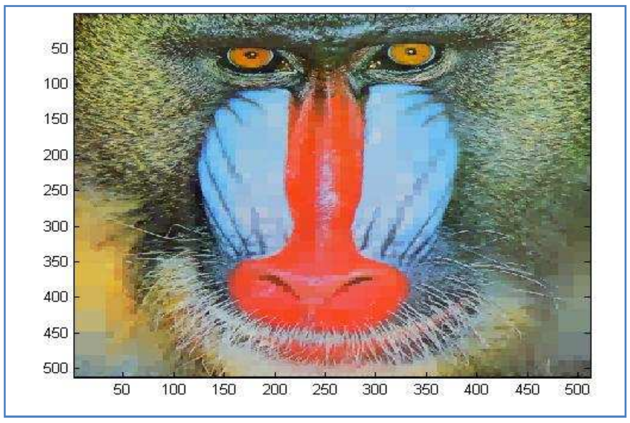

Figure 88: Decoded Image Baboon.tiff Threshold (0.8, 0.3, 0.8)

- Airplane.tiff

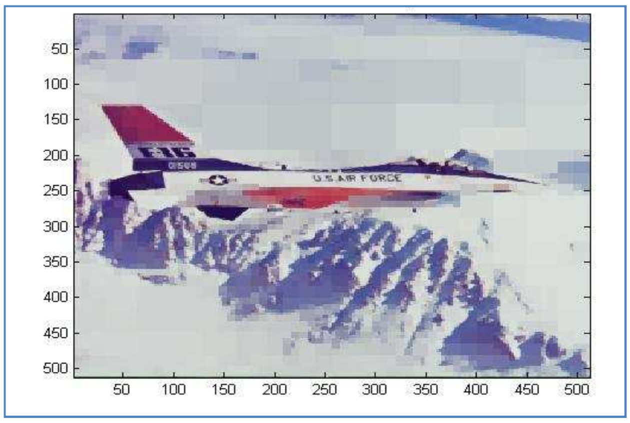

Figure 89: Decoded Image Airplane.tiff Threshold (0.3, 0.5, 0.7)

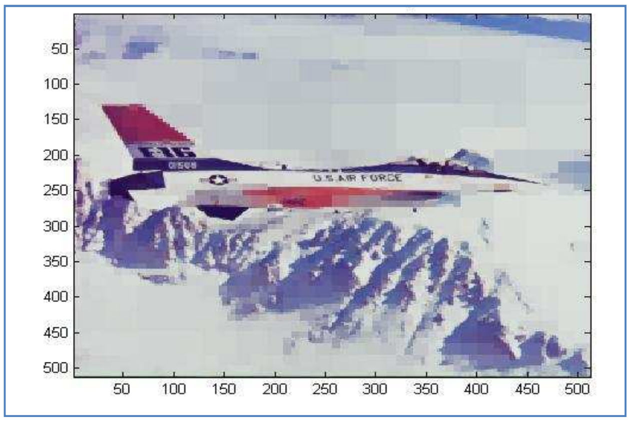

Figure 90: Decoded Image Airplane.tiff Threshold (0.3, 0.7, 0.5)

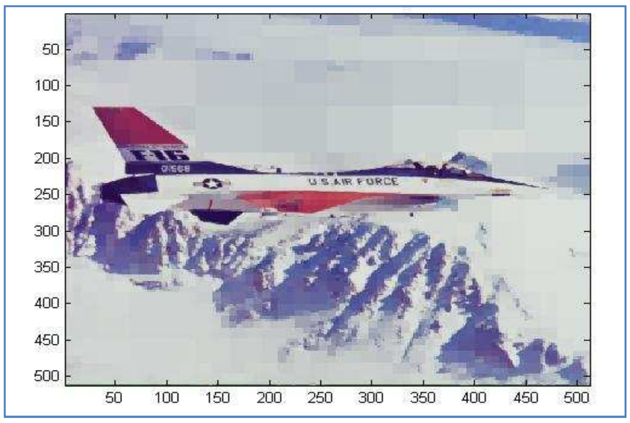

Figure 91: Decoded Image Airplane.tiff Threshold (0.5, 0.3, 0.7)

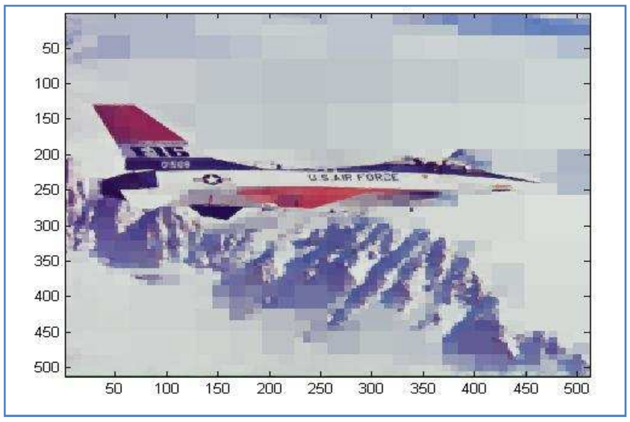

Figure 92: Decoded Image Airplane.tiff Threshold (0.5, 0.7, 0.3)

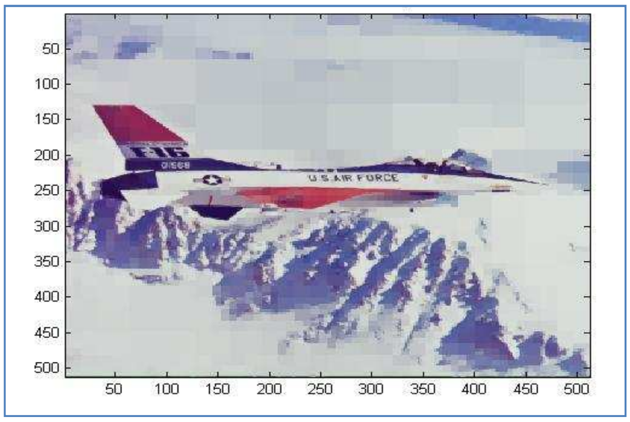

Figure 93: Decoded Image Airplane.tiff Threshold (0.7, 0.3, 0.5)

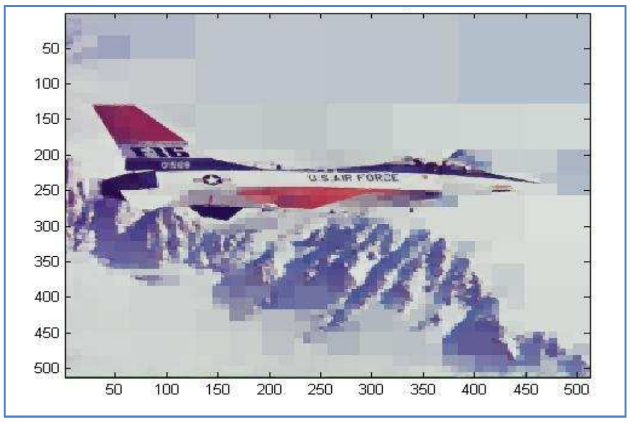

Figure 94: Decoded Image Airplane.tiff Threshold (0.7, 0.5, 0.3)

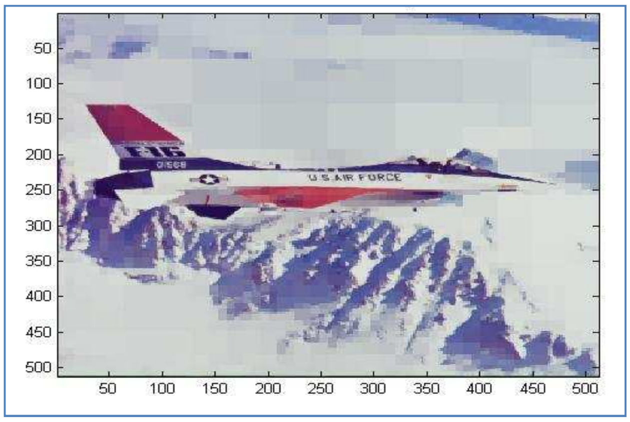

Figure 95: Decoded Image Airplane.tiff Threshold (0.8, 0.3, 0.3)

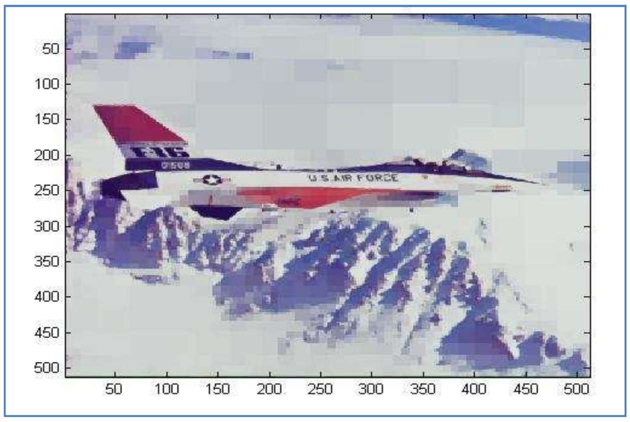

Figure 96: Decoded Image Airplane.tiff Threshold (0.3, 0.8, 0.3)

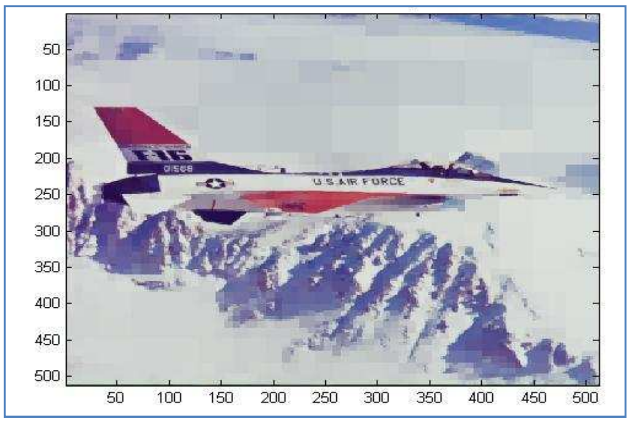

Figure 97: Decoded Image Airplane.tiff Threshold (0.3, 0.3, 0.8)

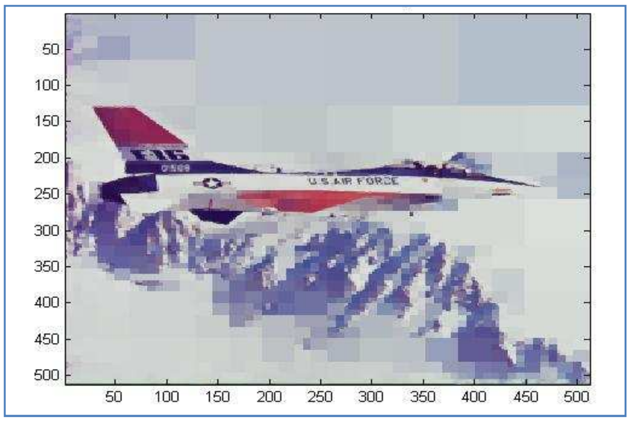

Figure 98: Decoded Image Airplane.tiff Threshold (0.8, 0.8, 0.3)

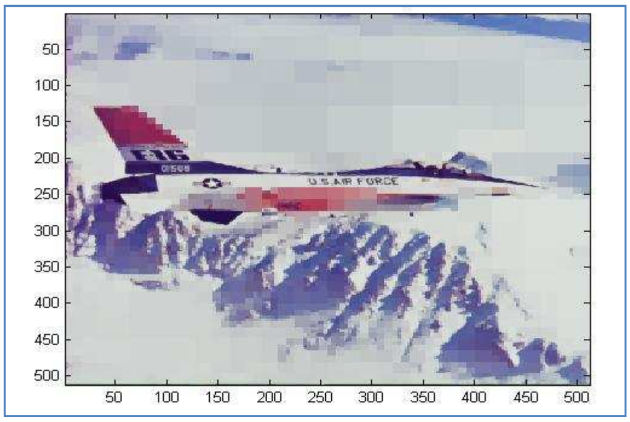

Figure 99: Decoded Image Airplane.tiff Threshold (0.3, 0.8, 0.8)

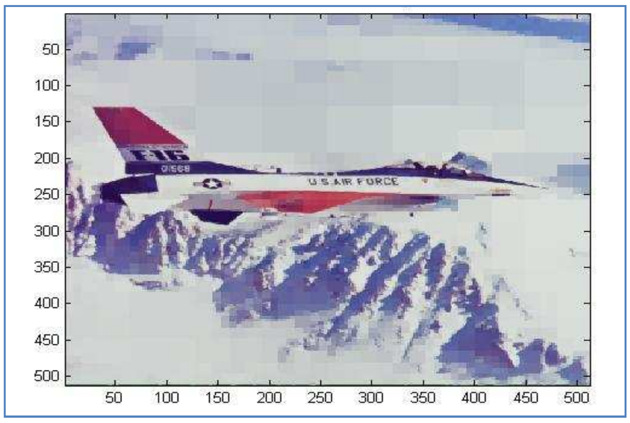

Figure 100: Decoded Image Airplane.tiff Threshold (0.8, 0.3, 0.8)

- Lena.png

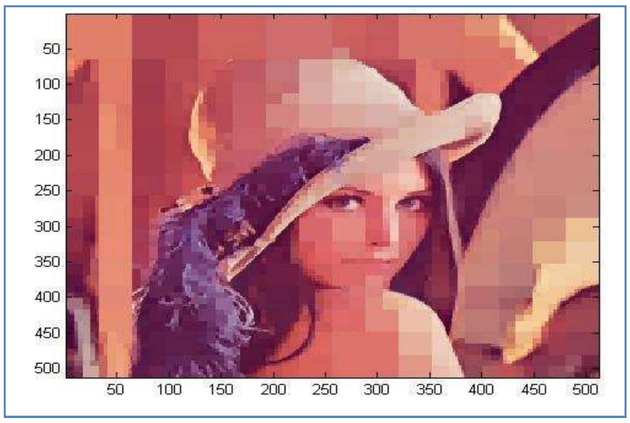

Figure 101: Decoded Image Lena.png Threshold (0.3, 0.5, 0.7)

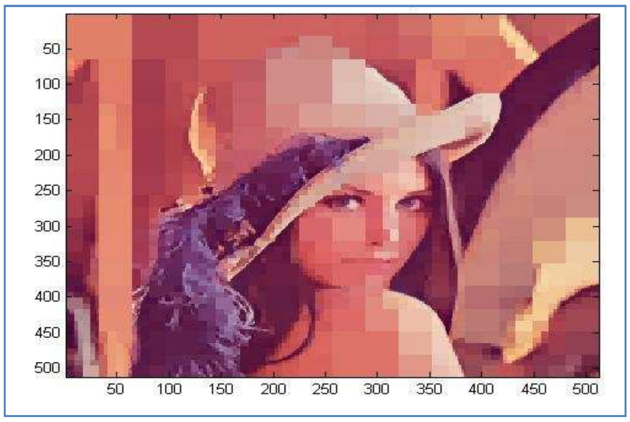

Figure 102: Decoded Image Lena.png Threshold (0.3, 0.7, 0.5)

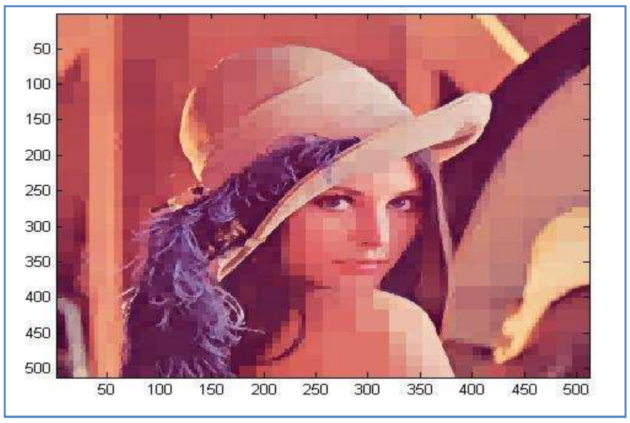

Figure 103: Decoded Image Lena.png Threshold (0.5, 0.3, 0.7)

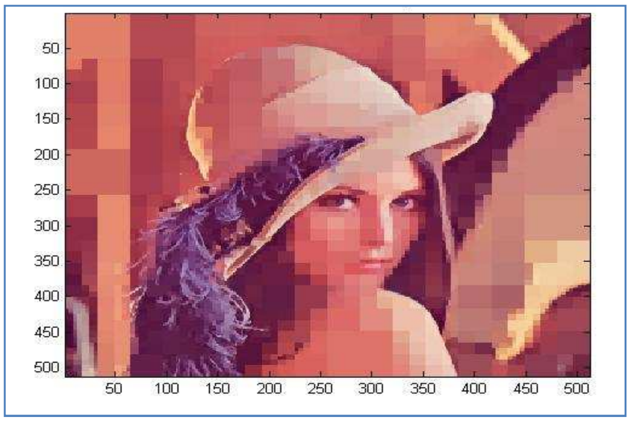

Figure 104: Decoded Image Lena.png Threshold (0.5, 0.7, 0.3)

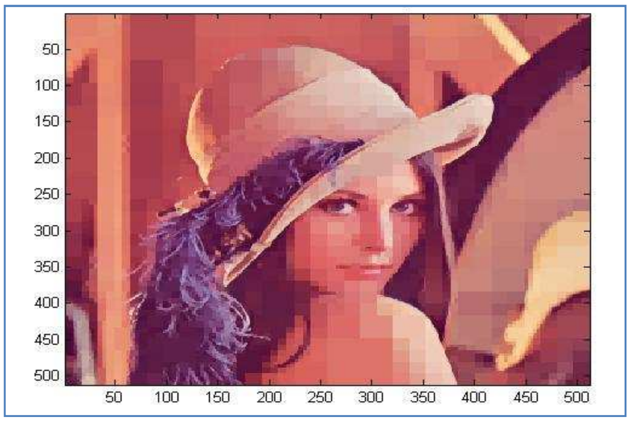

Figure 105: Decoded Image Lena.png Threshold (0.7, 0.3, 0.5)

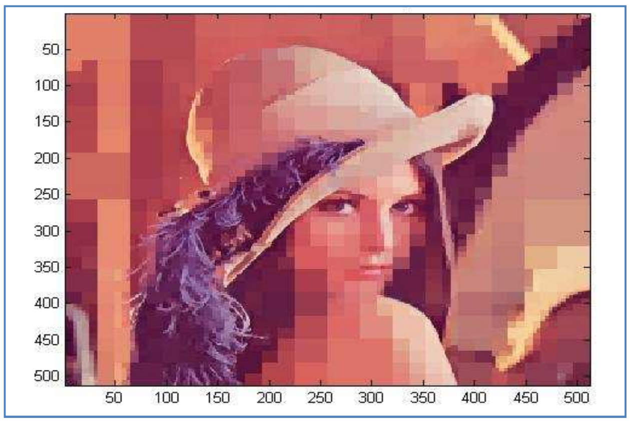

Figure 106: Decoded Image Lena.png Threshold (0.7, 0.5, 0.3)

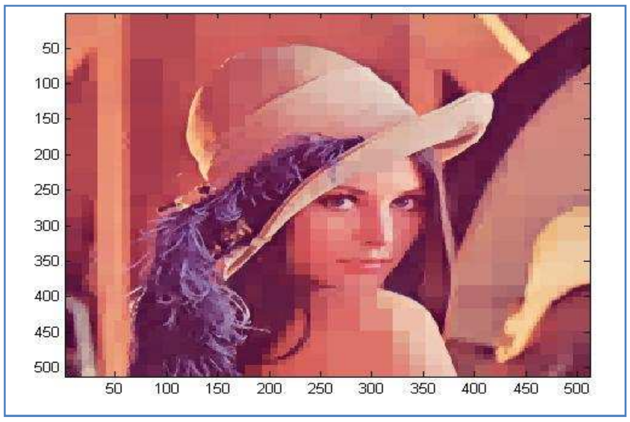

Figure 107: Decoded Image Lena.png Threshold (0.8, 0.3, 0.3)

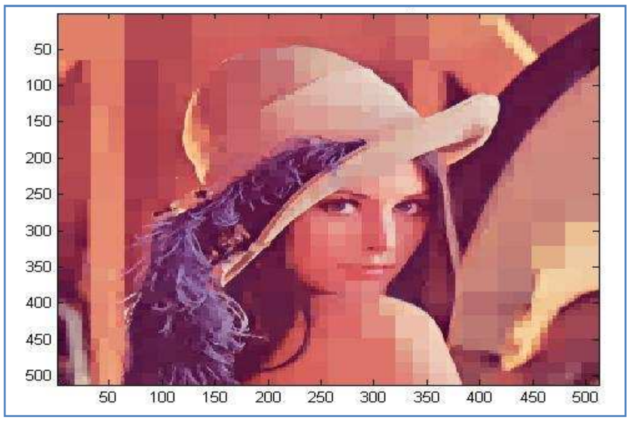
Figure 108: Decoded Image Lena.png Threshold (0.3, 0.8, 0.3)

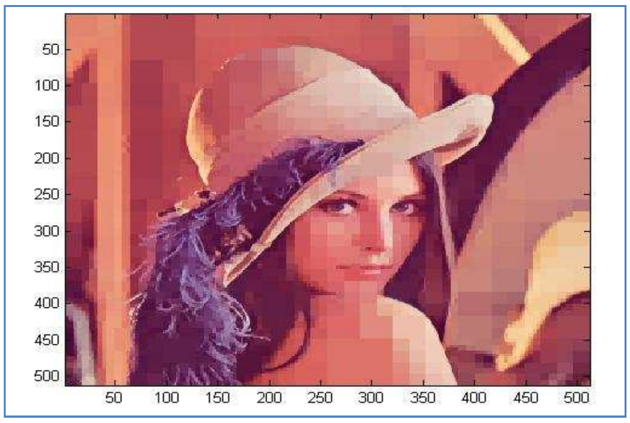
Figure 109: Decoded Image Lena.png Threshold (0.3, 0.3, 0.8)

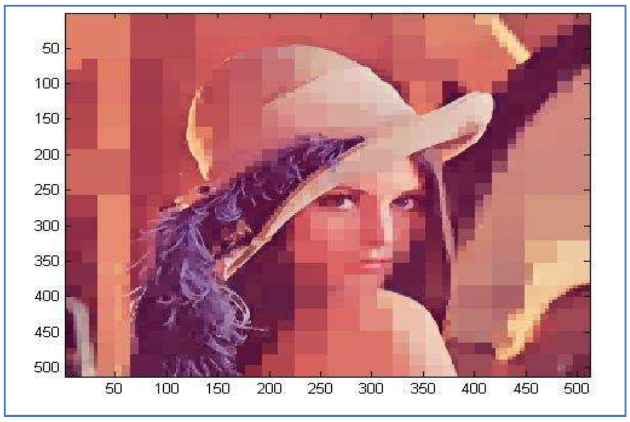
Figure 110: Decoded Image Lena.png Threshold (0.8, 0.8, 0.3)

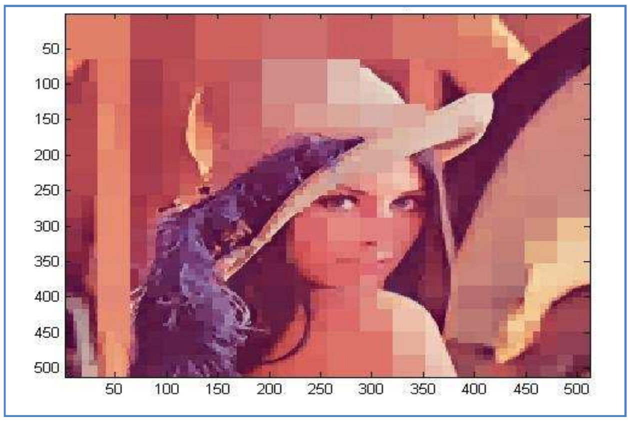

Figure 111: Decoded Image Lena.png Threshold (0.3, 0.8, 0.8)

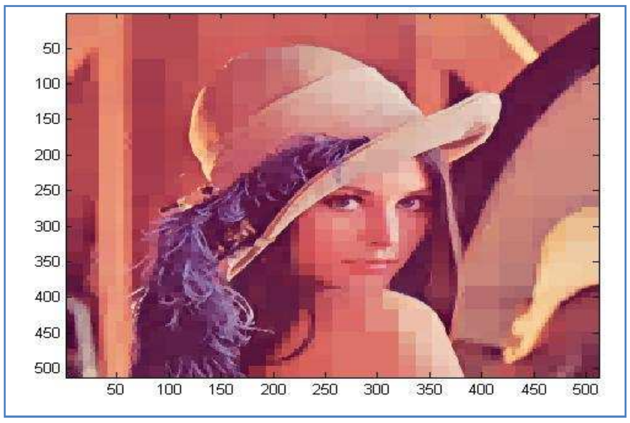

Figure 112: Decoded Image Lena.png Threshold (0.8, 0.3, 0.8)

For all of the images with the twelve variation of threshold, the quantitative analysis have been made including MSE, RMSE, PSNR, File size and CR. The analysis has been arranged in the table on the next page as followed:

➢ Peppers.tiff

Table 5: MSE, RMSE and PSNR for Peppers.tiff

No.	Threshold			MSE			RMSE			PSNR		
	R	G	B	R	G	B	R	G	B	R	G	B
1	0.3	0.5	0.7	62	111	145	7.874	10.536	12.042	30.2069	27.6776	26.5171
2	0.3	0.7	0.5	62	157	112	7.874	12.53	10.583	30.2069	26.1718	27.6386
3	0.5	0.3	0.7	107	71	128	10.3441	8.4261	11.314	27.837	29.6182	27.0587
4	0.5	0.7	0.3	107	157	68	10.3441	12.53	8.2462	27.837	26.1718	29.8057
5	0.7	0.3	0.5	134	71	99	11.5758	8.4261	9.9499	26.8598	29.6182	28.1745
6	0.7	0.5	0.3	134	112	63	11.5758	10.583	7.9373	26.8598	27.6386	30.1374
7	0.8	0.3	0.3	148	71	63	12.1655	8.4261	7.9373	26.4282	29.6182	30.1374
8	0.3	0.8	0.3	62	157	66	7.874	12.53	8.124	30.2069	26.1718	29.9354
9	0.3	0.3	0.8	56	68	128	7.4833	8.2462	11.314	30.6489	29.8057	27.0587
10	0.8	0.8	0.3	158	158	68	12.5698	12.57	8.2462	26.1442	26.1442	29.8057
11	0.3	0.8	0.8	62	163	161	7.874	12.767	12.689	30.2069	26.0089	26.0625
12	0.8	0.3	0.8	148	71	128	12.1655	8.4261	11.314	26.4282	29.6182	27.0587

Table 6: File Size and CR for Peppers.tiff

No.	Threshold			File Size		CR		
	R	G	B	Original	Decoded	R	G	B
1	0.3	0.5	0.7	35.7 KB	33.3 KB	1.43	2.00	3.33
2	0.3	0.7	0.5	35.7 KB	33.2 KB	1.43	3.33	2.00
3	0.5	0.3	0.7	35.7 KB	33.2 KB	2.00	1.43	3.33
4	0.5	0.7	0.3	35.7 KB	33.4 KB	2.00	3.33	1.43
5	0.7	0.3	0.5	35.7 KB	33.4 KB	3.33	1.43	2.00
6	0.7	0.5	0.3	35.7 KB	33.3 KB	3.33	2.00	1.43
7	0.8	0.3	0.3	35.7 KB	33.7 KB	5.00	1.43	1.43
8	0.3	0.8	0.3	35.7 KB	33.9 KB	1.43	5.00	1.43
9	0.3	0.3	0.8	35.7 KB	33.6 KB	1.43	1.43	5.00
10	0.8	0.8	0.3	35.7 KB	33.0 KB	5.00	5.00	1.43
11	0.3	0.8	0.8	35.7 KB	32.4 KB	1.43	5.00	5.00
12	0.8	0.3	0.8	35.7 KB	33.0 KB	5.00	1.43	5.00

- Baboon.tiff

Table 7: MSE, RMSE and PSNR for Baboon.tiff

No.	Threshold			MSE			RMSE			PSNR		
	R	G	B	R	G	B	R	G	B	R	G	B
1	0.3	0.5	0.7	60	101	132	7.746	10.0499	11.4891	30.3493	28.0876	26.9251
2	0.3	0.7	0.5	58	109	103	7.6158	10.4403	10.1489	30.4965	27.7565	28.0024
3	0.5	0.3	0.7	97	60	121	9.8489	7.746	11	28.2631	30.3493	27.3029
4	0.5	0.7	0.3	97	104	61	9.8489	10.198	7.8102	28.2631	27.9605	30.2775
5	0.7	0.3	0.5	105	60	102	10.247	7.746	10.0995	27.9189	30.3493	28.0448
6	0.7	0.5	0.3	114	98	62	10.6771	9.8995	7.874	27.5618	28.2185	30.2069
7	0.8	0.3	0.3	105	56	57	10.247	7.4833	7.5498	27.9189	30.6489	30.5721
8	0.3	0.8	0.3	54	84	61	7.3485	9.1652	7.8102	30.8069	28.888	30.2775
9	0.3	0.3	0.8	54	60	108	7.3485	7.746	10.3923	30.8069	30.3493	27.7966
10	0.8	0.8	0.3	140	135	62	11.8322	11.619	7.874	26.6695	26.8275	30.2069
11	0.3	0.8	0.8	60	136	153	7.746	11.6619	12.3693	30.3493	26.7954	26.2839
12	0.8	0.3	0.8	105	60	121	10.247	7.746	11	27.9189	30.3493	27.3029

Table 8: File Size and CR for Baboon.tiff

No.	Threshold			File Size		CR		
	R	G	B	Original	Decoded	R	G	B
1	0.3	0.5	0.7	54.7 KB	45.3 KB	1.43	2.00	3.33
2	0.3	0.7	0.5	54.7 KB	46.2 KB	1.43	3.33	2.00
3	0.5	0.3	0.7	54.7 KB	48.1 KB	2.00	1.43	3.33
4	0.5	0.7	0.3	54.7 KB	47.9 KB	2.00	3.33	1.43
5	0.7	0.3	0.5	54.7 KB	48.1 KB	3.33	1.43	2.00
6	0.7	0.5	0.3	54.7 KB	48.0 KB	3.33	2.00	1.43
7	0.8	0.3	0.3	54.7 KB	49.7 KB	5.00	1.43	1.43
8	0.3	0.8	0.3	54.7 KB	49.6 KB	1.43	5.00	1.43
9	0.3	0.3	0.8	54.7 KB	48.7 KB	1.43	1.43	5.00
10	0.8	0.8	0.3	54.7 KB	47.7 KB	5.00	5.00	1.43
11	0.3	0.8	0.8	54.7 KB	45.0 KB	1.43	5.00	5.00
12	0.8	0.3	0.8	54.7 KB	48.1 KB	5.00	1.43	5.00

➢ Airplane.tiff

Table 9: MSE, RMSE and PSNR for Airplane.tiff

No.	Threshold			MSE			RMSE			PSNR		
	R	G	B	R	G	B	R	G	B	R	G	B
1	0.3	0.5	0.7	61	107	81	7.8102	10.3441	9	30.2775	27.837	29.046
2	0.3	0.7	0.5	61	134	107	7.8102	11.5758	10.3441	30.2775	26.8598	27.837
3	0.5	0.3	0.7	99	63	88	9.9499	7.9373	9.3808	28.1745	30.1374	28.686
4	0.5	0.7	0.3	98	109	58	9.8995	10.4403	7.6158	28.2185	27.7565	30.4965
5	0.7	0.3	0.5	99	63	63	9.9499	7.9373	7.9373	28.1745	30.1374	30.1374
6	0.7	0.5	0.3	95	102	58	9.7468	10.0995	7.6158	28.3536	28.0448	30.4965
7	0.8	0.3	0.3	99	63	58	9.9499	7.9373	7.6158	28.1745	30.1374	30.4965
8	0.3	0.8	0.3	61	105	58	7.8102	10.247	7.6158	30.2775	27.9189	30.4965
9	0.3	0.3	0.8	56	63	58	7.4833	7.9373	7.6158	30.6489	30.1374	30.4965
10	0.8	0.8	0.3	118	121	58	10.863	11	7.6158	27.412	27.3029	30.4965
11	0.3	0.8	0.8	61	137	107	7.8102	11.7047	10.3441	30.2775	26.7636	27.837
12	0.8	0.3	0.8	99	63	91	9.9499	7.9373	9.5394	28.1745	30.1374	28.5404

Table 10: File Size and CR for Airplane.tiff

No.	Threshold			File Size		CR		
	R	G	B	Original	Decoded	R	G	B
1	0.3	0.5	0.7	33.7 KB	30.6 KB	1.43	2.00	3.33
2	0.3	0.7	0.5	33.7 KB	30.6 KB	1.43	3.33	2.00
3	0.5	0.3	0.7	33.7 KB	30.9 KB	2.00	1.43	3.33
4	0.5	0.7	0.3	33.7 KB	28.6 KB	2.00	3.33	1.43
5	0.7	0.3	0.5	33.7 KB	30.9 KB	3.33	1.43	2.00
6	0.7	0.5	0.3	33.7 KB	28.3 KB	3.33	2.00	1.43
7	0.8	0.3	0.3	33.7 KB	30.9 KB	5.00	1.43	1.43
8	0.3	0.8	0.3	33.7 KB	30.7 KB	1.43	5.00	1.43
9	0.3	0.3	0.8	33.7 KB	30.9 KB	1.43	1.43	5.00
10	0.8	0.8	0.3	33.7 KB	28.0 KB	5.00	5.00	1.43
11	0.3	0.8	0.8	33.7 KB	30.6 KB	1.43	5.00	5.00
12	0.8	0.3	0.8	33.7 KB	30.9 KB	5.00	1.43	5.00

➢ Lena.png

Table 11: MSE, RMSE and PSNR for Lena.png

No.	Threshold			MSE			RMSE			PSNR		
	R	G	B	R	G	B	R	G	B	R	G	B
1	0.3	0.5	0.7	63	99	91	7.9373	9.9499	9.5394	30.1374	28.1745	28.5404
2	0.3	0.7	0.5	63	130	99	7.9373	11.4018	9.9499	30.1374	26.9914	28.1745
3	0.5	0.3	0.7	92	62	73	9.5917	7.874	8.544	28.4929	30.2069	29.4976
4	0.5	0.7	0.3	106	133	66	10.296	11.5326	8.124	27.8777	26.8923	29.9354
5	0.7	0.3	0.5	92	62	73	9.5917	7.874	8.544	28.4929	30.2069	29.4976
6	0.7	0.5	0.3	124	106	66	11.136	10.2956	8.124	27.1966	27.8777	29.9354
7	0.8	0.3	0.3	92	61	66	9.5917	7.8102	8.124	28.4929	30.2775	29.9354
8	0.3	0.8	0.3	63	99	66	7.9373	9.9499	8.124	30.1374	28.1745	29.9354
9	0.3	0.3	0.8	63	62	73	7.9373	7.874	8.544	30.1374	30.2069	38.8142
10	0.8	0.8	0.3	124	133	66	11.136	11.5326	8.124	27.1966	26.8923	29.9354
11	0.3	0.8	0.8	63	130	99	7.9373	11.4018	9.9499	30.1374	26.9914	28.1745
12	0.8	0.3	0.8	92	62	73	9.5917	7.874	8.544	28.4929	30.2069	29.4976

Table 12: File Size and CR for Lena.png

No.	Threshold			File Size		CR		
	R	G	B	Original	Decoded	R	G	B
1	0.3	0.5	0.7	34.3 KB	30.1 KB	1.43	2.00	3.33
2	0.3	0.7	0.5	34.3 KB	30.1 KB	1.43	3.33	2.00
3	0.5	0.3	0.7	34.3 KB	31.6 KB	2.00	1.43	3.33
4	0.5	0.7	0.3	34.3 KB	30.7 KB	2.00	3.33	1.43
5	0.7	0.3	0.5	34.3 KB	31.6 KB	3.33	1.43	2.00
6	0.7	0.5	0.3	34.3 KB	30.5 KB	3.33	2.00	1.43
7	0.8	0.3	0.3	34.3 KB	31.7 KB	5.00	1.43	1.43
8	0.3	0.8	0.3	34.3 KB	31.2 KB	1.43	5.00	1.43
9	0.3	0.3	0.8	34.3 KB	31.6 KB	1.43	1.43	5.00
10	0.8	0.8	0.3	34.3 KB	30.4 KB	5.00	5.00	1.43
11	0.3	0.8	0.8	34.3 KB	29.9 KB	1.43	5.00	5.00
12	0.8	0.3	0.8	34.3 KB	31.6 KB	5.00	1.43	5.00

In this non-uniform threshold variation, we want to find which colour channel most contribute to the error. We will compare the average MSE and threshold value. By knowing this, we will consider that the threshold for that colour channel (highest average MSE) should be the lowest compared to other colour channels to get the better quality of image. So, the average MSE for each variation of threshold for each images have been calculated as followed:

Table 13: Comparison of Threshold and Average MSE

No.	Threshold			Average MSE			
	R	G	B	Peppers.tiff	Baboon.tiff	Airplane.tiff	Lena.png
1	0.3	0.5	0.7	106	98	83	84
2	0.3	0.7	0.5	110	90	101	97
3	0.5	0.3	0.7	102	93	83	76
4	0.5	0.7	0.3	166	87	88	102
5	0.7	0.3	0.5	101	89	75	76
6	0.7	0.5	0.3	103	91	85	99
7	0.8	0.3	0.3	94	73	73	73
8	0.3	0.8	0.3	95	66	75	76
9	0.3	0.3	0.8	84	74	59	66
10	0.8	0.8	0.3	128	112	99	108
11	0.3	0.8	0.8	129	116	102	97
12	0.8	0.3	0.8	116	95	84	76

Then, we analyze the comparison between threshold and average MSE for each images; Peppers.tiff, Baboon.tiff, Airplane.tiff and Lena.png. The average MSE being arranged in descending order, so we can observe the highest threshold belongs to which colour channel.

➢ Peppers.tiff

R	**G**	B	**Average MSE**
0.5	**0.7**	0.3	**166**
0.3	0.7	0.5	110
0.3	0.5	0.7	106
0.7	0.5	0.3	103
0.5	0.3	0.7	102
0.7	0.3	0.5	101

R	**G**	B	**Average MSE**
0.3	**0.8**	0.8	**129**
0.8	0.8	0.3	128
0.8	0.3	0.8	116

R	**G**	B	**Average MSE**
0.3	**0.8**	0.3	**95**
0.8	0.3	0.3	94
0.3	0.3	0.8	84

- For Peppers.tiff, the Green channel contributes the highest error when its threshold value is highest.
- So, to obtain better quality of image, the threshold value for Green channel should be lowest compared with Red and Blue channel.

➢ Baboon.tiff

R	G	**B**	**Average MSE**
0.3	0.5	**0.7**	**98**
0.5	0.3	0.7	93
0.7	0.5	0.3	91
0.3	0.7	0.5	90
0.7	0.3	0.5	89
0.5	0.7	0.3	87

R	G	**B**	**Average MSE**
0.3	0.3	**0.8**	**74**
0.8	0.3	0.3	73
0.3	0.8	0.3	66

R	G	**B**	**Average MSE**
0.3	0.8	**0.8**	**116**
0.8	0.8	0.3	112
0.8	0.3	0.8	95

- For Baboon.tiff, the Blue channel contributes the highest error when its threshold value is highest.
- So, to obtain better quality of image, the threshold value for Blue channel should be lowest compared with Red and Green channel.

➢ Airplane.tiff

R	**G**	B	**Average MSE**
0.3	**0.7**	0.5	**101**
0.5	0.7	0.3	88
0.7	0.5	0.3	85
0.5	0.3	0.7	83
0.3	0.5	0.7	83
0.7	0.3	0.5	75

R	**G**	B	**Average MSE**
0.3	**0.8**	0.3	**75**
0.8	0.3	0.3	73
0.3	0.3	0.8	59

R	**G**	B	**Average MSE**
0.3	**0.8**	0.8	**102**
0.8	0.8	0.3	99
0.8	0.3	0.8	84

- For Airplane.tiff, the Green channel contributes the highest error when its threshold value is highest.
- So, to obtain better quality of image, the threshold value for Green channel should be lowest compared with Red and Blue channel.

➢ Lena.png

R	**G**	B	**Average MSE**
0.5	**0.7**	0.3	**102**
0.7	0.5	0.3	99
0.3	0.7	0.5	97
0.3	0.5	0.7	84
0.5	0.3	0.7	76
0.7	0.3	0.5	76

R	**G**	B	**Average MSE**
0.3	**0.8**	0.3	**76**
0.8	0.3	0.3	73
0.3	0.3	0.8	66

R	**G**	B	**Average MSE**
0.8	**0.8**	0.3	**108**
0.3	0.8	0.8	97
0.8	0.3	0.8	76

- For Lena.png, the Green channel contributes the highest error when its threshold value is highest.
- So, to obtain better quality of image, the threshold value for Green channel should be lowest compared with Red and Blue channel.

From the analyses that have been made for non-uniform threshold variation, we also can determine the best non-uniform threshold combination. We can do the comparison between threshold combination and RMSE and also PSNR. The average values of RMSE and PSNR have been calculated to determine the best non-uniform threshold combination.

As we know, the values of MSE and RMSE are directly proportional between each other's and the values of MSE and PSNR are inversely proportional between each other's. From the quantitative analysis, the quality of images being determined by the lowest values of MSE and RMSE and highest value of PSNR. The average MSE and PSNR values with the respective threshold combination are as followed:

Table 14: Comparison of Threshold and Average RMSE, PSNR

No.	Threshold			Peppers.tiff		Baboon.tiff		Airplane.tiff		Lena.png	
	R	G	B	RMSE	PSNR	RMSE	PSNR	RMSE	PSNR	RMSE	PSNR
1	0.3	0.5	0.7	10.15	28.13	9.76	28.45	9.05	29.05	9.14	28.95
2	0.3	0.7	0.5	10.33	28.01	9.40	28.76	9.91	28.33	9.76	28.43
3	0.5	0.3	0.7	10.03	28.17	9.53	28.64	9.09	29.00	8.67	29.40
4	0.5	0.7	0.3	10.37	27.94	9.29	28.83	9.32	28.82	9.98	28.24
5	0.7	0.3	0.5	9.98	28.07	9.36	28.77	8.61	29.84	8.67	29.40
6	0.7	0.5	0.3	10.03	28.21	9.48	28.66	9.15	28.97	9.85	28.34
7	0.8	0.3	0.3	9.51	28.73	8.43	29.71	8.50	29.60	8.51	29.57
8	0.3	0.8	0.3	9.54	28.77	8.11	30.00	8.56	29.56	8.67	29.42
9	0.3	0.3	0.8	9.01	29.17	8.50	29.65	7.68	30.43	8.12	33.05
10	0.8	0.8	0.3	11.13	27.37	10.44	27.90	9.83	28.40	10.26	28.01
11	0.3	0.8	0.8	11.11	27.43	10.60	27.81	9.95	28.29	9.76	28.43
12	0.8	0.3	0.8	10.64	27.70	9.66	28.52	9.14	28.95	8.67	29.40

The graph of threshold combination versus RMSE & PSNR is plotted as in the next page. From the plotted graph, we can observe the best combination of non-uniform threshold.

➢ Peppers.tiff

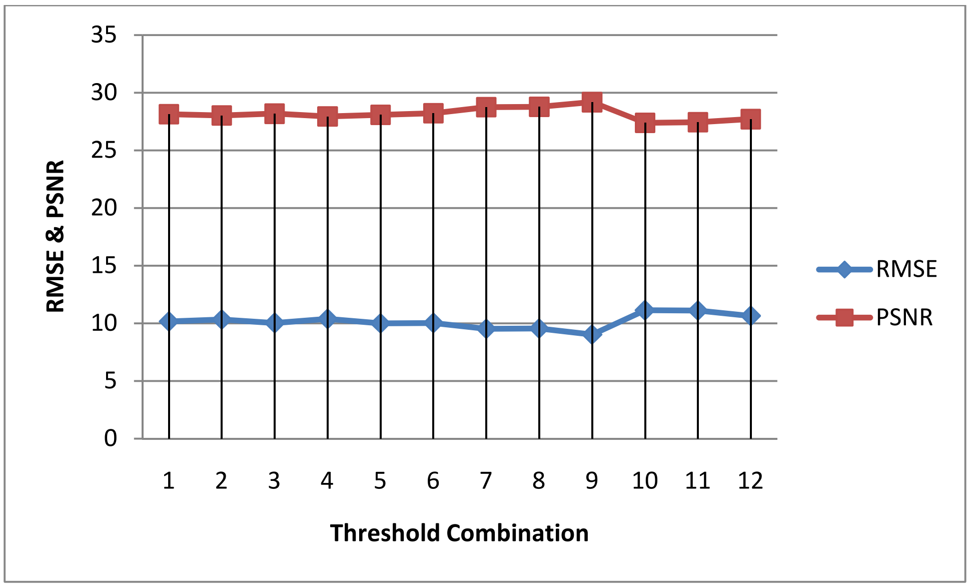

Figure 113: Threshold Combination versus RMSE & PSNR for Peppers.tiff

➢ Baboon.tiff

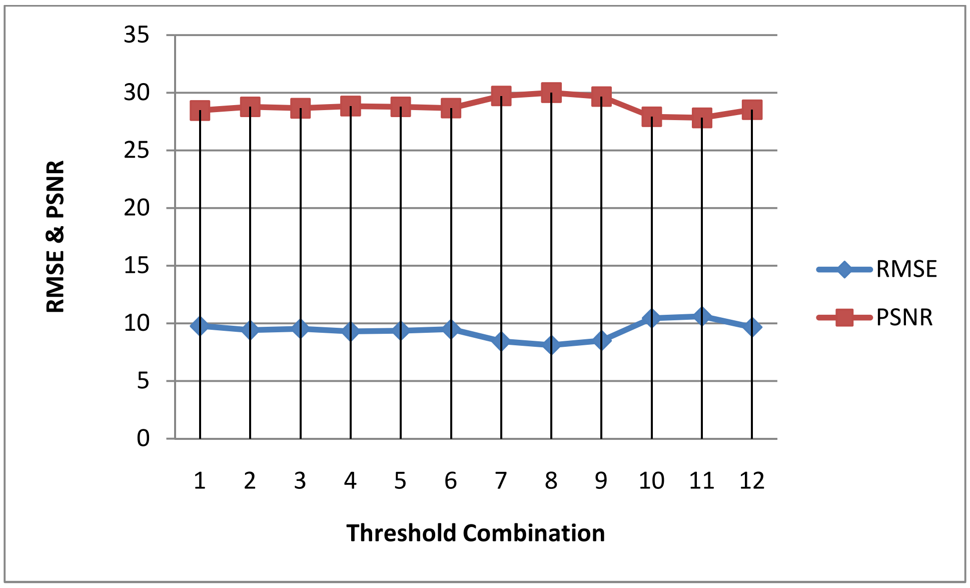

Figure 114: Threshold Combination versus RMSE & PSNR for Baboon.tiff

- Airplane.tiff

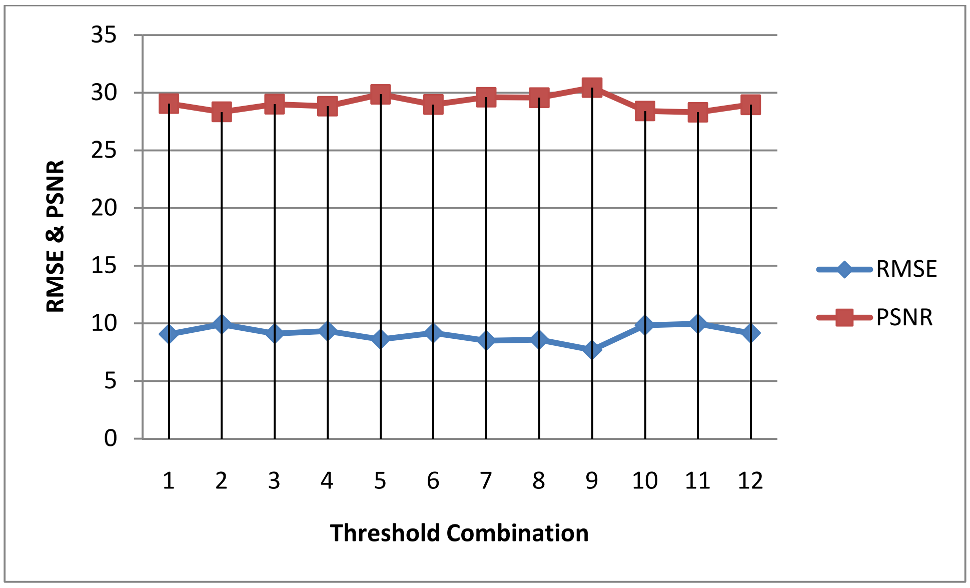

Figure 115: Threshold Combination versus RMSE & PSNR for Airplane.tiff

- Lena.png

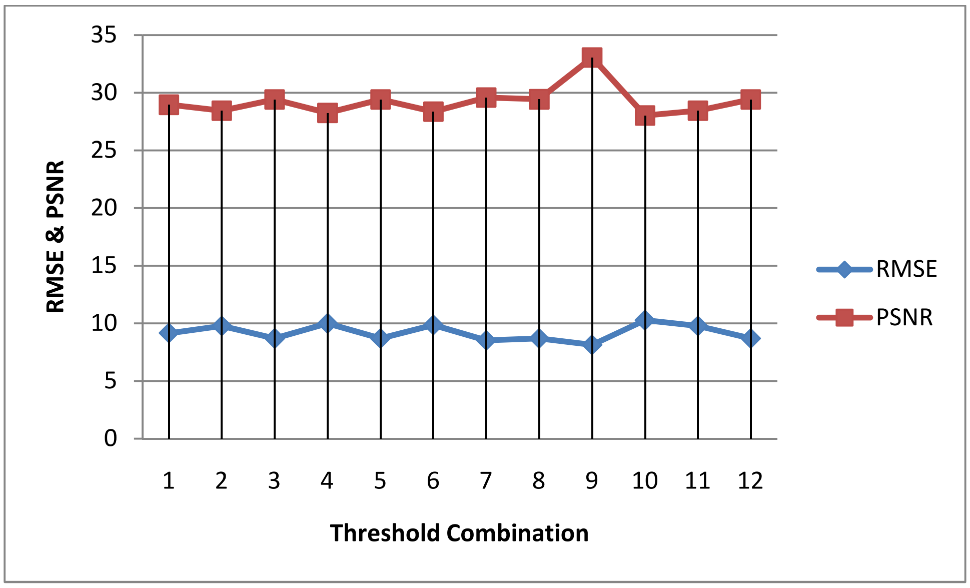

Figure 116: Threshold Combination versus RMSE & PSNR for Lena.png

From the plotted graph in the previous pages, for the Peppers.tiff image, from Figure 113, we can see the threshold combination which achieves lowest RMSE and highest PSNR is the ninth combination, which is 0.3, 0.3, 0.8. For the Baboon.tiff image, from Figure 114, we can see the threshold combination which achieves lowest RMSE and PSNR is the eighth combination, which is 0.3, 0.8, 0.3. For the Airplane.tiff image, from Figure 115, we can see the threshold combination which achieves lowest RMSE and PSNR is the ninth combination, which is 0.3, 0.3, 0.8. For the Lena.png image, from Figure 116, we can see the threshold combination which achieves lowest RMSE and PSNR is the ninth combination, which is 0.3, 0.3, 0.8.

For the RGB Quadtree Decomposition and Parametric Line Fitting method for image compression, from the analysis and output images of variation threshold in uniform and non-uniform patterns, we can see the quality of image Baboon.tiff is better than others even all the Red, Green and Blue channels are at high threshold. The Baboon.tiff image looks clear and less blur. The reason is we can see the pure colours of the image Baboon.tiff itself which contains all of the RGB colour components.

CHAPTER 5
CONCLUSION AND RECOMMENDATION

5.1 Conclusion

In summary, to define a Bézier curve of degree n, we need to choose $n + 1$ control points in space (R^3, where $s = 2$ or 3) so that they roughly indicate the shape of the desired curve while to define a Bézier surface, we need to choose $(n + 1)(m + 1)$ control points [26]. The concept of Bézier method including Bézier curves, Bézier surfaces, theory, properties and applications have been generated and proved by MATLAB simulation. The quadtree decomposition and parametric line fitting method for image compression also have been proved by MATLAB simulation. For the image compression, we can see the quality of image Baboon.tiff is better than others even all the Red, Green and Blue channels are at high threshold. The reason is we can see the pure colours of the image Baboon.tiff itself which contains all of the RGB colour components.

5.2 Recommendation

For the extension and future works, there are few recommendations that can be done:

- For image compression using the quadtree decomposition and parametric line fitting, we can try to use higher degree of line fitting such as quadratic or cubic instead of parametric line fitting.
- We can try to apply filtering such as using wavelet Bior 3.5 or Gaussian for the input image or output image of image compression using quadtree decomposition and parametric line fitting method.

REFERENCES

[1] R.E. Barnhill and W. Boehm 1984, Computer Aided Geometric Design, Amsterdam, North Holland

[2] Sambunath Biswas and Brian C. Lovell 2008, Bézier and Splines in Image Processing and Machine Vision, London, Springer

[3] D. Marsh 2004, Applied Geometry for Computer Graphics and CAD, Edinburgh, Springer

[4] http://en.wikipedia.org/wiki/Bézier_curve

[5] S. Kaleem and A. Abrahamsen 2000, Cubic Bézier Curves

[6] http://en.wikipedia.org/wiki/Bézier_surface

[7] G. Farin and D. Hansford 2000, The Essentials of CAGD, Arizona, A K Peters

[8] http://en.wikipedia.org/wiki/Bernstein_polynomial

[9] http://en.wikipedia.org/wiki/De_Casteljau's_algorithm

[10] http://en.wikipedia.org/wiki/Spline_(mathematics)

[11] http://en.wikipedia.org/wiki/Image_processing

[12] http://searchcio-midmarket.techtarget.com/sDefinition/0,,sid183_gci212327,00.html

[13] http://en.wikipedia.org/wiki/Image_scaling

[14] http://en.wikipedia.org/wiki/Bilinear_interpolation

[15] A. Klimke, Imgrescale Version 1.0, Universität Stuttgart, 2003

[16] Dr. Murtaza Khan, Approximation of Data Using Cubic Bézier Curve Least Square Fitting

[17] Sarah F. Frisken and Ron Perry, Simple and efficient traversal methods for quadtrees and octrees, Journal of Graphics Tools, 7(3):1-11, 2002

[18] Hanan Samet, Data structures for quadtree approximation and compression, Communications of the ACM, 28(9):973-993, 1985

[19] M. A. Khan, Exploiting Spline and Quadtree for Lossy Temporal Video Data and Lossless Synthetic Image Data Compression, Keio University

[20] M.A. Khan, A new method for video data compression by quadratic Bézier curve fitting, Bahrain, 2010

[21] Ghanbari, M.: Standard Codecs: Image Compression to Advanced Video Coding, new edn. Institution Electrical Engineers (2003)

[22] Wang, Y., Ostermann, J., Zhang, Y.Q.:Video Processing and Communications, first edn. Prentice Hall (2001)

[23] V. Perumal and Dr. J. Ramaswamy 2009, An Innovative Scheme For Effectual Fingerprint Data Compression Using Bézier Curve Representations, India

[24] http://design.osu.edu/Carlson/history/lesson20.html#melitta

[25] MATLAB demo, Copyright 1984-2002 The Mathworks Inc

[26] http://www.cs.mtu.edu/~shene/COURSES/cs3621/NOTES/spline/Bezier/bezier-construct.html

APPENDICES

APPENDIX A: BÉZIER DEMO

In the following figures, we can see the changing of Bézier curve by changing the control points.

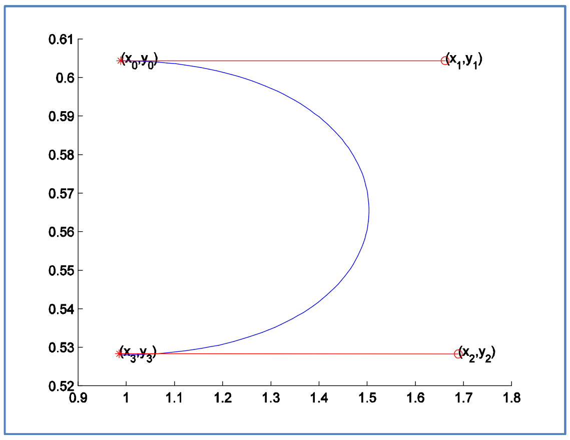

Demo 1

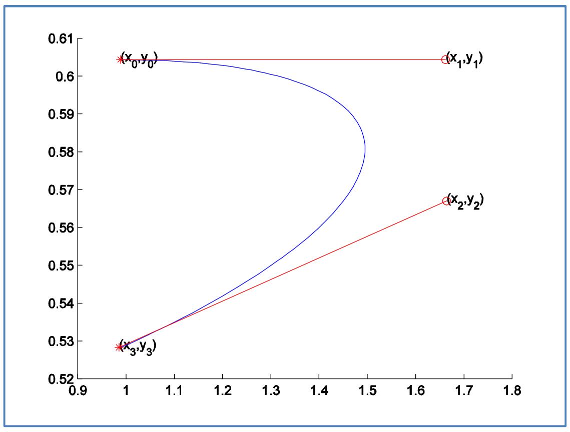

Demo 2

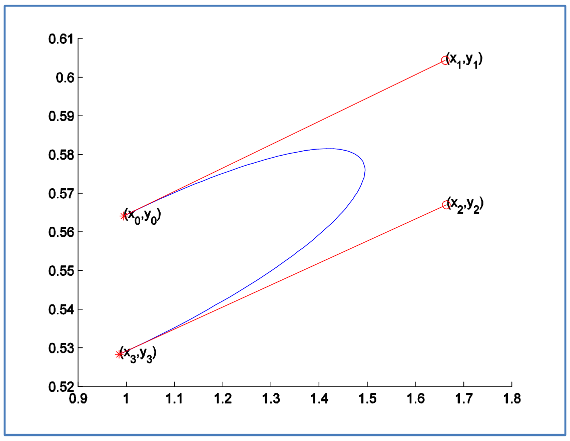

Demo 3

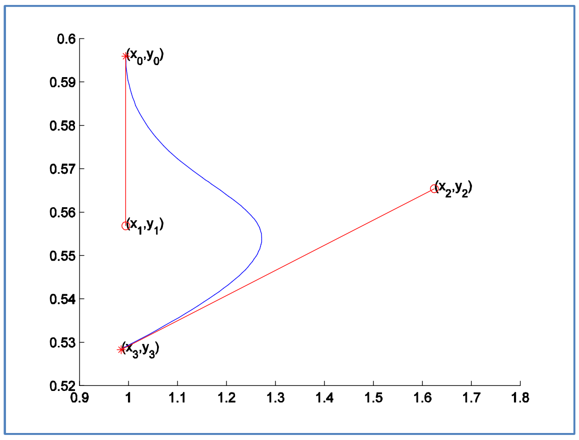

(x_0,y_0)
(x_1,y_1)
(x_2,y_2)
(x_3,y_3)
0.6
0.59
0.58
0.57
0.56
0.55
0.54
0.53
0.52
0.9
1
1.1
1.2
1.3
1.4
1.5
1.6
1.7
1.8

Demo 4

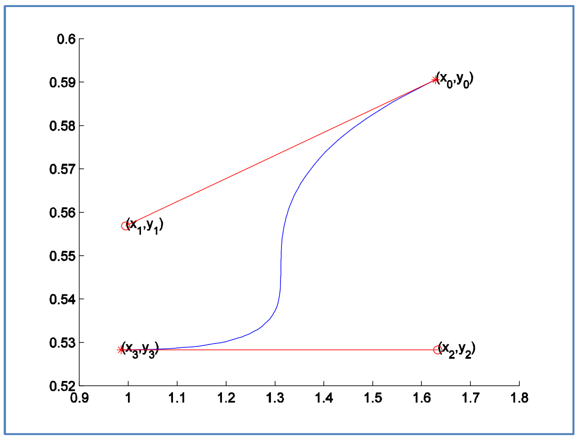

(x_0,y_0)
(x_1,y_1)
(x_2,y_2)
(x_3,y_3)
0.6
0.59
0.58
0.57
0.56
0.55
0.54
0.53
0.52
0.9
1
1.1
1.2
1.3
1.4
1.5
1.6
1.7
1.8

Demo 5

APPENDIX B: IMAGE RESCALING USING BILINEAR INTERPOLATION

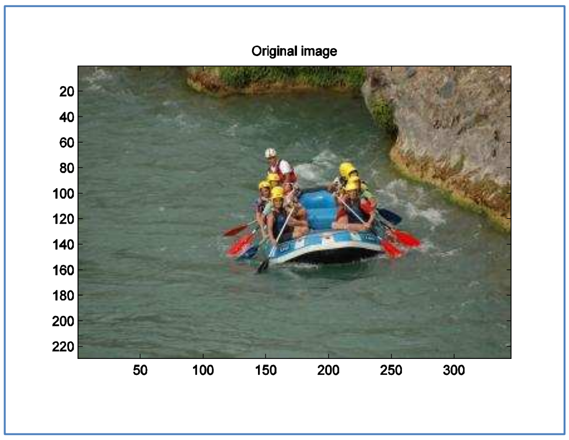

Original Image

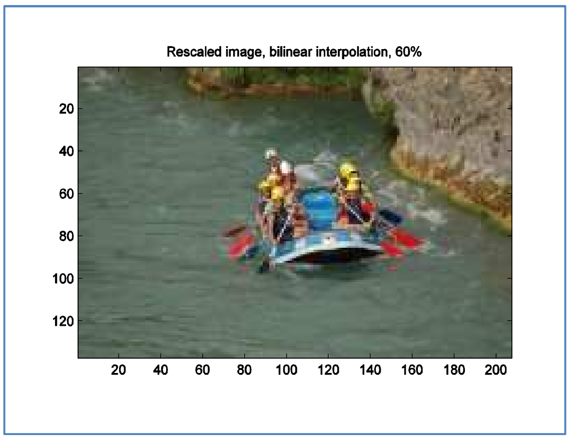

Rescaling 60%

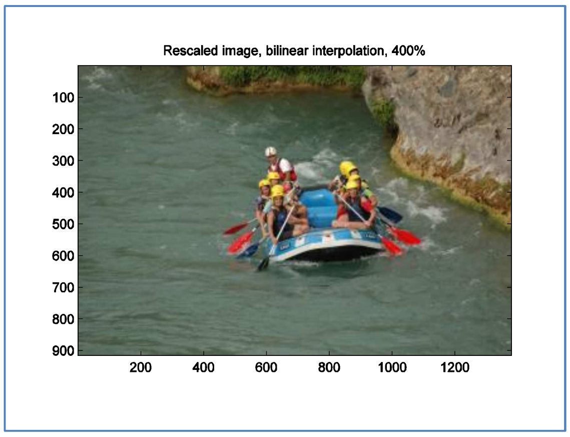

Rescaling 400%

APPENDIX C: UTAH TEAPOT

Utah Teapot 1

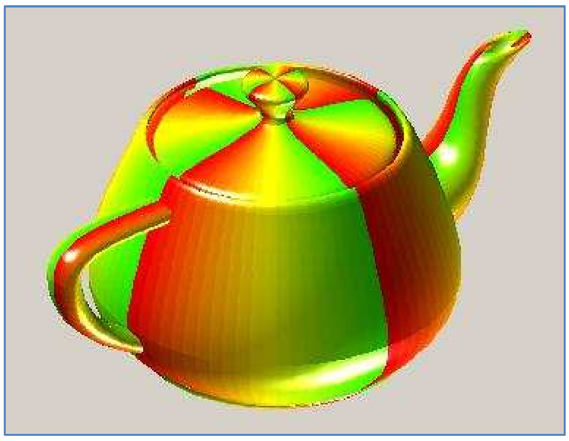

Utah Teapot 2

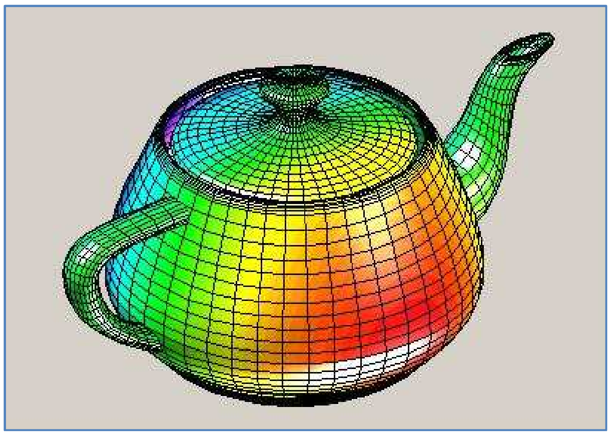

Utah Teapot 3